CHALMERS

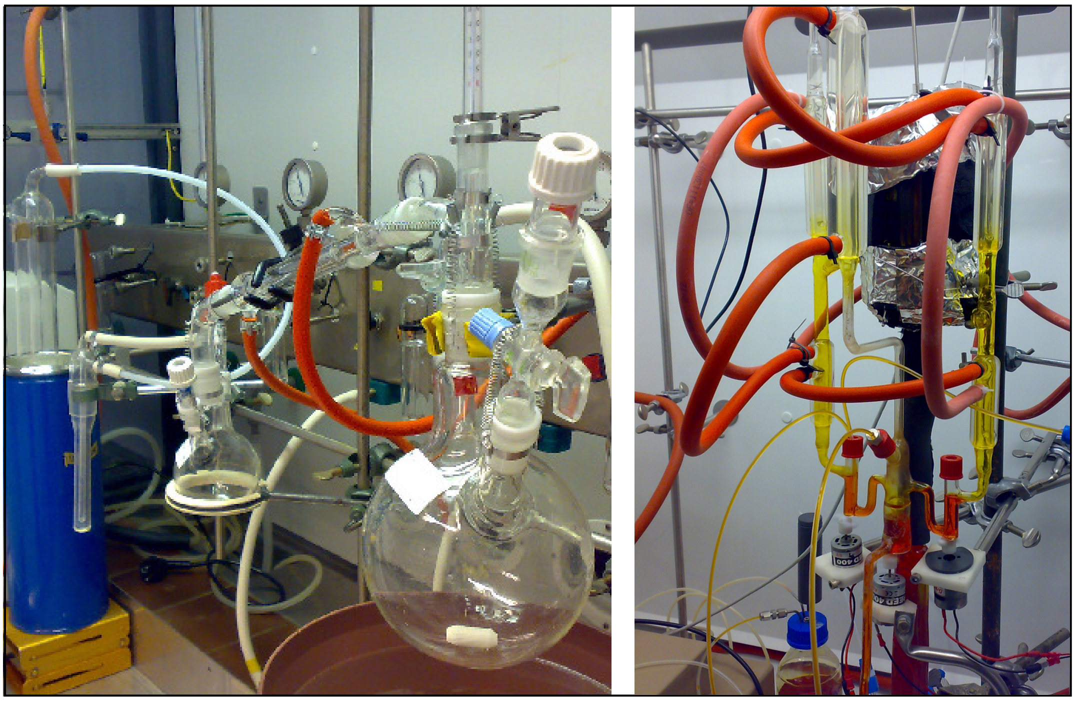

Optimisation of the Recovery Section of a Polyolefin Catalyst Manufacturing Process

Master´s Thesis in the Programme Innovative and Sustainable Chemical Engineering

JUKKA T. RÄSÄNEN

Department of Energy and Environment
Division of Heat and Power Technology
CHALMERS UNIVERSITY OF TECHNOLOGY
Göteborg, Sweden, 2010

MASTER'S THESIS

Optimisation of the Recovery Section of a Polyolefin Catalyst Manufacturing Process

A thorough study on
the methods of recovering the valuable components for reuse,
the effects of reuse on the catalyst properties,
the means of describing the nonideality of the mixtures,
and the economical effect of the optimised recovery section.

JUKKA T. RÄSÄNEN

SUPERVISOR(S):
Klaus Nyfors (Borealis Polymers Oy, Finland)
Mikko Lylykangas (Borealis Polymers Oy, Finland)

EXAMINER
Professor Lennart Vamling (Chalmers University of Technology)

Department of Energy and Environment
Division of Heat and Power Technology
CHALMERS UNIVERSITY OF TECHNOLOGY
Göteborg, Sweden 2010

Optimisation of the Recovery Section of a Polyolefin Catalyst Manufacturing Process

A thorough study on the methods of recovering the valuable components for reuse,
the effects of reuse on the catalyst properties, the means of describing the nonideality of
the mixtures, and the economical effect of the optimised recovery section.

Master´s Thesis in the Programme Innovative and Sustainable Chemical Engineering
JUKKA TAPANI RÄSÄNEN

jukka.t.rasanen@gmail.com

Department of Energy and Environment
Division of Heat and Power Technology
Chalmers University of Technology
SE-412 96 Göteborg
Sweden
Telephone + 46 (0)31-772 1000

Cover:
[Left: Laboratory scale batch evaporator (p. 31), Right: Yerazunis-type dynamic still for vapour-liquid equilibrium measurements (p. 30)]

Chalmers Reproservice
Göteborg, Sweden 2010

PREFACE

The work was performed at Borealis Porvoo (Finland) in February – July 2010. Parts of the work were performed in co-operation with Aalto University of Technology (Espoo, Finland). The thesis was instructed by Professor Vamling (Chalmers University of Technology) and tutored by Klaus Nyfors and Mikko Lylykangas (Borealis Polymers Oy).

I want to thank Professor Lennart Vamling (Chalmers University of Technology) for his instantaneous assistance and flexibility in the arrangements of this work. I valued your communicative approach greatly.

I owe a debt of gratitude to Jouni Kivelä, Klaus Nyfors and Mikko Lylykangas (Borealis Polymers Oy) for their great efforts in realising this work and for their engagement in supporting the project. I am thankful for the opportunity to work with persons truly skilled in their art.

Also, I want to thank the technicians at Borealis Porvoo for the numerous analyses and the personnel at the Porvoo Innovation Center for their support. Also, I want to thank dr Pokki (Aalto University of Technology) for professional assistance and the fruitful co-operation.

I express my great appreciation to my family, father Raimo, mother Taru, and sister Riitta. You gave me strength, taught me to work towards my goals and supported both my academic and private ambitions.

After the exhausting literature reviews, laboratory experiments, regressions and simulations I was always rewarded with the joy of sharing my time with my lovely girlfriend, Pauliina. You were always there.

Optimisation of the Recovery Section of a Polyolefin Catalyst Manufacturing Process
Master´s Thesis in the Programme Innovative and Sustainable Chemical Engineering
JUKKA T. RÄSÄNEN
Department of Energy and Environment
Division of Heat and Power Technology
Chalmers University of Technology

ABSTRACT

During the production of Ziegler-Natta catalysts, comparatively large amounts of washing effluents are generated. It is of significant importance – both in terms of economic competence and environmental concern – that these washing effluents are treated for recovering the components.

The objective of this work was to develop and optimise the separation processes of the recovery section of a catalyst manufacturing plant. The methods proposed in the initial design were proven suitable for the purposes. It was shown that it is possible and highly economical to recover the valuable components from the motherliquor and washing effluents. It was also proven, that these components can be efficiently reused in the washing stages without harmfully affecting the catalyst properties.

The recovery efficiency of a continuous evaporator was proven high: over 90 % of the most valuable component, titanium tetrachloride, was recovered. The evaporator was most feasible when operated at reduced pressures.

The separation of the key components via distillation was proven economically feasible. However, the toluene column condenser is proposed to be a partial condenser instead of total. The accumulation of light components in the toluene recovery cycle can be effectively avoided via bleeding the vapour from this condenser out from the process.

The accuracy of modelling the separation units was increased via regression of the binary interaction parameters of the key components. The parameters for describing the nonidealities were regressed from experimental vapour-liquid equilibrium data. Via these experiments it was also proven that there are no azeotropes within the studied binary mixtures and hence conventional distillation is possible.

The effects of the impurities in the washing liquids were shown to have practically no effect on the catalyst composition, morphology or polymerisation properties. Hence, these recovered components can be recovered and reused in the washing stages at the studied conditions.

Overall, the concept was proven technically and economically feasible. The variable operating cost of not having the recovery section was 158 €/kg$_{\text{catalyst}}$. The economic worth of the optimised recovery section with the proposed corrections was 86,3 € per unit quantity; thus reducing the variable operating cost to 71,7 €/kg$_{\text{catalyst}}$.

Key words:
Titanium tetrachloride, Titanium haloalkoxide, Vapour-Liquid Equilibrium (VLE), Separation, Evaporation, Regression, Optimisation

Abbreviations

atm	Atmospheric pressure (1013 mbar)
HC	Hydrocarbon
CAS	Chemical abstract system
ENCS	Existing and new chemical substances (list)
GC	Gas chromatography
HWL	Heptane washing liquid (feed to the washing stages)
HWE	Heptane washing effluent (washing waste)
LC	Liquid chromatography
MFR	Melt flow rate (mass of polymer flowing through a capillary in 10 min)
ML	Mother liquor
NRTL	Non-random two-liquid equation
OCT	Orto-chlorotoluene
PP	Polypropylene
PPR	Parallel pressure reactor
RHS	Right hand side (of equation)
SEM	Scanning electron microscope
TFE	Thin-film evaporator
TWL	Toluene washing liquid
TWE	Toluene washing effluent
UNIFAC	UNIQUAC functional-group activity coefficients (group contribution method)
UNIQUAC	Universal quasi-chemical equation
XS	Xylene solubles
ZN	Ziegler-Natta

Latin capital and lowercase letters

A, B and C	Antoine equation parameters
C_p	Specific heat capacity
D	Distillate molar flow
d	Fraction of distillate
F	Feed molar flow
f	Fugacity
g	Molar Gibbs free energy
H	Entropy
h	Molar entropy
K	Distribution factor
N	Number of moles
n	Number of moles
P	(Total) Pressure
t	T-value (in t-test)
W	Bottoms (concentrate) molar flow

w	Fraction of bottoms
R	Universal gas constant
S	Entropy
S_p^2	Sample variance
s	Molar entropy
T	Temperature
V	Volume
v	Liquid molar volume
x	Mole fraction in liquid
y	Mole fraction in vapour

Greek letters

γ	Liquid-phase activity coefficient
Λ	Wilson binary interaction parameters
μ	Population mean
Φ	Fugacity coefficient (of vapour)

Subscripts

D	Distillate
F	Feed
f	Formation (for example in enthalpy of)
i,j	Component i / j
V	Vapour
vap	Vaporisation (for example in enthalpy of)
W	Bottoms

Superscripts

E	Excess (for example in excess Gibbs free energy)
L	Liquid phase
O	Pure component
s	At saturation
v	Vapour phase

Table of contents

1 Introduction

1.1 Polypropylene and Ziegler-Natta catalysts

Polypropylene (PP), a thermoplastic polymerisation product of propylene, has been commercially produced since the 1950s. The popularity of PP has been sustained by its intrinsic properties: high stiffness, acid, alkali and solvent endurance and good tensile strength. In effect, the production capacity of PP has expanded up to 52 million tonnes per year (2008) and is estimated to continue to grow at 3,7 percent per annual (2010-2013). (Business Wire, 2010)

The development of PP capacity is and has been related to the development of polymerisation catalysts. The first findings of Karl Ziegler (Ziegler *et al* 1960) and further development by Natta and co-workers (Natta *et al* 1955) set the base for the evolutionary generations of catalysts nowadays known-as Ziegler-Natta (ZN) catalysts. The modern ZN-catalysts have enabled high-grade custom design polymers, thus enabling suitability in applications over other thermoplastic polymers. (ICIS, 2010) Despite the advances in metallocene and single site catalysts, the commercial manufacturing of PP relies predominantly on ZN-catalysts. The catalyst discussed in this thesis considers novel fourth generation Ziegler-Natta-polypropylene (PP) catalysts which allow (tubular) bulk-phase, gas phase reactors and combinations of each, for polymerisation of multimodal custom-design polypropylene.

In contrast to its advantages in polymerisation, the manufacturing of ZN-PP catalyst generates comparatively large amounts of waste liquids. These liquids, mainly washing effluents, compose of valuable components: hydrocarbons and excess reagents. It is of significant importance – both in terms of economic competence and environmental concern – that these washing effluents are treated for recovering the components.

1.2 Objectives

The objective of this work was to develop and optimise the separation processes of the recovery section of a fourth generation Ziegler-Natta PP catalyst manufacturing plant. The development consisted of defining the recovery stream design compositions and determination of the efficiency of separation. The optimisation covered the material-wise optimisation of the recovery section and the specification of the optimal operation parameters. The key elements that were to be delivered were:

- Verify the suitability of the separation techniques
- Quantify the recoverable amounts of the key components
- Study the effect of impurities in washing liquids on the catalyst physical properties and on the catalyst polymerisation properties
- Deliver the vapour-liquid equilibriums of the key component mixtures and regress the binary activity coefficients for an appropriate property method
- Optimise the material balances of the recovery section

1.3 Scope

The targets of this thesis were set to meet both the academic and the practical requirements in order to increase understanding of the process as well as to assist in the design of it. The boundaries of the study were set around the key unit operations of the separation processes in the recovery section of ZN-PP catalyst plant, whereas catalyst manufacturing in itself was not in the scope. In addition, auxiliaries were left outside of discussion.

1.4 Methods

In order to study the recovery of different components from the catalyst wastes and its effect on catalyst performance, experimental work was performed with laboratory-scale equipment. The experiments were for the most part performed at Borealis Innovation Centre in Porvoo, Finland. These experiments included catalyst synthesis using recycled solvents as well as test polymerisations. The catalysts were synthesized with a laboratory scale batch reactor system, Multimax RB04-50 (Mettler-Toledo), which has four parallel reactors. Polymerisations were performed with a minireactor system, Parallel Pressure Reactor (PPR) (Symyx), capable of performing 48 simultaneous polymerisations. Parts of the polymerisations were performed in a bench-scale polymerisation reactor. The catalyst preparation and polymerisations were performed at Borealis Innovation Centre in Porvoo.

To study the suitability of a continuous evaporation in the treatment of ZN-catalyst wastes, co-operation with an external manufacturer evaporators was established. The experiments performed with the external manufacturer were followed in-situ.

Another set of experiments aimed at acquiring data on the vapour-liquid equilibrium of relevant components was performed in co-operation with the Aalto University School of Science and Technology. The regression of thermodynamic data was performed with simulation software Aspen Plus 7.1 and compared to results acquired with VLEfit (a software developed at Aalto University). Aspen Plus was also used to simulate the separation units of the recovery section according to the planned plant flowsheet.

2 CATALYST PREPARATION plant

The development towards the discussed, industrially applicable fourth generation ZN-PP, catalyst has been performed in Porvoo (Finland) over a long period starting from the early 1980s. The work was performed to study possible configurations to handle the common effluents of catalyst manufacturing.

2.1 Recovery section

The waste liquids that are processed in the recovery section consist of mother liquor (reaction medium) and hydrocarbon washing effluents (toluene and n-heptane). The purpose of the hydrocarbon washes is to remove titanium haloalkoxides dissolved in titanium tetrachloride, $TiCl_4$, from the catalyst slurry. It is well established that these titanium haloalkoxides have an adverse effect on polypropylene catalyst activity (Pillai *et al.*, 1986) and are hence to be removed.

Motherliquor (ML) and toluene wash effluents (TWE) have high concentrations of titanium haloalkoxides. The compositions of ML and TWE are related in other terms as well, and hence it is expected that they can be treated in the same units. The heavies (primarily titanium haloalkoxides) are separated from ML and TWE in an evaporator, after which the components are purified by distillation. The heptane washing effluents (HWE) contain mostly n-heptane and toluene. Heptane is recovered as overhead product of distillation column; the bottom is forwarded to waste recovery. A block diagram of the effluent and recovery streams is given in Figure 1.

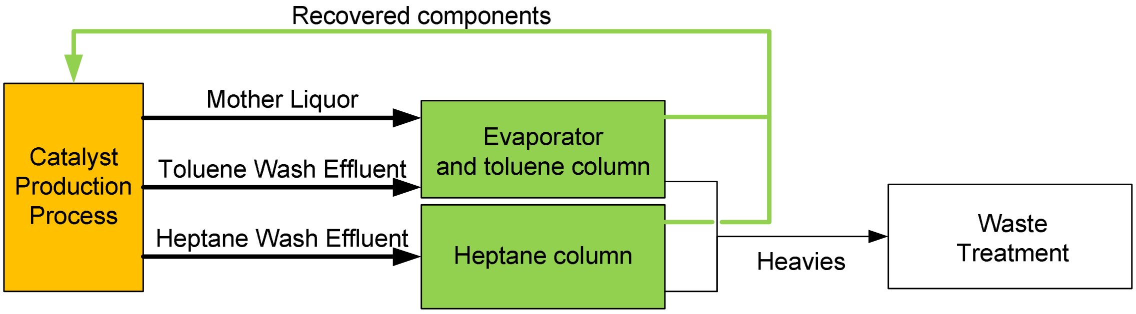

Figure 1 Block diagram of the component recovery in the catalyst preparation plant

2.2 Separation processes of the recovery section

In the studied material recovery system the components have qualities which were shown to necessitate special separation techniques. The selection of evaporation and distillation (Figures 2 and 3) units was motivated by the relatively low heat of evaporation of the recovered components and suitability for the feed conditions.

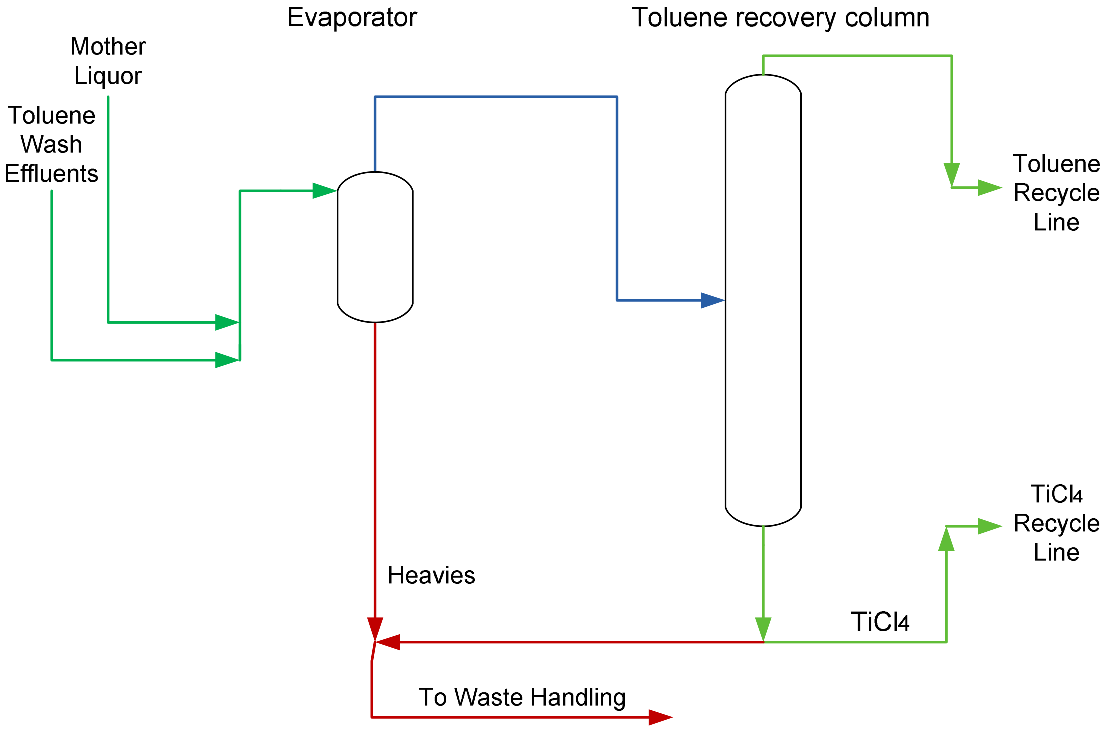

Figure 2 A schematic diagram of the recovery section of titanium tetrachloride and toluene in catalyst preparation plant recovery section

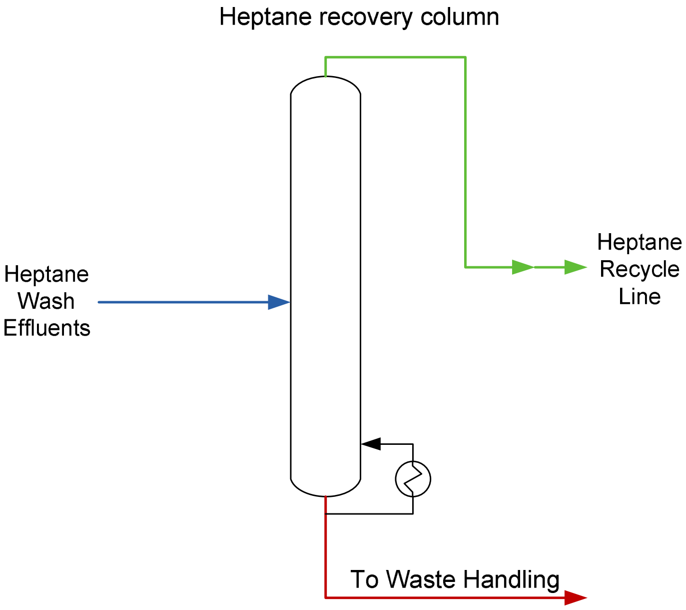

Figure 3 A schematic diagram of the purification units of heptane washing effluents in catalyst preparation plant recovery section

A systematic literature study on the existing processes (Table I) was carried out in order to evaluate different separation techniques. Later, the validity of assumptions was confirmed and scale-up data collected experimentally. The experiments are discussed later in Chapter 3.

Table I Main techniques of separation processes (Sinnot & Towler, 2009, p.553)

		Minor component		
		Solid	Liquid	Gas / Vapour
Major component	Solid	Sorting Screening Hydrocyclones Classifiers Jigs Tables Centrifuges Dense media Flotation Magnetic Electrostatic	Pressing Drying	Crushing Heating
	Liquid	Thickeners Clarifiers Hydrocyclones Filtration Centrifuges Crystallization Evaporators Precipitation Membranes Reverse osmosis Ion exchange Adsorption	Decanters Coalescers Solvent extraction Leaching Chromatography Distillation	Stripping
	Gas / Vapour	Gravity settlers Impingement settlers Cyclones Filters Wet scrubbers Electrostatic precipitators	Separating vessels Demisting pads Cyclones Wet scrubbers Electrostatic precipitators	Adsorption Absorption Cryogenic distillation Membranes

A suitable separation technique for the combined mother liquor and toluene wash effluents can be found from the Table I. Solids (titanium haloalkoxides) are present in the combined stream as a minor phase. The major phase is liquid and hence liquid-solid separation was to be selected. Evaporation was well suitable because the heat of evaporation of the recovered components is relatively low; e.g. the heat of evaporation of $TiCl_4$ is 15,28 kJ/mol (Patnaik, 2003). For comparison, the enthalpy of vaporization of water 40,65 kJ/mol. Toluene, heptane and $TiCl_4$ are collected in the evaporator overhead and later separated via distillation.

The predominant purpose of evaporation is to separate the solids in suspension: increase the concentration of solids in the liquid phase until a maximum viscosity is reached. Beyond the maximum viscosity (or concentration), the bottom solution can't be transferred via pumping. The vapour phase composes dominantly of two components: toluene and titanium tetrachloride, which can later be separated via distillation.

The suitable evaporator type is determined by the feed properties: viscosity, amount of solids, etc. The behaviour of the materials – fouling and heat-sensitivity – are determining in the selection of suitable evaporator type. Already in the early stages of the design process continuous evaporator was seen as a potentially efficient unit for the materials being processed. The intuition was supported by experience, published literature in the field (Chapter 2.2), and equipment selection guidelines (Guide for evaporator type selection (Sinnot & Towler, 2009, p. 602))

The feed stream entering the evaporator consists mainly of titanium tetrachloride and toluene (85 wt-% combined), minor amounts of heptane (5 wt-%) and by approximately 10 wt-% of thermally instable components, titanium haloalkoxides. Ti-haloalkoxides decompose (and form very viscous tarry gels) when heated above 130 °C for prolonged periods; hence, in order to evaporate titanium tetrachloride (boiling point 136,4 °C) without harmful side reactions, the evaporator should operate in partial vacuum with minimal residence time.

3 Theory

The said washing effluents of the catalyst production process consist mostly of the following components: toluene, titanium tetrachloride, n-heptane, titanium haloalkoxides, conventional electron donors and magnesium dichloride. Of these components titanium tetrachloride and titanium haloalkoxides are discussed in detail under Chapter 3.1.

The problem that arises from the purification of mother liquor and toluene washing effluents is that the mixture contains considerable amounts of titanium haloalkoxides, which have a tendency to decompose whilst heating to temperatures over 130 °C for prolonged periods. Therefore traditional distillation is not proficient for recovering the titanium tetrachloride (and hydrocarbons) from these solutions. Prior art on the possible means of recovering titanium is presented in Chapter 3.2. The mechanistic details and parameters for up-scaling of thin film evaporator are presented in Chapter 3.3 (proposed method for removing $TiCl_4$ by Basell patent (EP1834003 B1).

The thermodynamic property models and methods of acquiring vapour-liquid equilibrium are discussed under chapter 3.4.

3.1 Titanium compounds of interest

3.1.1 Titanium tetrachloride, $TiCl_4$

Titanium tetrachloride is a colourless or yellowish liquid in normal temperature and pressure. It has a molecular weight of 189,68 g/mol and its CAS registry number is 7550-45-0. A synonym for the compound is titanium (IV) chloride. (Patnaik, 2003)

It is not combustible; nevertheless it gives off irritating or toxic fumes in a fire. The most remarkable safety hazard of $TiCl_4$ is that it reacts violently with water to produce heat and corrosive fumes according to reaction:

$$TiCl_{4\,(l)} + 2\,H_2O_{\,(l)} \longrightarrow TiO_{2\,(s)} + 4\,HCl_{\,(g)} \tag{1}$$

$TiCl_4$ reacts even with the moisture in air to emit hydrochloric acid. Therefore it must be contained under inert conditions in closed containers. Physical and thermochemical properties of titanium tetrachloride are listed in Tables II and III, respectively.

Table II Physical properties of titanium tetrachloride (Patnaik, 2003)

Density (25°C) kg/dm^3	Freezing point °C	Boiling point °C	Critical temperature °C	Critical pressure atm	Critical volume cm^3/mol
1,73	-25	136,5	464,8	46,6	339

Table III Thermochemical properties of titanium tetrachloride (Patnaik, 2003)

ΔH_f (liq) kJ/mol	ΔH_f (gas) kJ/mol	ΔH_{vap} kJ/mol	ΔG_f (liq) kJ/mol	ΔG_f (gas) kJ/mol	S° (liq) J/deg mol	S° (gas) J/deg mol	C_p (liq) J/deg mol	C_p (gas) J/deg mol
-804,70	-763,67	15,28	-737,71	-726,83	252.46	353.34	145,28	99,46

3.1.2 Titanium haloalkoxides, Ti(O-2-ethylhexyl)Cl_3

The haloalkoxides present in the studied process are expected to compose mainly of trichloro(2-ethylhexan-1-olate)titanium (IV) (ENCS). It has synonyms 2-ethylhexyloxy titanium chloride (ECL) and titanium, trichloro(2-ethyl-1-hexanolato)-, (T-4)- (ASIA-PAC). The molecular weight is 283,46 g/mol and its CAS registry number is 27438-41-1. (SciFinder, 2010). The chemical structure is given in Figure 4.

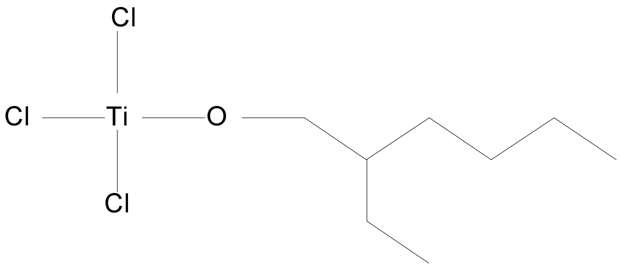

Figure 4 Chemical structure of Ti(O-2-ethylhexyl)Cl_3

The available data on the properties of Ti(O-2-ethylhexyl)Cl_3 is very limited. It is known that the component is solid in room temperature, but for instance no data on the boiling point could be found in the open literature. The melting point and boiling points of a titanium compound with similar chemical structure, titanium trichloroethoxy (CAS 3112-67-2), are 81-82 °C and 185-186 °C, respectively. (SciFinder, 2010) The melting and boiling points of trichloro(2-ethylhexan-1-olate)titanium are expected to be probably somewhat higher. Trichloro (2-ethylhexan-1-olate)titanium is later referred to as “titanium haloalkoxide” or Ti(O-2-ethylhexyl)Cl_3.

3.1.2.1 Reactions

Ti-haloalkoxides have a tendency to decompose thermally when heated above 130 °C for prolonged periods. The rapid reaction generates a dark-brown tarry residue which is very viscous whilst heated, and forms an almost solid tar at 20 °C with time (Ch. 3.1).

The titanium haloalkoxides are products of a side reaction during the activation stage of the catalyst synthesis. During the preparation of ZN-catalysts titanium tetrachloride reacts with the components of a magnesium complex, which contain magnesium alkoxides and free alcohol.. The main reaction of the activation stage can be described by following reactions (Leinonen[1]):

$$TiCl_4 + ROH \longrightarrow TiCl_3(RO) + HCl \quad (2)$$

$$2\ TiCl_4 + Mg(OR)_2 \longrightarrow 2\ TiCl_3(RO) + MgCl_2 \quad (3)$$

The reactions (2 and 3) represent the main reactions if titanium tetrachloride is present in excess. If a comparatively small amount of water (compared to equation 1) is present in the support material the reaction can be given by:

$$2\ TiCl_4 + H_2O \longrightarrow Cl_3Ti\text{-}O\text{-}TiCl_3 + 2\ HCl \quad (4)$$

Due to the fact that $TiCl_4$ is used in excess (in absence of water) in the current ZN-catalyst manufacturing process it is consistent to expect that only one of the chlorides of $TiCl_4$ has been substituted by the alkoxide group. It is however possible that two (or more) of the chloride ions of $TiCl_4$ have been substituted by the alkoxide, but the rate of this reaction has been considered low, and subsequently their concentrations small enough to be neglected (especially in process design).

The alkoxidation reaction has a central effect on the morphology of the support material and also the activity of the produced catalyst. Because the catalyst produced with the standard recipe has excellent activity, it can be concluded that practically all of the free alcohols and magnesium alkoxides have reacted with titanium tetrachloride to produce titanium haloalkoxides of type trichloro(2-ethylhexan-1-olate)titanium. (Leinonen[1])

3.1.2.2 Solubility

The solubility of $Ti(O\text{-}Et)Cl_3$in different industrial solvents has been measured by Garoff *et al.* (1990). These results are expected to be analogous to the solubility of $Ti(O\text{-}2\text{-}ethylhexyl)Cl_3$. However, the solubility of $Ti(O\text{-}2\text{-}ethylhexyl)Cl_3$ is expected to be lower for corresponding solvents.

$TiCl_4$ is expected, due to chemical similarity, to be the most efficient solvent for titanium (halo)alkoxides. Therefore, according to Garoff *et al.* (1990), the second most preferred solvent for $Ti(O\text{-}2\text{-}ethylhexyl)Cl_3$ is toluene. Acetone has a dissolving capacity close to half of toluene, but it is known to form a solid complex with $TiCl_4$, which in turn decreases the dissolving capacity of acetone. Also, condensation of acetone and $TiCl_4$ on the vessel walls can lead to solid formation which plugs easily the opening of the vessel. However, acetone has been found to be the most efficient solvent

---

[1] Timo Leinonen (M.Sc., Researcher, Borealis Polymers Oy) interviewed by the author in February 2010.

for dissolving solid residues containing inorganic components, like catalyst fines. (Garoff *et al.* 1990)

According to Garoff *et al.* (1990) the preferred industrial solvents for $Ti(O\text{-}Et)Cl_3$ in order are:

1. Toluene
2. Acetone
3. Chlorinated hydrocarbons
4. N-hydrocarbons (C_5-C_{10})

Temperature, as also pressure, affects the balance of intermolecular forces of the solvent-solute and the entropy change. Elevating the temperature close to the solvent boiling temperature increases the solubility. In accordance to theory, the dissolving capacity was shown to increase close to the double for most of the solvents when temperature was increased close to the boiling point of the industrial solvents. (Garoff[3])

3.2 Prior art for the separation of $TiCl_4$

The common methods for recovering a titanium compound from a waste solution are presented. The methods discussed comprise of treating a titanium containing waste of catalyst production; except for the article on adsorption in which the adsorption of metallic salts from titanium tetrachloride is discussed (useful in ore processes).

Shell Int Research (1990) patent EP0202715 describes a method for separating titanium haloalkoxides from mother liquor. In the process the contaminants of the formula $TiCl_3OR$, in which R is an alkyl or aryl, are separated by reacting the contaminants with an organic acid halide. The reaction product is thereafter precipitated as an addition complex and separated from the liquid phase. The reaction of acid halide (in a stroichiometric amount) with titanium haloalkoxide can be given by:

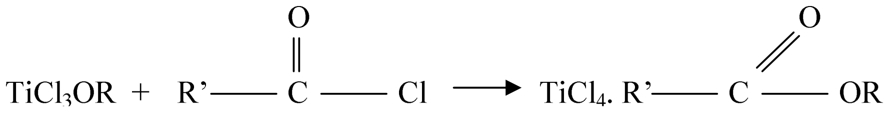

$$TiCl_3OR + R'-\overset{\overset{O}{\|}}{C}-Cl \longrightarrow TiCl_4.\,R'-\overset{\overset{O}{/\!/}}{C}-OR \qquad (5)$$

The liquid phase is said to comprise $TiCl_4$ and a halohydrocarbon (monochlorobenzene) in addition to contaminants. A proposed organic acid halide is benzoylchloride.

Mitsui Chemicals (2004) presents a method (US6790319) for recovering titanium halide by bringing titanium alkoxide into contact with a halogenating agent to convert titanium alkoxide to titanium halide (e.g.,$TiCl_4$, $TiBr_4$, TiI_4). In addition to organic acid halides, suitable halogenating agents are claimed to be inorganic halides and halogen gases (e.g., HCl, Cl_2). The inorganic halide is, for example a metallic halide or a non-metallic halide. Examples of metallic halides are $MgCl_2$, $AlCl_3$, and $FeCl_3$. Of these, $AlCl_3$ is preferable. Preferred non-metallic halide is $SOCl_2$. Reaction for recovering $TiCl_4$ with a non-metallic and metallic halide can be given by reactions (6) and (7), respectively.

$$Ti(OR)Cl_3 + SOCl_2 \longrightarrow TiCl_4 + SO_2 + RCl \tag{6}$$

$$Ti(OR)Cl_3 + AlCl_3 \longrightarrow TiCl_4 + Al(OR)Cl_2 \tag{7}$$

The aluminium containing residue of reaction (6) can be hydrolyzed to produce $Al(OH)_3$, hydrogen chloride and the alcohol, ROH. (Mitsui Chemicals 2004)

The method described by Choi and Lee (1988) comprises purifying titanium tetrachloride from low level volatile impurities (iron (III), aluminium and silicon chlorides) via adsorption. The adsorbent was silica gel of 70-230 mesh activated in air at 270 °C. The method was successful in removing Fe and Al, however Si was not successfully removed.

Akzo Nobel NV (2006) patent EP0837075 describes a batch-wise thermal treatment process for a waste stream comprising at least $TiCl_4$, one or more electron-donors and titanium haloalkoxides. The process is preferably conducted at temperatures of at least 180 °C in atmospheric pressure. In order to prevent the formation of $TiOCl_2$, a higher temperature (>200 °C) is preferred. Suitable equipment for the embodiment are stirred reactors equipped with a condenser, as well as conventional dryers and evaporators.

The thermal treatment decomposes the titanium haloalkoxides under formation of alkyl halide and Ti-halo-oxides. The formation rate of $TiCl_4$ is reported to be lower if reduced pressures (and correspondingly) lower temperatures are used. The final waste is claimed to compose of titanium halo-oxide and that the alkyl halide is also potentially recyclable. The final waste is a particulate material. (Akzo Nobel NV 2006)

Optionally the process contains a conventional distillation unit prior to the thermal treatment. In this process the condensate of the thermal treatment reactor is recycled into the distillation unit. (Akzo Nobel NV 2006)

Union Carbide Chem Plastic (2000) patent EP0837075 describes a 2-step purification process. The studied waste composes mainly of $TiCl_4$, reaction diluents (halohydrocarbon), titanium haloalkoxides and alkyl esters of aromatic acids. The halohydrocarbon is preferably orthochlorotoluene (OCT), an intermediate boiling solvent ($T_{bp,Ti\text{-}Haloalkoxide} > T_{bp,OCT} > T_{bp,TiCl4}$).

$TiCl_4$ is collected at 50-70 °C (with a part of the reaction diluents) as the lights component in the first column (operated at 50-200 mbar). The reaction diluent is selected so that it has sufficient solubility characteristics for the titanium haloalkoxides (heavies). The reaction diluents and heavies are collected as the bottom stream (80-105 °C) of the first column. The diluent (preferably OCT) is partially recovered in a second distillation column at 50-80 °C, operated at 50-200 mbar. The bottom product of second distillation column is collected at 80-120 °C and contains some reaction diluents to maintain waste solubility. (Union Carbide Chem Plastic 2000)

US5242549 (Shell Oil Co 1993) describes a process for separation of waste product components via 2-column distillation setup wherein a separation solvent is added to the waste product. The process is similar to Akzo Nobel's (2006) method (EP0837075): both of the distillation columns are operated in reduced pressure in the range of 50-200 mbar and $TiCl_4$ is collected as a light component in the first column. Difference is that in addition to $TiCl_4$ the reaction diluent is completely recovered in the first column. The separation solvent (added to the waste stream prior to first column) is partially recovered in the second distillation column as the distillate, and titanium haloalkoxides (dissolved), part of the separation solvent and organic esters as the bottom stream.

Basell Poliolefine SRL (2010) patent EP1834003 discloses a method for subjecting the $TiCl_4$ containing waste to a continuously operated distillation column and the bottom product thereafter to a thin-film evaporator. The distillation column is operated at reduced pressures ranging from 0.1 bar to 0.8 bar. During the preliminary distillation light hydrocarbons and part of $TiCl_4$ are removed.

The bottom product of the preliminary distillation column is continuously withdrawn and conveyed to the thin film evaporator. The thin film evaporator is operated at a normal pressure with the liquid temperature between 90-115 °C. $TiCl_4$ is collected as a vapour stream from the evaporator and the enriched titanium haloalkoxides and other by-products are discharged from the bottom of the evaporator. (Basell Poliolefine 2010)

The strengths and weaknesses of the presented methods are given in Table IV.

Table IV Summary of presented prior art

Applicant, Pub. number (A/B) (pub. year)	Inventive step	Claimed strengths	Weaknesses
Shell Int Research, EP0202715 (B1) (1990)	Organic acid halide	$TiCl_4$ prepared from titanium alkoxide, rapid reaction	Addition of a new component to the system, considered economically unfeasible
Mitsui Chemicals, US6790319 (B2) (2004)	Inorganic halide	$TiCl_4$ prepared from titanium alkoxide	Halogenation reaction contact time 2–4 hours
Akzo Nobel NV US7045480 (B2) (2006)	Thermal treatment	Solid residue, hazard of remaining waste reduced, no separation needed	Relatively high temp. required,violent evaporation →risk of entrainment
Shell Oil CO, US5242549 (A) (1993)	Vacuum distillation	Desired waste stream components recovered	Fouling, requires addition of a separation solvent, modest $TiCl_4$ recovery
Union Carbide Chem Plastics, EP0837075 B1 (2000)	Vacuum distillation	Desired waste stream components recovered	Fouling of the column, some $TiCl_4$ remains in the final waste
Basell Poliolefine, EP1834003 B1 (2010)	Thin-film evaporator	Short residence time, wipers enable percolation of highly concentrated viscose fluids	Hazardous residual product, clogging of the bottom

3.3 Thin film evaporator

Agitated thin film evaporators (TFE) as proposed by Basell (EP1834003 B1) are attractive for distillation, concentration and stripping of liquids especially when handling viscous, temperature sensitive substances that tend to foul or foam. (Glover, 2004) The rotating wipers allow short residence times and the large open space enables high vacuum distillations. It may function as a separator for partial distillation in a single-stage or multistage layouts, as well as a bottoms evaporator in a rectifying column. (Billet, 1992) In general, TFE has its advantages in applications where conventional distillation is not favourable.

3.3.1 Operation

A conventional thin-film evaporator consists of a vertical heated body and rotor blades, as given in Figure 5. The dilute preheated feed is fed to the top part of the evaporator onto a distribution ring. The distribution ring, which is mounted on the rotor, distributes the feed evenly on to the inner walls of the evaporator. The downwards flowing liquid film is kept in circulating motion in turbulent flow conditions with the rotating blades. The turbulent conditions combined with the thin, circulated liquid film generate optimal heat flux and consequently rapid vaporization and high separation efficiency. Clean vapours are collected from the vapour outlet on the top part to an external condenser and the concentrated liquid from the conical outlet at the bottom. (Glover, 2004)

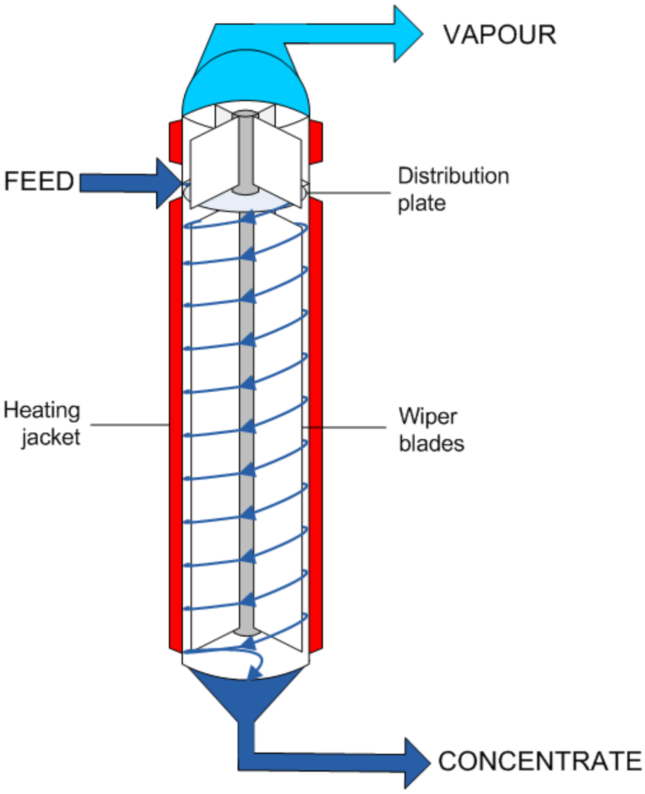

Figure 5 Agitated thin film evaporator of vertical design with a cylindrical body, wiper blades and distribution plate

The film thickness and the film flow are controlled with the internal rotating element. Different rotating element designs, also known as wiper systems, are given in Figure 6. Due to the turbulent conditions developed by the wipers, the evaporation rate is high and the product residence time short, usually less than one or two minutes. (Billet 1992)

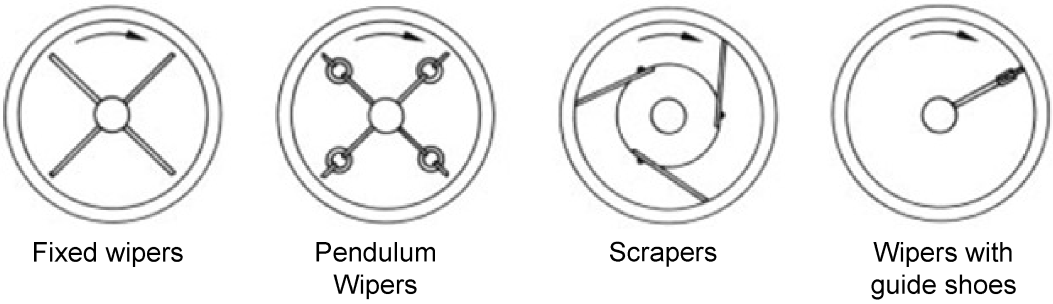

Figure 6 Wiper systems for agitated thin film evaporators (Billet, 2000)

There is no reflux, and hence the liquids flow only once through the column, subsequently requiring relatively large volatility difference for effective separation.

Consequently, the efficiency of the separation is defined by the boiling point difference of the substances in the system. (Billet, 1992)

3.3.2 Theory and efficiency of separation

The components that are to be collected as vapours in Basell process (EP1834003 B1) – $TiCl_4$, toluene and heptane – have largely different boiling points compared to the heavies, mainly 2-ethylhexyloxy titanium trichloride. The purpose is to achieve a bottom product of highly concentrated solids and a distillate greatly enriched by low-boilers ($TiCl_4$). The heavy key component is titanium haloalkoxide (Tbp > 185 °C). Heptane is the lightest component (boiling point of 108°C), followed by toluene (boiling temperature 111 °C). The light key component in the system is $TiCl_4$, which has boiling point of 136 °C.

The thermodynamic theory behind the separation in thin-film evaporators is that the low-boiler concentration between liquid (x) and vapour (y) reaches equilibrium (y*) in an infinitely small elemental area ($dh \cdot 2\pi r$) (Figure 7). The liquid concentration changes as a function of height of the heated surface as well as the evaporation dynamics.

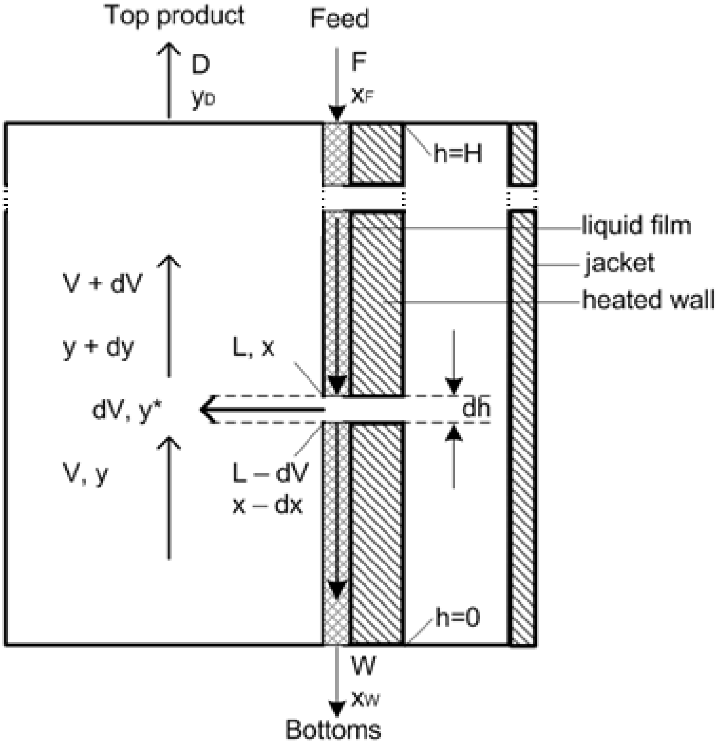

Figure 7 Continuous thin-film distillation model (Billet, 1992, re-drawn)

If the feed concentration of volatiles is high, then the evaporation rate is controlled by heat transfer. As the volatiles are evaporated from the liquid film the concentration of heavies increases (towards the bottom). At high heavies concentrations the evaporation rate changes to diffusion controlled, which can limit the separation efficiency. In order to minimize thermal degradation (and by-products of thermal decomposition), vacuum operation at correspondingly lower temperatures is an imperative. The application of partially vacuum conditions also generates higher relative volatility and higher separation efficiency. (Billet, 1992)

TFE can be modelled as a single-equilibrium stage separator. If $TiCl_4$ concentrations in the feed, x_F, and in the distillate, y_D, are known, the bottom concentration can be solved from the total molar balance, as given:

$$x_W = \frac{\mathrm{F}x_F - \mathrm{D}y_D}{\mathrm{W}} = \frac{x_F}{\mathrm{w}} - (1-\mathrm{w})y_D = \frac{1}{\mathrm{w}}x_F - \mathrm{d}y_D \tag{8}$$

, where w fraction of bottom, w= W/F
d fraction of distillate, d= D/F=(1-w)

Simple factors for studying the feasibility of the system are the residue per distillate ratio (R/D) and the percent of feed that is collected as distillate. Plotting the percent of feed that appears in the distillate (y-axis) as a function of the feed rate (on a square meter basis) (x-axis) gives quick insight into the achievable results. (Glover, 2004) The calculation of theoretical efficiency of partial distillation in TFEs is presented in more detail in Billet's (1992) article in Separations Technology, October 1992, 183-191.

In addition to the efficiency of separation other parameters are needed for upscaling. These parameters and their acquisition are discussed in the following chapter.

3.3.3 Bench-scale testing

Before performing experiments it should first be decided if the purpose is to determine the feasibility of the technique or to determine parameters for scale-up. This decision determines whether to select bench or pilot scale setup. According to Billet (1992), reliable determination of the minimum heat-transfer area can only be conducted in pilot plant trials. However, according to Glover (2004), under the right conditions bench top experiments can give reliable predictions (with some limitations) of the conditions for continuing to develop a process (V)

Table V Advantages and limitations of bench-scale experiments (Glover 2004)

Advantages	Limitations
Minimal feedrates → low cost of experiments	Scale-down may disturb operating behaviour:
Minimal production of by-product wastes	- liquid/vapour flow restrictions increased
Quickly configurable for (specific) use	- heat transfer coefficients reduced
Faster results → faster development of process	- pressure drop increased
Ability to provide initial parameters	Plugging or freezing of lines
Ability to demonstrate process feasibility	Transporting materials at small scale
Uncover process limitations (foaming, etc.)	Only careful predictions allowed

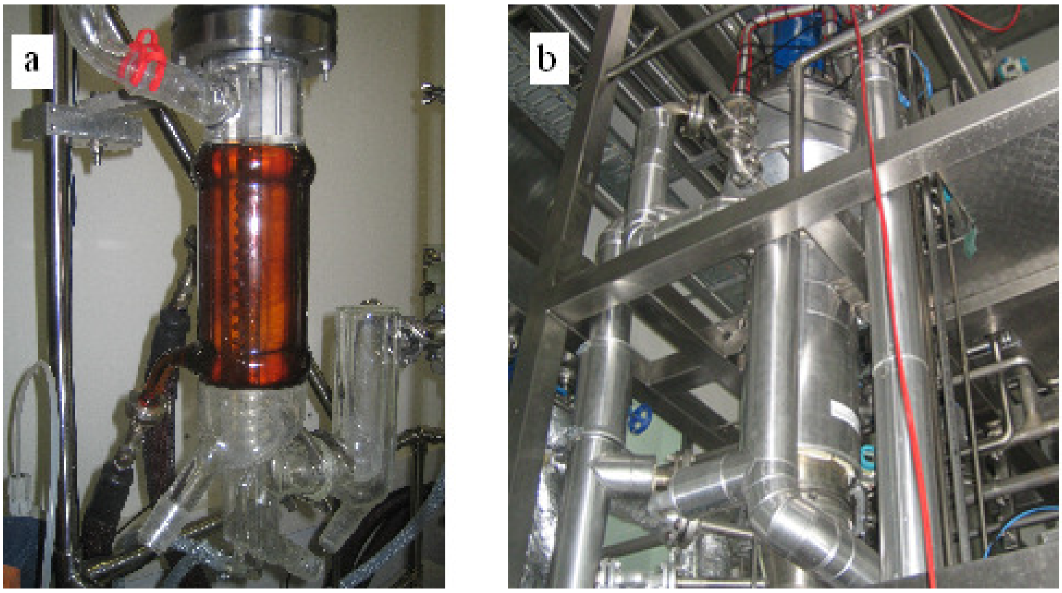

Figure 8 Bench- (a) and pilot-scale (b) thin-film evaporators

During bench-scale experimentation the parameters are optimised via varying feed rate, vacuum and heating temperature. Usually the bench experiments can be performed with only one type of rotor. The acquired process design parameters are limited, but nevertheless, the experiments provide quick insight of the feasibility of evaporator and at minimum the following (scale-up) parameters are acquired:

- Split distribution between the overhead and residue
- Operation pressure
- Heating oil temperature

The process design parameters are interrelated with physical properties and mechanical design parameters. (Glover 2004). With interrelation is meant that a change of value of a parameter can affect the values of other parameters. As an example, the composition of the feed material determines the physical properties (such as the heat of evaporation) which in turn are interrelated to the process design (type and temperature of heat transfer) and mechanical design (material thickness).

It has been proposed (Glover 2004), that even more detailed scale-up data can be acquired from bench-scale trials; however this case the material restrictions and differences in the surface wetting are should be minimised. Nevertheless, if the wall material in the bench-scale evaporator is same as in the full-scale unit, typically stainless steel, then the measurement of the overall heat transfer coefficient could ideally be performed (calculations described narrative in Glover’s article (2004)). With precise control, the feed per heated surface, kg/(s m_2), can then be acquired.

3.4 Thermodynamics of process design

Thermodynamic equations of ideal systems (standard states) are rarely adequate for accurate modelling. Therefore systems with nonideality need to be described through fugacity of gases and activity coefficients of liquids (or fugacity of liquids, phi-phi/EOS approach for pure hydrocarbon mixtures). In the following chapters the theory of describing and modelling nonideal systems together with vapour-liquid measurements are described in relation to the studied system. Chemical reaction equilibrium, energy conservation and energy transport processes are not discussed.

3.4.1 Thermodynamic property methods and models

Thermodynamic properties of mixtures containing $TiCl_4$ are poorly described in the literature. The activity coefficient database of Aspen Plus 7.1 does not include mixtures of $TiCl_4$ and hydrocarbons, mainly due to the reason that the databases are based on empirical data; and as mentioned, empirical data of mixtures containing titanium tetrachloride and hydrocarbons are few. For the same reason, estimation methods (UNIFAC) do not include titanium containing components.

Because the behaviour of these mixtures is expected to be nonideal, experimental research is required. In this chapter the phase equilibrium theory and the most-used thermodynamic models for describing real mixtures are described. Also a suitable property method for $TiCl_4$ containing components is proposed.

3.4.1.1 Phase equilibrium theory

Between two phases of a multicomponent mixture exist thermodynamic equilibrium, which can be given for every component, *i*, by equation:

$$f_i^V = f_i^L \tag{9}$$

Vapour-phase fugacity,f_i^V, can be given by (9) and liquid-phase fugacity,f_i^L , by (10):

$$f_i^V = P\Phi_i y_i \tag{10}$$

$$f_i^L = f_i^{OL}\gamma_i x_i \tag{11}$$

, where

P	total pressure, N/m^2
Φ_i	vapour fugacity coefficient (can be calculated with an appropriate EOS)
y_i	concentration of component *i* in the vapour phase
f_i^{OL}	standard state fugacity of the pure liquid
γ_i	liquid-phase activity coefficient

The distribution factor, K_i, or K-value, can be acquired via substitution of (9) and (10) into (11) and rearranging to equation (12).

$$K_i = \frac{y_i}{x_i} = \frac{\gamma_i f_i^{OL}}{P\Phi_i} \tag{12}$$

The standard state fugacity is a function of temperature, pressure, and liquid composition. For a pure liquid (x_i =1) it can be solved from equation (13). The exponential term on the RHS of equation (13) is termed the Poynting factor, or Poynting correction, which corrects for the pressure effects on the liquid-phase fugacity.

$$f_i^{OL} = P_i^O \Phi_i^s \left[exp\left(v_i^L \frac{P-P_i^O}{RT}\right)\right] \tag{13}$$

, where

P_i^O vapour pressure of pure component i, N/m^2

Φ_i^s fugacity coefficient of pure component i at saturation

v_i^L liquid molar volume, m^3/mol

The pure component vapour pressure can be calculated by the Antoine equation. The liquid molar volume can be estimated via structural contributions to molar volumes. The fugacity coefficient of the saturated vapour, Φ_i^s, can be calculated using the same EOS as was used to calculate Φ_i.

The pre-described approach is however less convenient for species in low pressure. In the studied case, the pressures in the systems are moderately low, ≤1 bar, and therefore the vapour-phase imperfections are not significant. With ideal gas assumption ($\Phi_i = 1$), and correlation for liquid-phase nonideality ($\gamma_i \neq 1$), the equation (11) reduces to modified Raoult's law:

$$K_i = \frac{\gamma_i P_i^O}{P} \tag{14}$$

3.4.1.2 P-v-T equations of state theory

Equations of state (EOS) describe relations between temperature, pressure and molar volume for real fluids. EOS are used for describing real gases in high pressures. In high pressures deviations from ideal behaviour in the vapour phase are significant and must be taken into account in process design. (Sinnot & Towler, 2009) Corrections for vapour-phase nonideality are assumed insignificant in the studied case and hence the common equations are only briefly described in Table VI. There exist guidelines for selecting the proper phase equilibrium model. In Appendix A is given the selection criteria map for VLE models in Aspen Plus 7.1.

Table VI	Common equations of state (Sinnot and Towler, 2009, p.455)

Equation (year published)	Description
Redlich-Kwong (1949)	Extension of Van der Waal's equation; not suitable near critical pressure; not suitable for liquids
Redlich-Kwong-Soave (1972)	Modified R-K to suit critical region and for use with liquids
Benedict-Webb-Rubin (1951)	8 empirical constants; accurate for vapour and liquid-phase hydrocarbons; useful for mixtures of light HCs with CO_2 and water
Lee-Kesler-Plöcker (1978)	Extension of B-W-R (accurate for a larger group of components); uses the principle of corresponding states; later modified further by Plöcker *et al.*
Chao-Seader (1961)	Accurate for light HCs and H_2; limited to T <530 K
Grayson-Streed (1963)	Extension of C-S (for H_2 rich mixtures); suitable for conditions of up to 200 bar and 4700 K
Peng-Robinson (1976)	Related to R-K-S; overcomes the instability in the R-K-S near the critical point
Brown K_{10} (1960)	Relates the *K*-value to 4 parameters: component, temperature, pressure and convergence pressure (at which all *K*-values approach 1); limited to low pressure (generally applied to vacuum systems)

3.4.1.3 Activity coefficient theory

The departures from ideal behaviour in liquid phase are revised and judged with liquid-phase activity coefficients. Liquid-phase activity coefficient models are set up based on excess Gibbs free energy, and their relation can be given by equation (15). (Lei *et al.* (2005).

$$RT\ \ln\gamma_i = \left[\frac{\partial(Ng^E)}{\partial(N_i)}\right]_{T,P,N_j} \tag{15}$$

, where

R	universal gas constant, 8,315 J/kmol·K
T	temperature, K
N	number of moles; subscripts: T-total; i-component i; j-component j, mol
g^E	excess molar Gibbs free energy

The excess molar Gibbs free energy is the sum of partial excess molar free energies and is related to excess molar enthalpy, h^E, and molar entropy, s^E, by:

$$g^E = h^E - Ts^E \tag{16}$$

In most applications (non-critical conditions), the liquid- phase activity coefficient can be assumed independent of pressure; and also, in the range of temperatures normally apparent in distillation column, independent of temperature. (Sinnot & Towler, 2009)

For an ideal mixture the value of activity coefficient is unity – which in turn means that the interaction between the similar or dissimilar molecules is identical. For nonideal mixtures the value deviates from unity. Positive deviations (from Raoult's law) account to values of γ_i >1. For the qualitative estimation of these deviations, Seader and Henley (2006) presented a classification, originally from Ewell, Harrison and Berg. The molecules are classified based on potential for forming hydrogen bonds, and thereafter each group is correlated with a type of deviation. In their classification $TiCl_4$, toluene and n-heptane all belong to the same group, "V". For a binary mixture of components from classes V+V, the molecule interaction does not consider H-bonds and the deviation is always positive or ideal. (Seader and Henley, 2006)

Examples of variation of activity coefficient with compositions in liquid phase are given in Figure 9. The roman numbering of components refers to the classification given in Seader and Henley (2006, p. 50). In Figure 9a the deviation from Raoult's law is strongly positive, in 9b negative, and in 9c the nonideality is adequately strong to result in the formation of two immiscible liquid phases.

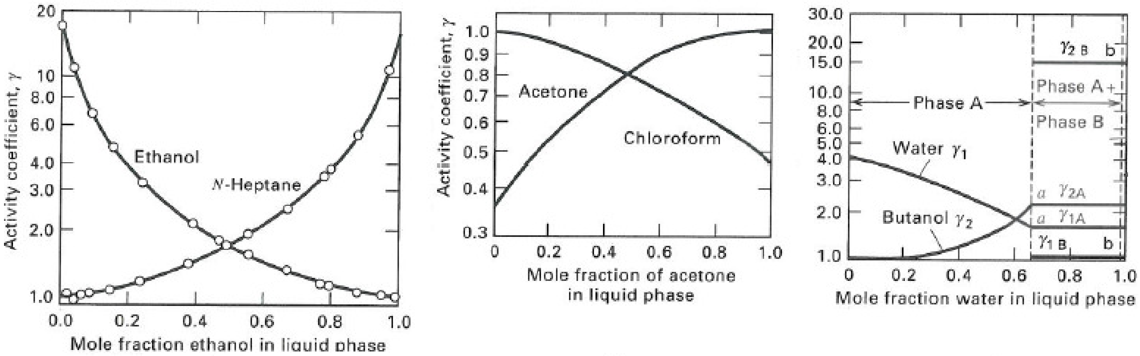

a b c

Figure 9 Variation of liquid-phase activity coefficients for binary pairs: (a) ethanol+n-heptane (II/V); (b) acetone+chloroform (III/IV); (c) water+n-butanol (I/II) (Seader and Henley, 2006)

Regular-solution model is fitting for regular, nonpolar species. For estimation of the liquid-phase activity coefficient via this theory requires only the pure species' molar liquid volume and the solubility parameter (volumetric internal energy of evaporation). However, as mentioned, regular-solution theory is not suitable for nonideal liquid solutions and hence more advanced approach is required.

3.4.1.4 Activity coefficient models

Several empirical and semitheoretical equations for liquid-phase activity coefficients exist. In Table VII the Margules, van Laar and Wilson two-constant equations, the Non-Random Two-Liquid (NRTL) three-constant equation and Universal Quasi-chemical (UNIQUAC) two-constant equations are presented. (Seader and Henley, 2006)

Table VII Liquid-phase activity coefficients equations (Seader and Henley, 2006)

Name		Equation for species 1		Equation for species 2
Margules	$\log\gamma_1=$	$x_2^2[\bar{A}_{12} + 2x_1(\bar{A}_{21} - \bar{A}_{12})]$	$\log\gamma_2=$	$x_1^2[\bar{A}_{21} + 2x_2(\bar{A}_{12} - \bar{A}_{21})]$
van Laar	$\ln\gamma_1=$	$\dfrac{A_{12}}{[1 + (x_1A_{12})/(x_2A_{21})]^2}$	$\ln\gamma_2=$	$\dfrac{A_{21}}{[1 + (x_2A_{21})/(x_1A_{12})]^2}$
Wilson	$\ln\gamma_1=$	$-\ln(x_1 + \Lambda_{12}x_2)$ $+x_2\left(\dfrac{\Lambda_{12}}{x_1 + \Lambda_{12}x_2} - \dfrac{\Lambda_{21}}{x_2 + \Lambda_{21}x_1}\right)$	$\ln\gamma_2=$	$-\ln(x_2 + \Lambda_{21}x_1)$ $-x_1\left(\dfrac{\Lambda_{12}}{x_1 + \Lambda_{12}x_2} - \dfrac{\Lambda_{21}}{x_2 + \Lambda_{21}x_1}\right)$
NRTL	$\ln\gamma_1=$	$\dfrac{x_2^2\tau_{21}G_{21}^2}{(x_1 + x_2G_{21})^2} + \dfrac{x_1^2\tau_{12}G_{12}}{(x_2 + x_1G_{12})^2}$	$\ln\gamma_2=$	$\dfrac{x_1^2\tau_{12}G_{12}^2}{(x_2 + x_1G_{12})^2} + \dfrac{x_2^2\tau_{21}G_{21}}{(x_1 + x_2G_{21})^2}$
	$G_{ij}=$	$\exp(-\alpha_{ij}\tau_{ij})$	$G_{ij}=$	$\exp(-\alpha_{ij}\tau_{ij})$
UNIQUAC	$\ln\gamma_1=$	$\ln\dfrac{\psi_1}{x_1} + \dfrac{\bar{Z}}{2}q_1\ln\dfrac{\theta_1}{\psi_1}$ $+\psi_2\left(l_1 - \dfrac{r_1}{r_2}l_2\right) - q_1\ln(\theta_1 + \theta_2T_{21})$ $+\theta_2q_1\left(\dfrac{T_{21}}{\theta_1 + \theta_2T_{21}} - \dfrac{T_{12}}{\theta_2 + \theta_1T_{12}}\right)$	$\ln\gamma_2=$	$\ln\dfrac{\psi_2}{x_2} + \dfrac{\bar{Z}}{2}q_2\ln\dfrac{\theta_2}{\psi_2}$ $+\psi_1\left(l_2 - \dfrac{r_2}{r_1}l_1\right) - q_2\ln(\theta_2 + \theta_1T_{12})$ $+\theta_1q_2\left(\dfrac{T_{12}}{\theta_2 + \theta_1T_{12}} - \dfrac{T_{21}}{\theta_1 + \theta_2T_{21}}\right)$

The Margules equation is used mostly due to its simplicity. The original Margules equation was presented as a one-constant equation (1895), however it correlates with symmetrical activity coefficient curves, which are rare. (Seader and Henley, 2006)

Van Laar equation fits many systems, and is derived from van der Waals equation of state. Van Laar equation cannot fit activity coefficient deviation curves that pass through a maximum (unusual) or minimum. Van Laar coefficients can be acquired accurately via nonlinear regression (Txy, Pxy) or rapidly via infinite dilution method (extrapolation of experimental data). The drawback of van Laar equation is that with nonpolar molecules that exhibit strong nonideality the equation can deviate in the dilute regions. When activity coefficient values exceed approximately 7, van Laar equation may erroneously predict phase splitting. (Seader and Henley, 2006)

Wilson model fits well binary systems of strong nonideality, but is restricted to miscible systems. As given in Figure 9c, the deviation curves are not continuous through the entire composition region, and hence Wilson prediction does not fit these two-liquid phase systems. Despite this drawback, Wilson is widely used, mostly because it is superior to the Margules and van Laar equation for highly nonideal, miscible mixtures. The Wilson equation can be extended to multicomponent mixtures via assuming a pseudo-binary mixture. In this case the multicomponent equation involves only binary interaction constants. As van Laar equation, Wilson model does not predict a minima or maxima of deviation curves. The binary parameters (Λ_{12}, Λ_{21}) for Wilson model can be acquired from a best fit to experimental data (Txy,Pxy), infinite-dilution or single-point (azeotropic conditions) methods. (Seader and Henley, 2006)

The NRTL method is an extension of Wilson to obtain more universal expressions for liquid-phase activity coefficients. The equation is suitable for multicomponent vapour-liquid, liquid-liquid and vapour-liquid-liquid systems. The tendency of non-random distribution of species i and j is described with parameter α_{ij}. Values for α_{ij} can be acquired from experimental data, but are often selected according to guidelines. Values α_{ij} <0.426 predict phase immiscibility. (Seader and Henley, 2006)

UNIQUAC model is, as well as Wilson and NRTL equations, based on local concentration concept. The difference is that instead of local volume or local mole fractions, UNIQUAC uses local area fraction θ_{ij}. The local area fraction is based on two structural parameters: the volume parameter, r, and the surface parameter, q. These values are calculated from the angles and distances of bonds. If not found in the literature, these values can be estimated by the group-contribution method (UNIFAC). (Seader and Henley, 2006)

UNIFAC (UNIQUAC functional-group activity coefficients) method is used for predicting liquid-phase activity coefficients based on the UNIQUAC equation. The method relies on treating the solution as a mixture of functional groups instead of molecules. For the estimation of activity coefficients, size parameters for each functional group (calculated from theory) and binary interaction parameters for each pair of the functional groups are necessitated (back-calculated from existing phase equilibrium, and thereafter used with the size parameters to predict the phase-equilibrium of the current system). (Seader and Henley, 2006)

3.4.2 Selection of appropriate model

There exist guidelines for selecting an appropriate activity coefficient model for the liquid-phase (Figure 10). These models can be combined with an appropriate vapour phase EOS. For example possible EOS for Wilson liquid-phase activity model in Aspen 7.1 are ideal gas law, Redlich-Kwong, Hayden-O'Connel, Nothnagel and HF equation of state. A more complete property method selection map is given in Appendix A.

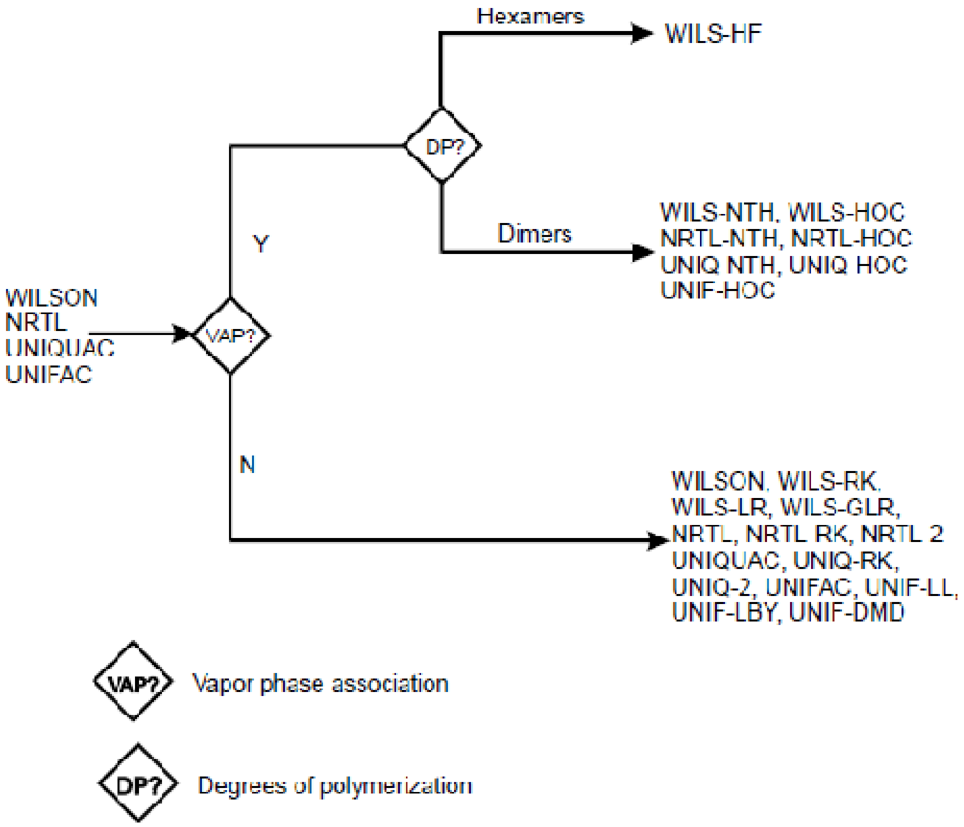

Figure 10 Guidelines for selecting activity coefficients model in Aspen 7.1 for non-electrolyte systems with polar components in pressure <0.5 MPa (from Aspen manual)

Due to the absence of $TiCl_4$ in UNIQUAC database, the method (and its devotee UNIFAC) is not suitable for the system. NRTL and Wilson method predictions were compared to experimental data of heptane + toluene binary VLE (Yerazunis *et al.*, 1964). The empirical and predicted VLEs of heptane + toluene binary system at 101 kPa are presented in Chapter 3.4.4 (Figures 12 and 13). Comparing these two predictions, it can be concluded that Wilson prediction fits the experimental curve more accurately, and is especially superior in the region close to pure heptane. Also importantly, Wilson is suitable for the system since no phase split occurs.

The components in the simulated system (recovery area) do not form immiscible mixtures and hence there are no restrictions for selecting Wilson. Even so, should there be liquid-liquid split, the Wilson model can be extended for these systems with its modification T-K-Wilson.

The Wilson prediction for liquid-phase activity coefficient together with vapour-phase ideal-gas law EOS was selected. The Wilson property method is commonly used, sophisticated and well established. The regressions of the VLE parameters for the studied binary systems will be performed to acquire Wilson equation coefficients.

3.4.3 Vapor-liquid equilibrium

Accurate measurement of the vapour-liquid equilibrium for $TiCl_4$ with present hydrocarbons was of importance due to deficient published literature. Thermodynamic consistency of the models applied in simulations requires highly accurate empirical data. Measurements are often time-consuming and tedious (Moser and Kistenmacher, 1987) and therefore purchasing or building apparatus for measuring VLE and thereafter learning to use the equipment was not considered sensible in the given timeframe. Thus, co-operation with Aalto University School of Technology and Science was established.

3.4.3.1 Measurement methods

Namely three groups of methods exist: static, dynamic and infinite dilution methods. (Raal and Ramjugernath, 2005). Of these three, the dynamic method, originally developed by Yerazunis *et al.* (1964), is discussed. For a person interested in general theory of different measurement techniques of vapour-liquid equilibrium the chapter 5 (static and dynamic) and chapters 13 and 14 (infinite dilution) in the book edited by R.D. Weir and T.W. de Loos (Measurement of the Thermodynamic Properties of Multiple Phases, 2005) are suggested. Another recommended review on the methods and computations is given by Raal and Mühlbauer (1998).

3.4.3.2 Dynamic stills

In the dynamic equilibrium method the mixture brought to boil at a set pressure in a heating vessel. The boiling mixture rises through a Cottrell pump to the equilibrium still, where the vapour and liquid settle into equilibrium. The vapour is collected from the top of the equilibrium chamber and condensed, and the liquid from the bottom of the still and condensed. Thereafter the vapour and liquid are mixed in a mixing chamber and returned to the heating vessel. The mixture is kept in circulation until the equilibrium conditions (temperature, pressure, compositions of liquid and vapour) stay constant. It takes conventionally 15-30 minutes to settle into steady state. (Pokki[2])

At steady state the equilibrium reached represents one equilibrium step and representative samples of the liquid and vapour can be collected. In addition to the composition of the liquid, x, and vapour, y, the corresponding temperature , T, and pressure, P, are also recorded. The measurements can be performed at constant pressure (isobaric) or temperature (isothermal). The principle of dynamic still is given in Figure 11.

---

[2] Juha-Pekka Pokki (D.Sc (eng.), Teaching researcher, Aalto-University School of Science and Technology) interviewed by the author on June 11th 2010.

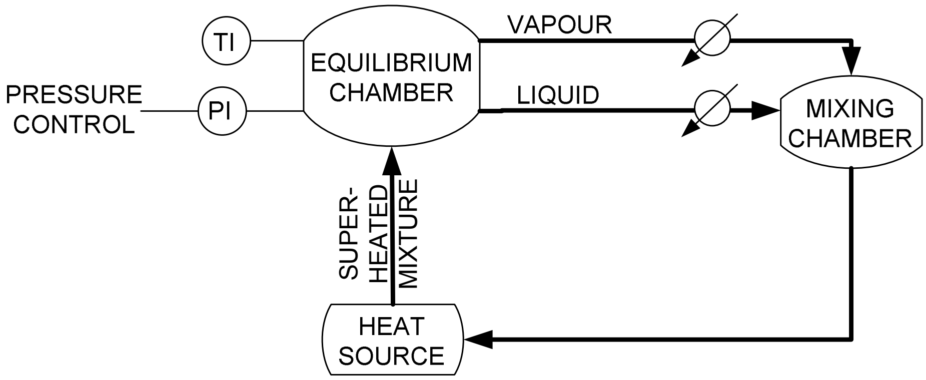

Figure 11 The principle of dynamic still (Uusi-Kyyny 2004)

3.4.3.3 Thermodynamic consistency

After acquisition, the data has to be evaluated for thermodynamic consistency. Conventional methods are the area test (Herington, 1947, Redlich and Kister 1948) and the point test of Van Ness *et al.* (1973).

The area test follows from the Gibbs-Duhem (binary mixture) equation:

$$x_1 d \ln \gamma_1 + x_2 d \ln \gamma_2 = \frac{-H^E}{RT^2} dT + \frac{V^E}{RT} dP \tag{17}$$

For isothermal VLE data the excess enthalpy, H^E, does not arise, and the excess volume term, V^E, is neglible. Hence, integration of (17) over the whole composition range gives:

$$\int_{x1=0}^{1} \ln \frac{\gamma_1}{\gamma_2} \mathrm{d}x_1 = 0 \tag{18}$$

According to Joseph *et al.* (2002) the test requires the integrand to be zero. The criterion of the test is that the difference of the integrand areas divided by the sum of the (absolute) areas should be ≤ 0,1. The test is claimed to be required, yet insufficient due to the ignorance of pressure in the test.

The point test method is based on using any of the three measured variables (x, y, T, P) to calculate and the value of fourth variable. This variable, usually the vapour phase composition, is then compared with the experimental value. The deviations between the predicted and experimental phase compositions are thereafter used to evaluate the thermodynamic consistency. The average absolute deviation between the calculated and experimental value must be less than 0.01. (Joseph *et al.* 2002)

There exists a possibility for the data regression to converge without errors, but with unsuitable results. Indicators of a bad fit are (Aspen Plus Manual[3]):

- A standard deviation for a regressed parameter is 0.0, indicating the parameter is at a bound.
- A large residual root mean square error value. Normally, this value should be less than 10 for VLE data and less than 100 for LLE data.
- VLE data fails the thermodynamic consistency test.

3.4.4 Relevant VLEs in literature

Experimental data for several thousand binary and many multicomponent systems are presented virtually in the DETHERM database. DECHEMA manages the database, which allows free access to search for component or mixture data sets. Despite the fact that the distillation of toluene and $TiCl_4$ is presented well in the literature, no data of the vapour-liquid equilibrium was found in this database (Dechema, 2010). Therefore the vapour-liquid equilibrium of toluene + $TiCl_4$ and heptane + $TiCl_4$ binary mixtures were to be measured. The experiments and results are described in Chapter 3.5.

3.4.4.1 VLE for the binary system of n-heptane + toluene

The vapour-liquid equilibrium of n-heptane and toluene was measured by Yerazunis, Plowright and Smola (Yerazunis *et al.*, 1964) to show the strong liquid-phase nonideality of the system behaviour. In accordance to the experimental results, the Wilson liquid-phase activity coefficient model predicts strong positive deviation from Raoult's law. However, interaction in NRTL has not been regressed using experimental data and consequently fails to predict the nonideality. Subsequently, the temperature-composition diagram plotted with NRTL property method (Figure 13) is not consistent to the experimental diagram, Figure 12 (Yerazunis *et al.,* 1964). Wilson property method correlates with the empirical data, especially in the region close to the mole fractions of pure heptane.

---

[3] Aspen Plus 7.1 APrSystem Help, Using the Aspen Physical Property System: Regressing Property Data: Using Regression Results: Examining Regression Results: How to Identify Unsatisfactory Data Regression Results

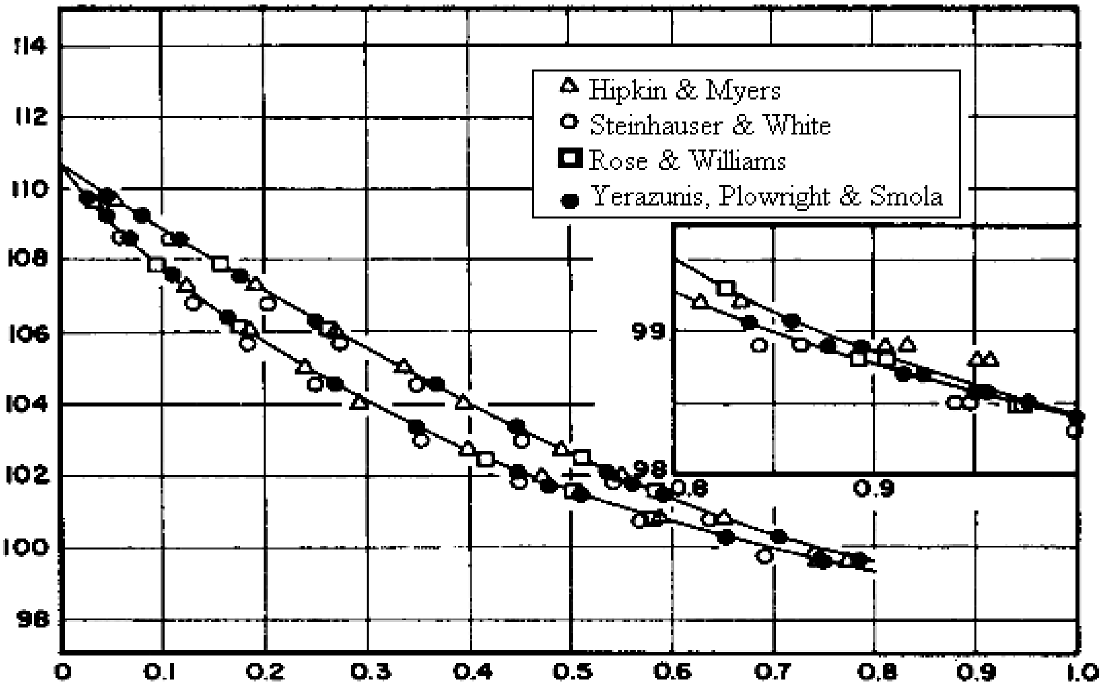

Figure 12 Experimental temperature-composition diagram of n-heptane + toluene at 101 kPa (Yerazunis *et al.* 1964)

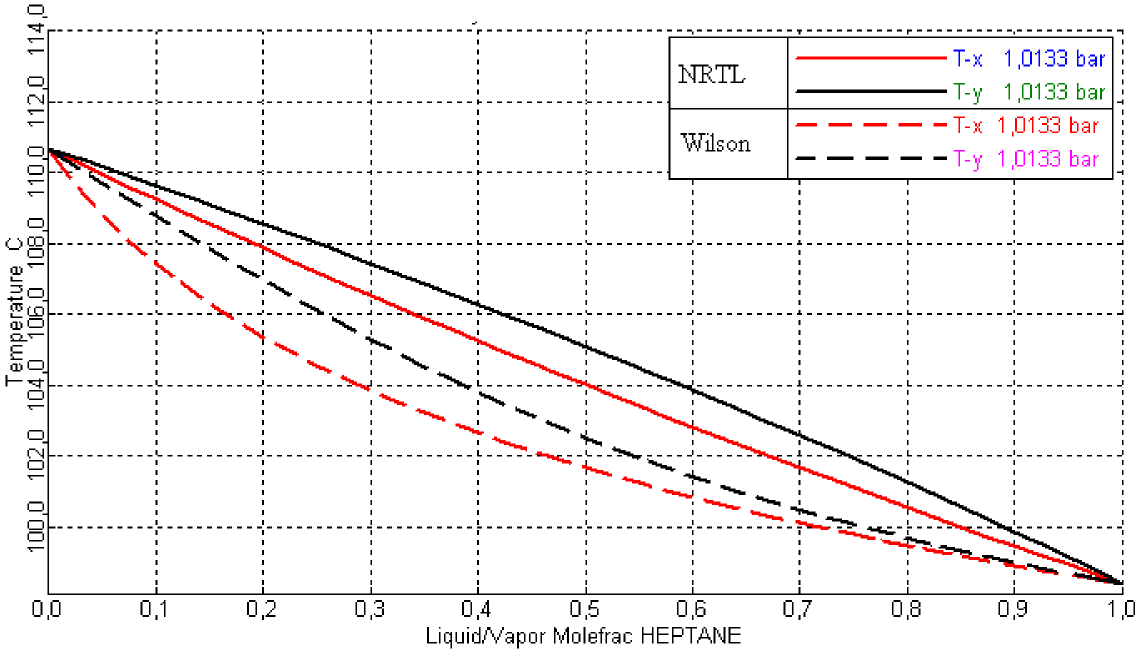

Figure 13 Predicted temperature-composition diagram of n-heptane-tToluene at 101 kPa. Aspen Plus 7.1, with NRTL (upper two lines) and Wilson property methods (cut lines).

4 Experiments and results

4.1 Evaporation – Setting the initial specifications

In order to be able to set design specifications for the simulation of the continuous evaporator the maximum achievable bottom product concentration had to be known. The bottom concentration is not only determined by the solubility of the haloalkoxides: it is strongly dependent on the evaporation temperature and residence time. The Ti-haloalkoxides are well known to form gel-like structures when they are heated over 130 °C for prolonged periods. Experiments were performed without top condenser to minimize the impact of refluxing. A set of experiments was performed with reduced pressure. The pressure was reduced to decrease the boiling point of $TiCl_4$ to < 90 °C.

4.1.1 Materials

Samples were collected from the catalyst pilot plant (located in Porvoo Finland). Samples of the motherliquor (ML) and the toluene wash effluents (TWE) were combined in a 1:1 weight ratio. In the campaign only one toluene wash stage was used.

4.1.2 Equipment

The test series were prepared with laboratory-scale evaporation equipment (Figure 14) under argon atmosphere. The boiling flask was dimensioned to be comparatively large in order to achieve larger heat-transfer area (1000 ml). The haloalkoxides are thermally sensitive and therefore refluxing was minimized by using no vertical column.

Figure 14 Setup of the short-path distillation experiments

The pressure was controlled by using the air-free Schlenk-technique (1 atm trials) and a Büchi Vacuum System B-178 pump/controller (200 mbar trials). The boiling flask was heated with an oil-heater and the horizontal condenser was cooled with tap water (15

°C). The gas traps between the system and the vacuum pump were filled with heptane and cooled to -20 °C in order to condense possibly evaporated $TiCl_4$.

4.1.3 Evaporation at 1 atm

The system was batched with 147 g (149 ml) of the combined solution of ML and TWE (Table IX). The oil bath temperature was set to 120 °C, knowing from previous experiments that the temperature between the oil and the boiling flask needs to be 15-20 °C, and that heptane has the boiling point of 98,4 °C. The next boiling component, toluene has its boiling point at 110,6 °C and $TiCl_4$ eventually at 136,4 °C.

The heptane was collected rather aggressively with a yellowish colour. The colour indicates that already in the beginning, $TiCl_4$ evaporates; subsequently indicating binary activity of the two components. Toluene started to evaporate very shortly after the heptane. After 40 minutes from the startup $TiCl_4$ was collected. Evaporating the last remains of liquid in the boiling flask was not possible expectedly due to the size of the boiling flask: the mass of the generated vapours was not large enough (compared to the size of the vapour space in the boiling flask) to drive the evaporation to the extreme end. In the purpose of evaporating all possible $TiCl_4$ the residence time was extended and the oil bath temperature was raised to 150 °C. The evaporation rate of $TiCl_4$ decreased to 1 drop per 5-8 seconds in the end.

The maximum bottom concentration was reached after 1 h. The solidification reaction was fast and resulted in a tar-like solution. The amount of collected, reddish-yellow distillate was 100 g. The material balance is given in Table VIII.

4.1.4 Evaporation at 200 mbar

The equipment (Figure 14) was connected to a Büchi Vacuum System B-178, with which the pressure was controlled. The pressure set point was 200 mbar and the controller threshold was 5 mbar, equalling operating pressure of 200 ± 5 mbar.

The first trial of the vacuum experiments failed because the toluene (and other light components) boiled violently carrying Ti-haloalkoxides to the distillation flask. The first trial was performed by preheating the oil bath to 60 °C, feeding the system with 147 g (149 ml) of solution and lowering the pressure to 200 mbar. Then the temperature of the oil bath was gradually raised to 105 °C. The response to the oil temperature was slow, and therefore there was no boiling before the oil temperature of 105 °C. However, after the boiling vessel had thoroughly heated to this temperature the boiling began violently – thus resulting in over-flooding of the haloalkoxides. The presence of Ti-haloalkoxides could be observed from the brown colour of the distillate. Pure distillate would have been orange (because $TiCl_4$ colours toluene even in small concentrations) and would had changed to a more reddish colour as more $TiCl_4$ is collected.

Another trial was therefore performed. The oil bath was preheated to 80 °C and the boiling flask was let in contact with the oil for 30 min in order to heat up the glass. 149 g (150 ml) of combined ML and toluene wash effluents was fed into the boiling flask and the pressure was gradually lowered. The boiling began at 300 mbar, at which heptane was expectably collected. The pressure was dropped to 200 mbar and the oil bath temperature was slowly raised to 87 °C. Toluene was collected at 66-68 °C at 200 mbar. The oil temperature was gradually elevated to 110 °C and $TiCl_4$ was collected at 76 °C. The amount of the collected distillate was 123 g and bottom 22 g. Distillate had a reddish colour, indicating strong presence of $TiCl_4$ in toluene.

The final concentration was reached without solidification in the bottom. However, in order to ensure that all of the possible TiCl4 was evaporated the oil bath temperature was gradually raised to 150 °C. After less than 15 minutes at this temperature, the bottom solidified rapidly. First the solution's viscosity rose rapidly. This could be observed from the foaming of the solution. Within seconds the solution formed a viscose, dark brown gel that could not be mixed. The tarry bottom was conserved under inert and dry conditions for 2 weeks. During a fortnight the solution turned from very viscous gel to almost solid.

4.1.5 Results

The weights of the feed, distillate and bottom were measured (Table VIII). The accuracy of procedure was calculated by the summed weights of overhead and bottom divided by the amount fed into the system (Out/In).

Table VIII Weights of collected fractions of the evaporation experiments, *Calculated as the residual of feed and overhead

1 atm	Amount g	Of feed %	$\frac{\text{Out}}{\text{In}}$	**200 mbar**	Amount g	Of feed %	$\frac{\text{Out}}{\text{In}}$
Feed	147,04	-		Feed	149,11	-	97,3 %
Overhead	100,04	68	100 %	Overhead	123,30	83	
Bottom	47,00*	32		Bottom	21,85	15	

At 1 atm experiment the bottom residue reacted to form a tar-like gel. However, at 200 mbar the reaction was avoided and thus the bottom was flowable.

The feed material was analysed with ICP-AES (Mg, Ti), GC (toluene, heptane, 2-ethylhexanol (hydrolysis product of Ti-alkoxides), pentane and octane) and with LC (DOP). The composition of the feed material is given in Table IX. The compositions of the feed material (combined ML and TWE) and overhead were both analysed with ICP-AES (Titanium and Magnesium). Thus the titanium tetrachloride balance was obtained (Table X). The entrainment of Ti-alkoxide was assumed neglectable (all elemental titanium in overhead was assumed to originate from $TiCl_4$).

Table IX Composition of the feed material of evaporation trials at 1 atm and 200 mbar and the methods of analysis and their estimated accuracies (Quin[4])

Component	wt-%			Measurement method	Lower detection limit	Estimated accuracy
					ppm	% (rel.)
TiCl4	27,5	±	2,75	ICP-AES	0,1	10
TiCl3OEHA	7,4	±	0,02	GC (EHA)	10	0,25
Toluene	40,7	±	0,10	GC	10	0,25
n-heptane	6,6	±	0,02	GC	10	0,25
Pentane	1,4	±	0,00	GC	10	0,25
Octane	1,2	±	0,00	GC	10	0,25
MgCl2	0,4	±	0,04	ICP-AES	0,1	10
DOP	1,3	±	0,13	LC	20	10
Sum	86,5	±				

Table X Titanium tetrachloride balances and recoveries of evaporation experiments at 1 atm and 200 mbar; F–feed, O–overhead, B–bottom

		1 atm			200 mbar		
		F	O	B	F	O	B
Weighed total	g	147,04	100,04	46,99	149,11	123,30	21,85
$TiCl_4$	g	40,4	26,1	n.a.	41,1	52,0	n.a.
Calc. $TiCl_4$				14,3			-11,0
$TiCl_4$	wt-%	27,5	26,1		27,5	42,2	
$TiCl_4$ recovery	%		64,6			126,8	
Titanium	mol	0,25127	0,13752	n.a.	0,25481	0,27433	n.a.

87 wt-% of the feed composition was explained by the analysis (Table IX). The sources of error are discussed in Chapter 5.6. As given in Table X, the amount of $TiCl_4$ (and elemental titanium) in overhead of 200 mbar distillation was higher than the amount fed into the system. The overhead titanium was analysed with two independent samples to give weight fractions of 0,104 and 0,109 for elemental titanium and their average was used in calculations. It can be concluded that there was a measurement error (dilution of samples etc.) or that the sample that was used (as feed material) in the 200 mbar experiments does not represent the analysed composition due to improper mixing of solution prior to feeding.

Nevertheless, a larger amount of distillate was collected at 200 mbar compared to normal pressure. The feed to distillate ratio was 83 % at 200 mbar and 68 % at 1 atm. Similarly, the recovery of titanium tetrachloride was increased with reduced pressures.

---

[4] David Quin (Ph.D., Researcher, Borealis Polymers OY) interviewed by author in July 16 2010.

The titanium recovery at 0.2 bar was 127 % and at 1 atm 65 %. Assuming zero entrainment (all Ti-haloalkoxides in the bottom) results in bottom Ti-haloalkoxide concentrations of 23,2 and 50,5 wt-% for 1 atm and 200 mbar trials, respectively. In addition to higher recovery, also the operability was enhanced with lower pressure (and corresponding temperature): the bottom did not react to form tarry gel during the trials.

4.2 Evaporation and distillation

The distillation of the overhead product of evaporation was to be performed as recourse for the determination of the effect of recycled components on the catalyst activity. The experimental procedure was as follows:

1. Evaporation of combined ML and TWE at 200 mbar
2. Collect the overhead product. Analyse the composition.
3. Dilute the bottom product with toluene (prevents solidification), collect a sample and analyse the composition
4. Feed the collected overhead product to a boiling flask. Separate titanium tetrachloride from low-boiling components (toluene fraction) by distillation at 1 bar
5. Use the collected toluene fraction in catalyst washing stages
6. Polymerisation of the synthesized catalyst

The experimental procedure of steps 1-4 is described in the following subchapters and the steps 5-6 in Chapter 4.4.1. The experiment of step 1 had a secondary purpose of verifying the results of the evaporation experiments described in Chapter 4.1.

Material used in the experiments was acquired from the catalyst pilot and composed of 1:1 weight ratio of ML and TWE. The material was same as used in the prior experiments (Chapter 4.1).

4.2.1 Equipment

The evaporation equipment was similar to the vacuum evaporator described in chapter 3.1.2. The distillation was performed at 1 atm in inert conditions by using the Schlenk technique. The boiling flask was a 500 ml 3-necked round flask, to which a feeding/sampling socket and a 300 mm Vigreux column were attached. The distillate collection vessel was connected to the argon line (pressure control) and had a sampling socket. The vapour temperature was measured. As later was noticed, the Vigreux column was not efficient enough to purify the toluene to a wanted level and therefore additional distillation with 350 mm packed column (Raschig rings, D_o=6,5 mm, D_i=4 mm, L=7,5 mm) was performed at atmospheric pressure.

4.2.2 Evaporation at 200 mbar

The boiling vessel was batched with 380 g of combined ML and TWE. The oil bath temperature was set to 70 °C. Based on previous experience the boiling point of the lights was approached by reducing the pressure. At 300 mbar the first drops were collected with vapour temperature of 50 °C, the total amount being roughly 5 ml. The pressure was stabilized to 200 ± 4 mbar and the vapour temperature rose to 62 °C, indicating the shift from n-heptane to toluene.

The oil bath temperature was set to 85 °C to collect vapour (65 °C) at a steady rate of 2 drops per second. Instead of a clear shift in vapour temperature (from toluene to $TiCl_4$) the vapour temperature rose steadily from 65 °C to 75 °C. In order to secure steady distillation rate, the oil bath temperature was risen gradually to 105 °C. If the behaviour of the mixture would had been ideal, then the temperature shift from evaporating toluene to evaporating $TiCl_4$ would had been more clear. The evaporation was continued until the rate of distillate decreased to below 1 drop per 3 seconds, without solidification reaction of the bottom product.

4.2.3 Distillation of evaporation overhead at 1 atm

The overhead product of the evaporation experiment was collected and 257 g was fed to the boiling vessel equipped with a Vigreux-rectifying column. The distillation was performed under argon in atmospheric pressure. The oil temperature was set to 130 °C and the first distillate was collected at 97-100 °C (5 ml). The vapour temperature rose to 108 °C, and continued to rise at rate 1 °C/10 min. The largest fraction was collected at 110 – 112 °C. The distillation was continued until 115 °C to ensure sufficient evaporation of toluene (from $TiCl_4$). Overall the distillation took 55 minutes.

The collected distillate had a rose colour, indicating strong presence of $TiCl_4$. The high concentration of $TiCl_4$ was confirmed via ICP-AES analysis to be 20 wt-%. In order to separate $TiCl_4$, the distillate (D1) was treated in a second distillation unit.

150 g of D1 was fed to a boiling flask equipped with a packed (Raschig) column. The oil bath temperature was set to 130 °C and the first vapour was collected at 100 °C, after which the temperature rose to 108 °C. The temperature rose constantly from 108 to 111.5, after which the experiment was finished. The second distillation lasted 65 minutes and the oil bath temperature in the end was 140 °C. Distillation rate was rather constant at 10 drops per 8 seconds. Compared to the first distillation, refluxing was stronger and subsequently lower $TiCl_4$ concentration was observed in the distillate. The yellow-orange distillate (D2) was analysed to compose 4 wt-% $TiCl_4$.

4.2.4 Results

The collected fractions were weighed (Table XI) and the overall mass balances were found to be very accurate, 98,7–99,7 %.

Table XI Overall weighed mass balance of the evaporation and distillation trials. F–feed, O–overhead, B–bottom.

	Evaporation			Distillation 1			Distillation 2		
	Amount	Of feed	Out/In	Amount	Of feed	Out/In	Amount	Of feed	Out/In
	g	%	%	g	%	%	g	%	%
F	379,79			256,90			149,90		
O	293,31	77,2	98,7	196,64	76,5	99,7	82,71	55,2	99,1
B	81,37	21,4		59,40	23,1		65,81	43,9	

Similar analysis methods (ICP-AES, GC, LC) were used as earlier described to analyse concentration the components in each fraction: feed, overhead and bottom. The component weights were calculated by simply multiplying the concentration with the weighed amount. The compositions of each fraction in the trials are given in Table XIII.

Table XIII Compositions of fractions of the evaporation and distillation trials. F–feed, O–overhead, D-distillate, B–bottom; n.a.–not analysed; *negative value resulted from the subtraction of the added toluene amount (added to keep the solids soluble).

		Evaporation			Distillation 1			Distillation 2		
		F	O	B	F	D	B	F	D	B
$TiCl_4$	g	137,6	90,3	31,3	82,1	33,8	59,1	29,9	3,6	19,5
Tialkox.	g	30,6	0,0	22,5	0,0	0,0	0,0	n.a.	n.a.	n.a.
Toluene	g	117,7	164,0	-2,4*	150,3	94,6	11,1	96,3	56,7	36,6
Heptane	g	12,2	25,2	0,0	21,3	19,9	0,1	15,7	14,7	0,0
Octane	g	3,4	4,7	0,1	4,1	2,9	0,9	2,2	0,8	1,3
$MgCl_2$	g	1,9	0,0	1,7	0,0	0,0	0,0	0,0	0,0	0,0
Sum	g	303,4	284,2	53,2	257,8	151,2	71,2	144,1	75,8	57,3
Weighed	g	379,8	293,3	81,4	256,9	196,6	59,4	149,9	82,7	65,8

The titanium tetrachloride balances were quite accurate (Table XIII), 77,3–88,4 % in all trials. However, toluene mass balances were shown to be incorrect. The concentration of titanium haloalkoxides in the evaporation bottom was low, 28 wt-%.

The bottom fraction of the evaporation trial was diluted with toluene in order to keep the Ti-alkoxides soluble. However, the toluene analyses were shown to be corrupted, and subtraction of the added amount from the total toluene amount in the evaporation bottom resulted in a negative value.

The titanium tetrachloride was recovered by 65,6 wt-% via evaporation and was successfully purified as a bottom product in distillation 1. ICP indicated that the distillation 1 bottom was 99,5 wt-% of $TiCl_4$. In contrary, GC indicated toluene and heptane. Based on the measured temperature, their presence in bottom was questionable. The distillate of distillation 1 was explained only by 77 wt-% (sum of component masses versus weighed total amount). Again, the largest source of error was indicated to be toluene. Toluene mass balance in distillation 1 was explained only by 70,3 % (loss of toluene was 44,6g out of 150,3 g). It can therefore be concluded that the toluene analysis results of the evaporation trial and distillation 1 were incorrect.

Toluene was collected as major overhead product of distillation 2. This overhead fraction was used in the toluene washing stage of catalyst preparation to study the effect to the catalyst (Chapter 4.4.1).

4.3 Continuous evaporator

For the purpose of gaining “proof of concept” on the treatment of combined ML and TWE in a continuously operated evaporator, experimental work was performed in co-operation with an external partner. The purpose of performing experiments with a benchtop unit was to ensure fast results on the feasibility of the unit.

4.3.1 Material

Three types of material were used in the experiments: A,B and C. All materials were collected from Porvoo catalyst pilot plant and had minor differences, the most important of them being the storage time, and the second being the content of toluene. Materials B and C were collected approximately 2,5 months prior to the experiments; whereas material A had been collected 18 days prior to the trials. The compositions of the materials are presented in Table XIV.

Table XIV Composition of materials used in the continuous evaporator trials

Component	A wt-%	B wt-%	C wt-%
Toluene	41,4	55,5	61,3
$TiCl_4$	30,8	17,2	21,4
n-Heptane	6,5	4,9	3,8
Ti-haloalkoxides	7,6	5,9	5,9
DOP	1,2	1,2	2,5
$MgCl_2$	0,4	0,3	1,4
Sum	87,8	85,0	96,3

4.3.2 Equipment

The experiments were performed with a bench-scale evaporator, equipped with a vacuum pump and manual pressure and feedrate controls. The experiments were performed under argon atmosphere in water-free conditions. The heating oil temperature was controlled with Julabo SE-6 (stability ±0,01 °C). The vacuum was pumped with Edwards E2M1.5 two-stage oil-sealed rotary vane pump.

4.3.3 Experiments

Before the trials the system was inertised by venting the system three times with nitrogen. As a safety precaution, one flange on the vacuum pipe between the cold trap and the vacuum system was attached loosely (avoiding possibility of forming over-pressure inside the system). One of the three flasks on each side (residue and distillate) was used to collect material from the start-up and intermediate phases. The products of the experiments were then collected to the remaining two vessels. After completion the system was vented with inert gas, and the collected samples were taken off and weighed. The most important operation parameters are the feed rate and the temperature difference between the jacket and the boiling point. Typically the jacket temperature was kept about 40 °C above the boiling point of the light component (toluene). For example, at 0.2 bar the oil temperature was 100 °C (toluene boils at c. 62 °C and $TiCl_4$ at c. 82 °C).

Three programmes were applied at given pressures, 0,2, 0,4 and 1 bar:

1. High recovery – low feedrate at given pressure, modest temperature difference
2. High throughput – high feedrate at given pressure, modest ΔT
3. Extreme – high feedrate, high ΔT

4.3.4 Results

The operation conditions, feedrates and the obtained distillate and residue weights of the performed experiments are given in Table XV. The sum of heavies in the feed was 7,4 – 9,2 wt-% (Table XIV). Taking into account the heavies not included in the analysis (additive ~0,3 wt-%), the total amount of heavies was approximately 10 wt-%. The obtained feed to distillate ratio in the experiments was at minimum 75 %, and at maximum 90 %. Therefore, at best the volatiles were collected seemingly close to 100 % (test 1), although the unit was not laid out to handle highly viscous residues.

Table XV Results of the continuous evaporation experiments; (* 300 ml of B, 200 ml of A)

	Material	Temp °C	Pressure mbar a	Time min	Residual g	Distillate g	R/D g/g	Feedrate g/min	D/F %
1	C	60	220	26	10,4	99,0	0,11	4	90
2	C	80	450	90	34,9	187,5	0,19	2,5	84
3	B	70	240	15	26,6	79,8	0,33	7	75
4	B	80	250	24	43,9	143,3	0,31	8	77
5	B/A*	110	1000	16	12,5	80,4	0,16	6	87
6	B/A*	110	400	14	41,6	133,7	0,31	13	76

The trials 1 and 2 were performed with modest feedrate in order to maximize the yield. The R/D were 0,11 and 0,19 for trials 1 and 2, respectively, and the corresponding feed to distillate ratios (D/F) were 90 and 84 %. In experiment 1 (high recovery) the residue became viscous and hardly flowing due to the very high feed to distillate ratio: the bottom accounted for only 10 wt-% of the feed. Heating the bottom with a heat blower did not enhance flowing. In the case of experiment 2 the recovery rate was lower and therefore the bottom residue (16 wt-% of the feed) was better flowing.

Experiments 3 and 4 led to similar R/D ratios (0,33; resp. 0,31) although the heating oil temperature was increased by 10 °C in experiment 4. The fact that R/D did not change more by the increased heating temperature could be due to a diffusion limitation towards the bottom of the still, i.e. the evaporation rate is limited by the diffusion rate of gases to the surface of the film, not by the heat transfer through the wall.

At ambient pressure and 110 °C thermal oil temperature (experiment 5) the residue turned very viscous and hardly flowing already at 87 wt-% feed to distillate ratio. Lumps of tarry residue were formed which implies that lower pressure and temperature are favourable for the operation of the evaporator.

In the final test run (experiment 6) the feedrate was elevated in order to see if the separation was still effective at shorter contact times (about 1 minute). The residue in experiment 6 was less viscose. Lumps of the residue from experiment 5 were flushed by the residue of experiment 6, and thus the actual amount of residue formed in experiment 6 was less than measured and higher for experiment 6. Hence, the material balances of these two experiments were slightly corrupted.

The experiments are presented in table XVI from the operability point-of-view.

Table XVI Comments on the trials; R–residue, D–overhead/distillate

Trial	Feed material	Temp (°C) / P (mbar)	Description	Comments
1	C	60 / 220	High recovery trial	R viscose, slowly flowing; D colour clean
2	C	80 / 450	High recovery trial	R flowing (80°C might be advantageous)
3	B	70 /240	High-throughput	R ok; D ok
4	B	80 / 250	High-throughput	Temperature increase 70->80 did not result in significant change in operability
5	B/A (3/2)	110 / 1000	Comparison	R very viscose, lumps of sticky R
6	B/A (3/2)	110 / 400	Extreme	R very viscose, yet flowing

In the light of these results, the industrial continuous evaporator should be operated under vacuum. By lowering the pressure and temperature, the formation of tarry residues from titanium haloalkoxides is reduced.

Samples from experiments 1 and 6 (distillate and residue) were analysed. All titanium was assumed to be present either as $TiCl_4$ or Ti-haloalkoxide ($TiCl_3OEHA$). The calculated amount of these components was based on analysis of Ti and 2-ethylhexanol (2-EHA). The molar amount of titanium tetrachloride was calculated by:

$$n_{\mathrm{TiCl4}} = n_{\mathrm{Ti,\,total}} - n_{\mathrm{Ti,\,TiCl3OEHA}} \tag{19}$$

, where $n_{\mathrm{Ti,\,TiCl3OEHA}} = n_{\mathrm{EHA}}$

The material balances based on methods described above are given in Tables XVII (experiment 1) and XVIII (experiment 6). The bottom residual sample of experiment 6 was partly solidified and hence a representative sample could not be taken.

Table XVII Material balance of the trial 1 (P=220 $mbar_a$, T=60 °C, Feed=4 g/min)

FEED	$TiCl_4$	$TiCl_3EHA$	Toluene	DOP	$n\text{-}C_7$	$MgCl_2$	$\Sigma_{calc.}$	$\Sigma_{meas.}$
mol	0,123	0,023	0,728	0,007	0,041	0,016	0,938	
g	23,40	6,43	67,06	2,74	4,16	1,50	105,28	109,4
wt-%	21,4	5,9	61,3	2,5	3,8	1,4	96,2	
RESIDUAL	$TiCl_4$	$TiCl_3EHA$	Toluene	DOP	$n\text{-}C_7$	$MgCl_2$	Σx_i	
mol	0,010	0,016	0	0,003	0,000	0,007	0,037	
g	1,98	4,47	0,00	1,29	0,04	0,63	8,42	10,4
wt-%	19,0	43,0	0	12,5	0,4	6,1	81,0	
DISTILLATE	$TiCl_4$	$TiCl_3EHA$	Toluene	DOP	$n\text{-}C_7$	$MgCl_2$	Σx_i	
mol	0,113	0,000	0,780	0	0,048	0	0,942	
g	21,40	0,09	71,87	0,00	4,85	0,02	98,23	99
wt-%	21,6	0,1	72,6	0	4,9	0	99,2	

Table XVIII Material balance of the trial 6 (P=400 $mbar_a$, T=110 °C, Feed=13 g/min)

FEED	$TiCl_4$	$TiCl_3EHA$	Toluene	DOP	$n\text{-}C_7$	$MgCl_2$	Σ	$\Sigma_{meas.}$
mol	0,209	0,041	0,949	0,000	0,114	0,000	1,313	
g	39,69	11,52	87,40	2,10	11,39	0,56	152,68	175,3
wt-%	22,6	6,6	49,9	1,20	6,5	0,3	85,9	
RESIDUAL	$TiCl_4$	$TiCl_3EHA$	Toluene	DOP	$n\text{-}C_7$	$MgCl_2$	Σx_i	
g								41,6
DISTILLATE	$TiCl_4$	$TiCl_3EHA$	Toluene	DOP	$n\text{-}C_7$	$MgCl_2$	Σx_i	
mol	0,219	0,003	0,881	0	0,081	0	1,184	
g	41,54	0,87	81,16	0,00	8,16	0,02	131,74	133,7
wt-%	26,4	0,7	60,7	0	6,1	0	93,8	

Toluene was recovered by over 93 % (weight, analysed). Titanium tetrachloride was recovered by 91,5 % (molar) in experiment 1 and by 104,6 % in experiment 6. There are two alternative causes for the >100 % yield in experiment 6:

1. The feed material was a combination of material A and B, and the material balance calculation was based on 40/60 (wt-%) mixture of these two. This calculation causes error for the mass balance.
2. It is possible that free $TiCl_4$ was formed during the experiment by the reactions between the titanium haloalkoxides and $MgCl_2$. One of the possible reactions could be a halogenation reaction, as described in patent US6790319 (Mitsui Chemicals Inc 2004). $MgCl_2$ (present in the feed) could, according to the patent, act as a halogenating agent, where R is an alkyl (2-ethylhexyl) via reaction:

$$Ti(OR)Cl_3 + MgCl_2 \longrightarrow TiCl_4 + Mg(OR)Cl \qquad (20)$$

The analysis showed no DOP entrainment in the overhead product and only minor entrainment of titanium haloalkoxides. In case of the latter, it is not certain, however, if the entrained compound was titanium haloalkoxide or free 2-ethylhexanol. The analysis of Ti-haloalkoxide was done by first hydrolysing the sample and then analyzing the amount of 2-ethylhexanol by GC. The boiling point of 2-ethylhexanol is 185 °C at normal pressure, i.e. it would – in case present in the feed – evaporate and end up in the distillate more easily than the Ti-haloalkoxide which is solid at room temperature.

In any case the entrainment was very low: less than 2% of 2-EHA ended up in the distillate in experiment 1. Furthermore, the possibility of entrainment is inherently higher in the bench-scale evaporators, compared to industrial evaporators because of transport distances. Hence, even the minor entrainment can supposedly be reduced, if not even avoided completely, in the large scale unit.

In principle, the volatiles were "easily" separated from the Ti-haloalkoxides without the formation of gel-like tarry residue. The most feasible operation was evaluated at lowered pressures.

From the operability point-of view the best conditions were observed at trial 4: temperature of 80 °C, pressure of 250 mbar and feedrate at 8 g/min. At these conditions 77% of feed was collected as distillate and the residue was well flowing.

4.4 The effect of impure washing liquids to the catalyst

After the catalyst is successfully solidified and the motherliquor removed, the catalyst is washed with hydrocarbons. The washing is performed by two toluene washes followed by two heptane washes, as illustrated in Figure 17. It is of increased environmental and economical concern, that the recovered components can be utilized in all of the washing stages without any harmful side-effects on the catalyst properties performance.

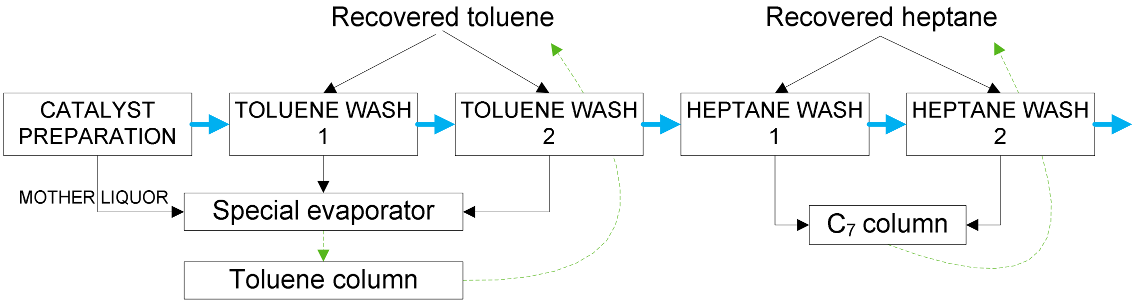

Figure 17 Schematic diagram of the washing and recovery stages

4.4.1 Toluene washing liquid

The distillate from the toluene column is collected to a storage vessel, wherefrom it is designated to be forwarded for use in the toluene washing stages. The primary purpose of the column is to separate $TiCl_4$ as the bottom product and toluene as distillate. However, depending on the configuration of the toluene column (Chapter 4.6.3.1), some impurities (heptane and $TiCl_4$) must be allowed in the recovered toluene stream. The purpose of examining these conditions was to determine how heptane, $TiCl_4$ and possible of thermal decomposition products could affect the catalyst if present in TWL.

4.4.1.1 $TiCl_4$

Purpose of $TiCl_4$ in the synthesis of Ziegler-Natta catalysts is to activate the $MgCl_2$ crystal structure by reacting with the alcohol and coordinating to the activated $MgCl_2$ (Garoff *et al.* 1990). During the catalyst production, excessive amounts of $TiCl_4$ are used to promote the reactions towards the favourable direction. Due to the excess $TiCl_4$, the titanium haloalkoxides are also kept soluble.

Having an additional washing stage with pure $TiCl_4$ between the hydrocarbon washes has been shown to have a positive effect on the catalyst activity. Nevertheless, based on internal (Borealis) studies, the effect of < 10 wt-% of $TiCl_4$ has been shown to have minor or no effect on the catalyst activity or xylene solubles of PP and very minor effect on the PP melt flow rate. (Denifl[5]) According to Denifl, the amounts of titanium tetrachloride present in the recovered toluene stream (≤5 wt-%) should have only minor (if any) positive effect on the catalyst activity and thus can be considered acceptable.

4.4.1.2 Heptane

N-heptane in approximate amounts of <30 wt-% present in the toluene washing stages is considered to have an inconsequential effect on the catalyst activity and polypropylene XS-% or MFR. (Denifl[6]) Thus, heptane is considered inert in this context.

On the other hand the solubility of Ti-haloalkoxides in toluene was found to be over 40-times higher than in heptane (at 20 °C) (Garoff *et al.* 1990). The solubility of Ti(O-2-

---

[5] Peter Denifl (D.Sc., Researcher, Borealis Polymers OY) interviewed by author on April 17 2010.

ethylhexyl)Cl_3 is expected to be comparable to the studied alkoxide. The washout efficiency of Ti-haloalkoxides with toluene is more efficient and hence, if heptane is present in the recovered toluene, larger total flow rate is expectedly required to reach the same washout efficiency as with pure toluene. In addition, n-heptane has a lower boiling point than toluene and can accumulate in the recovery cycle; however this circumstance is considered in more detail in Chapter 4.6 (Optimisation).

4.4.1.3 Decomposition products

As the toluene washes (and motherliquor) undergo thermal processing (evaporation and distillation) the risk of decomposition of Ti-haloalkoxides present. Contrary to $TiCl_4$ and heptane, these decomposition products could have detrimental unfavourable effects on the catalyst if they are recycled back into washing stages. Therefore a study was performed by washing the catalyst with recovered toluene. The toluene recovery is described in Chapter 4.2. For comparison of effects on the catalyst a washing mixture (with identical composition) was prepared from pure $TiCl_4$, toluene and n-heptane.

4.4.1.4 Material

The composition of recovered toluene was analysed in order to prepare a comparative mixture from pure components. The comparative mixture was prepared to be identical in composition to the recovered with the exception that only the three main components were present: toluene, $TiCl_4$ and n-heptane. The composition was normalized so that their relative ratio was identical to the recovered (Table XIX) and rounded for easy measurement (volumetric). The purpose of using the comparative mixture was to reveal whether there are unknown (low-boiling) decomposition products in the recovered toluene that result in differences in catalyst performance.

Table XIX Compositions of materials used in the toluene washing stages of the catalyst synthesis; (* sum of analysed composition)

	Recovered toluene wt-%	Comparative mixture wt-%
$TiCl_4$	4,3	5,0
Toluene	68,5	75,3
n-Heptane	17,8	19,7
Octane	1,01	0
sum	91,7 *	100,00

4.4.1.5 Experimental design, synthesis and polymerisations

For these experiments resources were allocated for two catalyst synthesis and two bench-scale polymerisations. Therefore the experiments were designed simply: recovered toluene was used in the toluene washing step of one catalyst and synthetic mixture in the toluene washing step of the other.

The catalysts were synthesized with a parallel reactor system (Multimax) and polymerized in a bench-scale reactor. In the catalyst synthesis only one toluene washing is used (in laboratory scale – in industrial scale plant there are two toluene washes). The bench-scale polymerisations were performed at 80 °C with 36–37 bar pressure. The activity, melt flow rate (MFR) and xylene solubles were determined.

4.4.2 Heptane washing liquid

The predominant role of the heptane washes is to remove toluene from the end-product. Toluene could hypothetically have detrimental effect on the catalyst. Therefore extensive research was carried out to studying the effect of toluene in HWL.

The purification of heptane washing effluents (HWE) was designed to be performed via distillation. The overhead product, heptane, is thereafter reused in the washing stages of the catalyst manufacturing process. The toluene concentration in the overhead heptane was determined by simulations of the recovery section heptane column to be app. 5,6 wt-%. The purpose of these experiments was to study the effects of impure HWL (6 wt-% toluene added) and the effect of prolonged settling time. The target was to determine whether the design parameters of the heptane column are achievable and that the change in settling time whilst up-scaling has any significant effect on the catalyst polymerisation properties.

4.4.2.1 Response variables

The key response variables and their analysis methods are given in Table XX.

Table XX Key response variables; * conventional; ** alternative

Response variable	Measurement method	Unit	Description
Polymerisation activity of the catalyst	Yield of PP (per used amt of cat) * Propene uptake**	$kg_{PP}/(g_{cat}\ h)$	PP yield measured in a 1 hour standard polymerisation
Average molecular weight of PP	GPC		Chromatographic instrument
Xylene soluble of PP	Gravimetric* FIPA**	%XS (by weight)	Flow injection polymer analysis, gives the content of xylene soluble PP
Isotacticty	FTIR	% (isotactic PP)	Mid-IR Fourier transform spectrometry
Crystallinity, thermal properties	DSC	%, °C	Differential scanning calorimetry, gives the degree of crystallinity of a substance, melt temperature and glass transition temperature

The activity was calculated by dividing PP yield versus the amount of catalyst and reaction time. The uptake is measured by the pressure of the reactor; partial pressure of propene decreases as it reacts to coordinate in the polymer chain. FIPA provides information on the amount of PP soluble in cold xylene (Vestberg[6]). FTIR measures the structural tacticity based on the intensities of the bands. Classical bands are 998 cm^{-1} for isotactic, 868 cm^{-1} for syndiotactic, and 975 cm^{-1} as an internal standard. (Ozzetti *et al.*, 2002)

An indirect measure of the isotacticity can also be acquired via differential scanning calorimetry (DSC). In DSC, the energy absorbed (or produced) is measured by monitoring the difference in energy input into the studied sample and a reference as a function of time. Consequently a measure of the crystallinity of the substance can be acquired. In general, the greater the crystallinity the greater the isotacticity is. Crystallinity correlates positively with the substance stiffness, tensile strength and softening point. (Tripathi, 2002)

4.4.2.2 Design factors

Following each of the washes, the catalyst particles are allowed to settle and the liquid is siphonated away. In order to estimate the scope of change in the toluene concentration of the final product (catalyst) solution a response study was performed. The response study was performed with mass balance calculations via keeping the composition of the solution in the reactor prior to heptane washes constant and then varying the toluene content of the HWL. The toluene content before the heptane washes was 97,9 wt-% . The siphonation efficiency was kept constant at 85 % (by weight).

The removal efficiency, $\eta_{siphonation}$, of siphonation can be given by:

$$\eta_{siphonation} = \left(1 - \left(1 - x_{siphonation}\right)^{N_s}\right) 100\% \tag{21}$$

, where N_s the number of siphonations

$x_{siphonation}$ mass fraction of the siphonated liquid

The toluene fed with the first HWL is removed with removal efficiency of 97,75 % (undergoes two siphonations) and the toluene fed in the second HWL with the removal efficiency of 85 % (by weight). 3 wt-% of toluene in the first HWL and 0 wt-% in second, results in a toluene concentration change of 0,37 wt-% in the final reaction liquid (compared to washing with pure HWL in both washes). 3 wt-% of toluene in both of the washes results in a change of 2,77 wt-%. Therefore it was concluded that the toluene concentration of the second heptane wash is (as expected) determinant for the

---

[6] Torvald Vestberg (D.Sc., Researcher, Borealis Polymers OY) interviewed by author on April 29–28 2010.

toluene content of the remaining reaction liquid. Despite the dominant role of the second heptane wash to the final reactor liquid toluene content, also the first heptane wash toluene content was selected as a design factor.

The settling time in the lab synthesis differs significantly from the commercial-scale catalyst plant. The settling time of the first heptane wash was seen dominant in this case because it has a higher initial toluene concentration compared to the second heptane wash. The settling time of the first heptane wash was selected as a third variable.

4.4.2.3 Design factor levels

The levels of the experimental design are given in Table XXI. The settling time at the commercial-scale plant is 4 hours; however it was impractical to study such long settling times at the lab. Hence, settling time of 120 min was used as the upper level and 15 min as the lower (normal settling time in lab synthesis).

Table XXI Levels of design factors of the catalyst activity study

Factor	Parameter		Low (-)	High (+)
A	Toluene in 1st C_7 wash	wt-%	0	6
B	Toluene in 2nd C_7 wash	wt-%	0	6
C	Settling time of 1st C_7 wash	min	15	120

4.4.2.4 Design of experiments

The experiments were designed as a reduced (modified) three-factor factorial design (Table XXII), with of 8 experiments. A full *k* factor factorial design requires 2^k runs and would have resulted (three factors) in 8 experiments. The error caused by the preparation procedure was, however, expected to be higher than the change in response. Therefore there was stronger need for replicas, than for a full factorial design. Hence, the experimental design was reduced to 4 experiments and replicated once.

Table XXII Experimental design of the catalyst activity study

Run	Treatment combination	A	B	C
1	(1)	-	-	-
2	a	+	-	-
3	ab	+	+	-
4	abc	+	+	+

The modified design was preferred instead of a traditional 2^{3-1} experimental design (Montgomery 2009) for the following reasons:

- Interest in the interaction effect of treatment combination ab
- Factor C is practical to study only at high level of A
- In practise, variable B would never be at high level when A is at low level (first wash the catalyst with pure heptane and then with impure heptane)

- Clear reference point (A,B and C at low factor level) was demanded
- Very low, if any, differences in responses were expected in the first 3 runs
- The target was to determine whether the added toluene in HWL has an effect on the catalyst activity, not to draw conclusions on the strength of effect

4.4.2.5 Catalyst synthesis

The complexity of Ziegler-Natta catalysts reduces the reliability to predict the activity of the catalyst based on information of the catalyst composition. The composition of the catalyst does not describe the detailed chemistry of active sites, and thus does not describe the behaviour of the active sites during polymerisation. Other factors, such as the temperature and residence times at different catalyst preparation stages, and especially the polymerisation conditions (bulk, semi-bulk, temperature, pressure) may have a more major effect on the catalyst polymerisation activity. (Denifl[7])

The 8 catalyst synthesises (with 4 recipes) were performed with Multimax parallel reactor system (Mettler-Toledo). Multimax RB04-50 has 4 parallel reactors; volume of each is 50 ml. recipes. The recipe 1 represented a "standard" catalyst recipe washed twice with pure heptane. The differences in recipes 2-4 compared to the reference are described in Table XXIII.

Table XXIII Overview of catalyst recipes; RMAN--- – Catalyst batch code

Recipe	RMAN---	Description
1	041,042	Reference, clean HWL
2	043,044	1st HWL 6 wt-% toluene, 2nd clean
3	045,046	1st and 2nd HWL 6 wt-% toluene
4	047,048	1st and 2nd HWL 6 wt-% toluene, 1st HWL with 120 min settling

4.4.2.6 Polymerisation with Parallel Pressure Reactor (PPR)

PPR is a 48 reactor system with 6 modules and 8 blocks. The polymerisations were randomized in the following manner: recipes 1-2 (RMAN041-044) in modules 1-3, and recipes 3-4 (RMAN045-048) in modules 4-6. There were 6 replicates (R_i) of each catalyst, which were labelled R_1, R_2, ... R_6 according to their position in the reactor: R_1 and R_2 were found in the left-most module (R_1=A-D, R_2=E-H), R_3 in the second left-most module and so forth.

---

[7] Peter Denifl (D.Sc., Researcher, Borealis Polymers OY) interviewed by author on April 17 2010.

The polymerisations were performed in semi-bulk conditions at 70 °C. The catalyst was slurried in Primoil prior to the polymerisations and mixed with a magnetic stirrer to generate homogeneous slurry. By mixing the slurry the morphology of the catalyst was sacrificed in order to achieve incorrupt catalyst concentration and subsequently reliable results. All of the catalysts were stirred prior to polymerisation and therefore the effect was equivalent for each.

In order to compare the results, and whether there was any statistically significant difference between the samples (or recipes), a two-sided *t*-test was performed. Tukey's test is similar; however *t*-test is more convenient as the mean values of recipes 2,3 and 4 are compared only against recipe 1 (reference). The comparison was made by the two-sample *t*-test with the assumptions:

H_0: $\mu_1 = \mu_2$ (avg. MW identical / activities identical)
H_1: $\mu_1 \neq \mu_2$ (avg. MW different / activities different)

If $|t_{\text{calculated}}| > t_{\alpha/2,\, n1+n2-2}$, then H_0 is rejected and it can be concluded that the average MW (or activity) of the compared samples differ. α/2 is the upper percentage point in distribution with n_1+n_2-2 degrees of freedom. The two sample *t*-value was solved from:

$$t_0 = \frac{\bar{y}_1 - \bar{y}_2}{S_p\sqrt{\frac{1}{n_1}+\frac{1}{n_2}}} \tag{22}$$

, where $\bar{y}_i$ is the sample i mean, n_i the size of sample i, and $S_p = \sqrt{S_p^2}$. The estimate of the common variance is calculated from:

$$S_p^2 = \frac{(n_1-1)S_1^2+(n_2-1)S_2^2}{n_1+n_2-2} \tag{23}$$

, where S_i are the individual sample variances

4.4.2.7 Bench-scale polymerisations

The polymerisations were performed at 80°C and 36–37 bar (5,09 bar, 70 mmol H_2). The Al/Ti was 250 and Al/D (donor) was 10. The reaction time for 1,4 kg of propylene was 60 min with mixing at 450 rpm.

4.4.3 Results

The effects of impurities in TWL and HWL (to the catalyst) were studied separately: their interaction effect was seen less important.

4.4.3.1 The effect of impure TWL to the catalyst

Compositions of the washing liquids used in the catalyst synthesis are given in Table XIX. The resulting catalyst composition is given in Table XXIV. Washing the catalyst with recovered toluene increased the Mg-content of the catalyst slightly, but also the mean particle size (from 33,1 µm to 36,7 µm). The increment in size is, however, diminutive and within specifications (Denifl[8]). The results of the bench polymerisations are presented in Table XXV.

Table XXIV Compositions of the catalysts prepared with recovered and comparative toluene washing mixtures (Cat. Batches RMAN077 and 078) and specifications for the catalyst (* indicative)

		Recovered toluene	Comparative mixture	Specification Min	Target	Max
Ti	wt-%	4,05	4,04	2	3	4
Mg	wt-%	14,1	12,7		12,5 *	
Al	wt-%	0,31	0,31			
DOP	wt-%	33,2	33,5	26	31	36
Coulter size, mode	µm	38	34,6			
Coulter size, mean	µm	36,7	33,1			
Coulter, 10%	µm	24,9	20,3			
d_{50}, Coulter, 50%	µm	36,7	34,1	30	35	45
Coulter, 90%	µm	50,7	46			

Table XXV Results of bench-scale polymerisation of the catalyst prepared with recovered toluene and comparative toluene washing mixture (Polym. Batches ALHB187 and 189). Weight introduced to the piston in MFR was 2,16 kg

		Recovered toluene	Comparative mixture
Activity	$kg_{PP}/(g_{cat}$ h)	35,5	34,5
MFR (2,16)	g/10min	4,74	5,49
XS	%	1,1	1,4

According to the studies, the activity was not reduced due to hypothetical decomposition (or other light unknown) products in the recovered toluene. In fact, comparing the results of recovered toluene catalyst versus the comparative mixture catalyst, the activity was a bit higher: 35,5 $kg_{PP}/(g_{cat}$ h) and 34,5 $kg_{PP}/(g_{cat}$ h), respectively. The melt flow rate (MFR 2,6) and xylene solubles (XS) were a little lower: 4,74 g/10min and 1,1 % for recovered, 5,49 g/10min and 1,4% for comparative mixture.

Images of the catalysts were taken with Scanning Electron Microscope (SEM). SEM images are given in Appendix B, and revealed only minor changes in the catalyst morphologies. The catalyst washed with recovered toluene had fines attached to the particles. However, the particles were compact, spherical, and uniform in size.

---

[8] Peter Denifl (D.Sc., Researcher, Borealis Polymers OY) interviewed by author in June 2010.

Overall, the differences in catalyst polymerisation properties (Table XXV) were minor, and the results do not allow further conclusions on the effects (Leinonen[9]). Therefore it is safe to conclude that the toluene can be recovered and reused in the washing stages at the studied conditions without apparent harmful side-effects.

4.4.3.2 The effect of impure HWL to the catalyst

The toluene (6wt-%) in heptane washing liquid had practically no effect on the catalyst composition (Table XXVI) – not even with prolonged settling time (recipe 4). The composition and sizes are within specifications (given in Table XXIV).

Table XXVI Results of the catalyst synthesis

Batch code	Recipe	Ti %	Mg %	DOP %	Coulter, mean size µm	Coulter, d_{50} µm	Yield g
RMAN041	1	3,68	12,8	33,1	38,8	37,8	1,5
RMAN042		3,63	12,0	33,0	37,1	36,7	1,7
RMAN043	2	3,81	12,4	34,8	37,9	35,8	1,5
RMAN044		3,78	12,5	34,2	39,0	38,5	1,3
RMAN045	3	3,41	13,2	34,1	33,9	34,3	1,4
RMAN046		3,54	12,7	33,9	34,6	34,5	1,3
RMAN047	4	3,64	14,2	34,3	37,3	37,5	1,4
RMAN048		3,77	13,1	33,0	41,2	41,4	1,6

Comparison of the Coulter mean sizes between the synthesized catalysts enables quick inspection – however for more in-depth analysis the size distribution is a requisite. The Coulter particle size distribution by differential volume of catalysts RMAN041-RMAN048 is given in Appendix C. The size distributions were found to be generally identical. It should be however noticed that comparison of the (by weight or volume) 50 % cumulative size, d_{50}, is generally applied and adequate.

The catalyst SEM images are presented in Appendix D. Minor imperfections in the morphologies of catalysts RMAN043 and RMAN045 were revealed.

There were ellipsoid catalyst particles in RMAN043; however if it was due to the toluene content then ellipsoid particles would be present in RMAN044 as well (same recipe). Hence the RMAN044 particles were spherical, it can be concluded that the imperfections in RMAN043 were not due to the toluene content in HWL.

According to Denifl[10], the most likely explanation for elliptic shape (RMAN043) is a change in droplet viscosity during the solidification of catalyst. As a result of slightly

---

[9] Timo Leinonen (M.Sc., Researcher, Borealis Polymers Oy) interviewed by the author on June 3rd 2010.

[10] Peter Denifl (D.Sc., Researcher, Borealis Polymers OY) interviewed by author on June 8 2010.

reduced solidification rate and turbulent mixing the still solidifying catalyst is stretched and retains the elongated shape after solidification. A change in the bulk viscosity does not expectedly result in a change in the catalyst density and hence is not the cause for ellipsoid shape; however, it may affect the particle size.

Agglomerates in RMAN045 are unlikely due to increased toluene content, because RMAN046 shows no similar behaviour of particle agglomerations (same recipe). The agglomerates in RMAN045 are loosely bounded and most probably the particles would be separated under mixing.

If the 6 wt-% toluene content in HWL would affect the catalyst morphology (or other properties) the strongest impact would be observed by comparing catalyst produced with recipe 4 against the reference. The recipe 4 catalyst was washed twice with impure heptane and in addition the settling time (catalyst contact time with the HWL) was expanded from 15 to 120 minutes. However, as can be observed by comparing images of RMAN047 and 48 against RMAN041 and 42, no clear effect on the catalyst morphology was observed.

After successful synthesis the PPR polymerisations were performed. Two outliers were identified and removed from the data. The first outlier (RMAN044 R_5) was due to a possible hydrogen leakage, which resulted in excess propane uptake, and subsequently to very high average molecular weight (442 028 compared to overall mean, 192 789). The second outlier (RMAN045 R_3) was a result of interruption in the propene uptake The uptake curve (Figure 18, y-axis) should be linear against the quench time (x-axis).

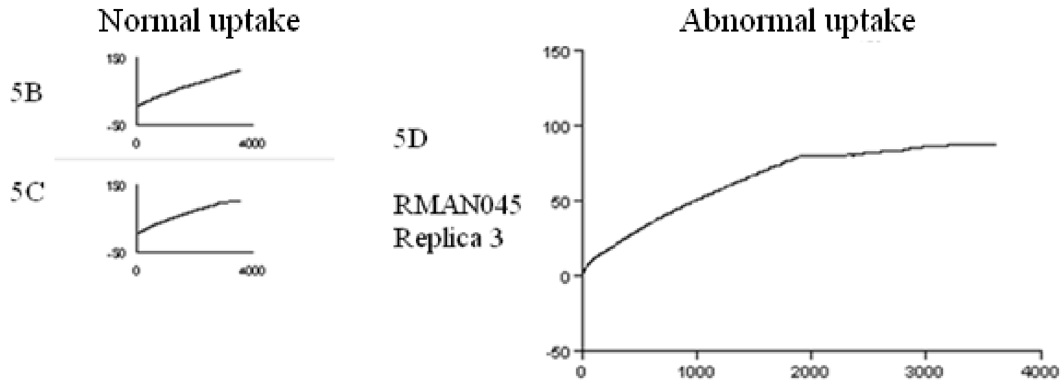

Figure 18 Propene uptake (psi) and quench time (0-3600 seconds) for three polymerisations performed in PPR at 80 °C and 10 bar a. 5B: RMAN047 R_3, 5C: RMAN046 R_3, 5D: RMAN045 R_3

As given in Table XXVII, the avg. MW of the recipe 4 (mean of polymerisations of catalysts RMAN047-48), compared to recipe 1 was statistically significantly lower ($t<t_{statustic}$). The deviation from the reference was negative for all test samples, thus possibly indicating a trend of change in average molecular weight (due to increased

toluene content in HWL). The number average molecular weight, M_n, and M_w/M_n are presented in Appendix E.

Table XXVII Average molecular weights, M_w, of the catalysts polymerized in PPR. The statistic *t*-value was $t_{0.025,22}$=2,074 (α=0.05, N=24, dF=24-2=22). Outliers (RMAN044 R_5 and RMAN045 R_3) were removed. R_i–ith replica.

RMAN 0--	R_1	R_2	R_3	R_4	R_5	R_6	Mean (replicates)	Mean (same recipes)	Std dev	*t*-value
	k	k	k	k	k	k	k	1000	%	
41	172,5	207,4	200,5	225,7	201,7	195,3	200,5	201	8	
42	209,0	178,9	202,5	223,8	186,9	209,0	201,7			
43	187,3	186,5	229,3	180,6	181,3	205,4	195,1	191	9	-1,42
44	188,6	163,8	176,1	207,8	0,0	198,4	187,0			
45	199,9	210,8	0,0	197,1	193,1	191,5	198,5	193	5	-1,45
46	199,1	190,8	177,6	190,7	179,9	187,9	187,7			
47	166,6	199,2	196,9	199,3	171,2	189,2	187,1	186	7	-2,56
48	187,7	196,2	171,8	197,1	187,1	169,1	184,8			

The t-test method requires the samples to be drawn from independent, normally distributed populations, or from populations with equal variances. (Montgomery 2009) The normality assumption was verified from normal probability plots (Appendix F).

The activity was calculated by dividing the yield (g_{PP}) by the amount of catalyst ($g_{catalyst}$) and reaction time (1 hour).A two-sided *t*-test was performed to compare the sample (recipe) mean activities against the reference (Table XXVIII).

Table XXVIII Activities of the catalysts polymerized in PPR. The statistic *t*-value was $t_{0.025,22}$=2,074 (α=0.05, N=24, dF=24-2=22). Outliers (RMAN044 R_5 and RMAN045 R_3) were removed. R_i–ith replica.

	R_1	R_2	R_3	R_4	R_5	R_6	Mean (replicates)	Mean (same recipes)	Std dev.	*t*-value
	kg_{PP} / (g_{cat} h)								%	
41	1,11	0,98	1,65	1,34	1,28	1,06	1,24	1,13	19	
42	0,86	0,96	1,12	1,10	1,19	0,94	1,03			
43	0,90	1,12	1,04	1,22	1,23	0,86	1,06	0,99	15	-1,79
44	0,82	0,86	1,09	0,98		0,87	0,92			
45	1,42	1,35		1,07	1,04	0,99	1,17	1,23	13	1,25
46	1,47	1,22	1,30	1,35	1,13	1,28	1,29			
47	1,33	1,37	1,21	1,30	1,16	1,14	1,25	1,20	11	0,92
48	1,27	1,20	1,30	1,17	0,96	0,99	1,15			

According to *t*-test, the activities do not differ significantly ($t_{\text{calculated}} < t_{0.025,22}$) and hencee H_0 can not be rejected. Therefore it can be concluded that the increase by 6 wt-% toluene in HWL does not (statistically significantly) affect the activity of the catalyst even with prolonged settling time.

In order to acquire more information on the possible causes of the “trend” of lowered avg. MW, DSC measurement was performed. Due to the large number of samples (48-2 outliers= 46) three replicas of each catalyst were selected for analysis. The replicas with the lowest avg MW, the highest avg MW, and also the replica closest to the mean value were selected among each polymerized catalyst. The results are given in Appendix G.

The standard deviation of Cr was low for each polymerized catalyst (0-3,8 %), except for RMAN042 (6,8 %). The standard deviation was between 0-1,4 % for T_m and 0,2-1,4 % T_c. Thus, no clear evidence of reduced isotacticity was shown.

Flow injection polymer analysis, FIPA, reveals information on the amorphous content of PP, and should correlate with crystallinity, as the XS-% that is acquired is a measure of low-chain-length polymer. FIPA requires – compared to yields acquired via PPR, ~0,2 g per reactor – large amount of sample. Therefore the polymerisations of each catalyst recipe were combined, mixed and analysed. Of the same samples also the FTIR (Fourier transform infra-red) analysis was performed. Analysis results of FIPA and FTIR are given in Table XXIX.

Table XXIX Isotacticity (FTIR) and xylene solubles XS (FIPA) of the products (PP) of PPR polymerisations. The products of same recipes were combined for analysis.

Recipe	Catalyst	XS FIPA %	Isotacticity FTIR wt-%
1	RMAN041, 042	2,0	95,1
2	RMAN043, 044	2,5	95,3
3	RMAN045, 046	2,9	95,5
4	RMAN047, 048	4,0	95,3

Isotactic centres have a tendency to result in higher activities. There was no significant change in catalyst activity (Table XXVIII) between the samples and from this perspective the isotacticities (Table XXIX) were consistent: no significant difference was observed. Isotacticity is correlated with polymer crystalline content (measured with DSC, Appendix G), and also these results were in analogy: no trend of change was observed.

However, the XS% measured with FIPA was alarmingly high and showed an increasing trend towards the “more impure” recipes 3 and 4. Because FTIR results (Table XXIX) are correlated with XS and no change was observed, it was assumed that the FIPA analysis was not reliable.

In order to conclude whether the FIPA results were incorrect, catalyst of recipe 4 (RMAN047) and a reference catalyst (RMAN041) were polymerized in a bench reactor. Compared to PPR, bench-scale polymerisation results in higher yields and higher productivity because of different reaction conditions: PPR polymerisations were performed in slurry, whereas bench polymerisation in bulk. Also, polymerisations in smaller scale (PPR) are more sensitive to catalyst poisoning. Via larger yields (larger sample size), alternative XS-measurement method, gravimetric measurement, can be performed. In addition to XS-%, the melt flow rate of the bench-scale PP was measured. The results of bench polymerisation of RMAN041 and 047 are given in Table XXX.

Table XXX Bench polymerisations of the catalysts prepared with recipes 1 and 4 (clean reference and the most impure TWL with long contact time). (Polym. Batches ALHB166 and 167). Weight introduced to the piston in MFR was 2,16 kg

Catalyst	Activity kgPP/gcat	MFR (2,16) 2,16	XS (%) gravimetric %
RMAN041	40,14	5,9	1,2
RMAN047	38,32	5,8	1,3

Via MFR, also the avg. M_w of the recipes 1 and 4 was confirmed. MFR correlates negatively with molecular weight: high melt flow rate corresponds to low average molecular weight. Thus, would there be a significant decrease in PP average molecular weight due to impure HWL (as PPR results suggested, Table XXVII) an increase in MFR be have been observed. However, as given in Table XXX, the MFR of RMAN047 was comparable to the reference RMAN041; the difference in MFR was diminishingly low.

The gravimetrically analysed xylene solubles of bench scale polymerisations for RMAN047 and RMAN041 were different from the FIPA results of PPR polymerisations. The increase in gravimetric XS was unsubstantial.

Overall, no strong indication that the studied conditions (6 wt-% of toluene in HWL) would harm the catalyst was identified. Thus it can be concluded that heptane can be recovered and reused in the washing stages at the studied conditions without clearly damaging the catalyst.

4.5 Vapour-liquid equilibrium

For achieving accurate data professional equipment and resources are required. Hence, co-operation with Aalto University was established for isobaric and isothermal VLE measurements of toluene+$TiCl_4$ and n-heptane+$TiCl_4$. From the data (x, T, P.) the required parameters for describing phase equilibrium can be extracted. Also the vapour pressure of titanium tetrachloride was measured.

4.5.1 Material

The materials used were pure, untreated chemicals of synthesis quality. The chemicals used were titanium tetrachloride (Millenium Chemicals), n-heptane (DHC Solvent Chemi) and toluene (Aspo Chemicals).

4.5.2 Equipment

In apparatus of Yerazunis *et al.* (1964) type (Figure 19) the boiling liquid is forced via Cottrell pump to the equilibrium cell, in which the phases set into equilibrium. The equilibrium is ensured by packing, (traditionally stainless steel wire mesh packing) (Raal and Ramjugernath, 2005). Sampling of the liquid-phase composition was performed in situ via density measurement (Anton Paar GmbH, DMA 512P). Vapour phase was not recycled through the density meter for the economy of effort. Recycling the sample through the density measurement apparatus changes the dynamics of the system and increases the time to reach steady state. Reaching equilibrium took 30 minutes, whereas stabilized conditions are normally reached in 15–20 minutes (Pokki[11]).

In order to ensure thermodynamic consistency (Raal and Ramjugernath 2005), the experiments were performed with very high accuracy. The experiments were performed under argon atmosphere in water-free conditions.

A precision thermometer (ASL F200) with a PT 100 temperature sensor was used for monitoring the temperature of the system. The pressure was monitored with a pressure transducer. The accuracy of temperature measurement was ±0,005 °C and pressure ±0,05 kPa.. The density measurement apparatus was calibrated for the mixtures at 15–25 °C.

---

[11] Juha-Pekka Pokki (D.Sc (eng.), Teaching researcher, Aalto-University School of Science and Technology) interviewed by the author on June 11th 2010.

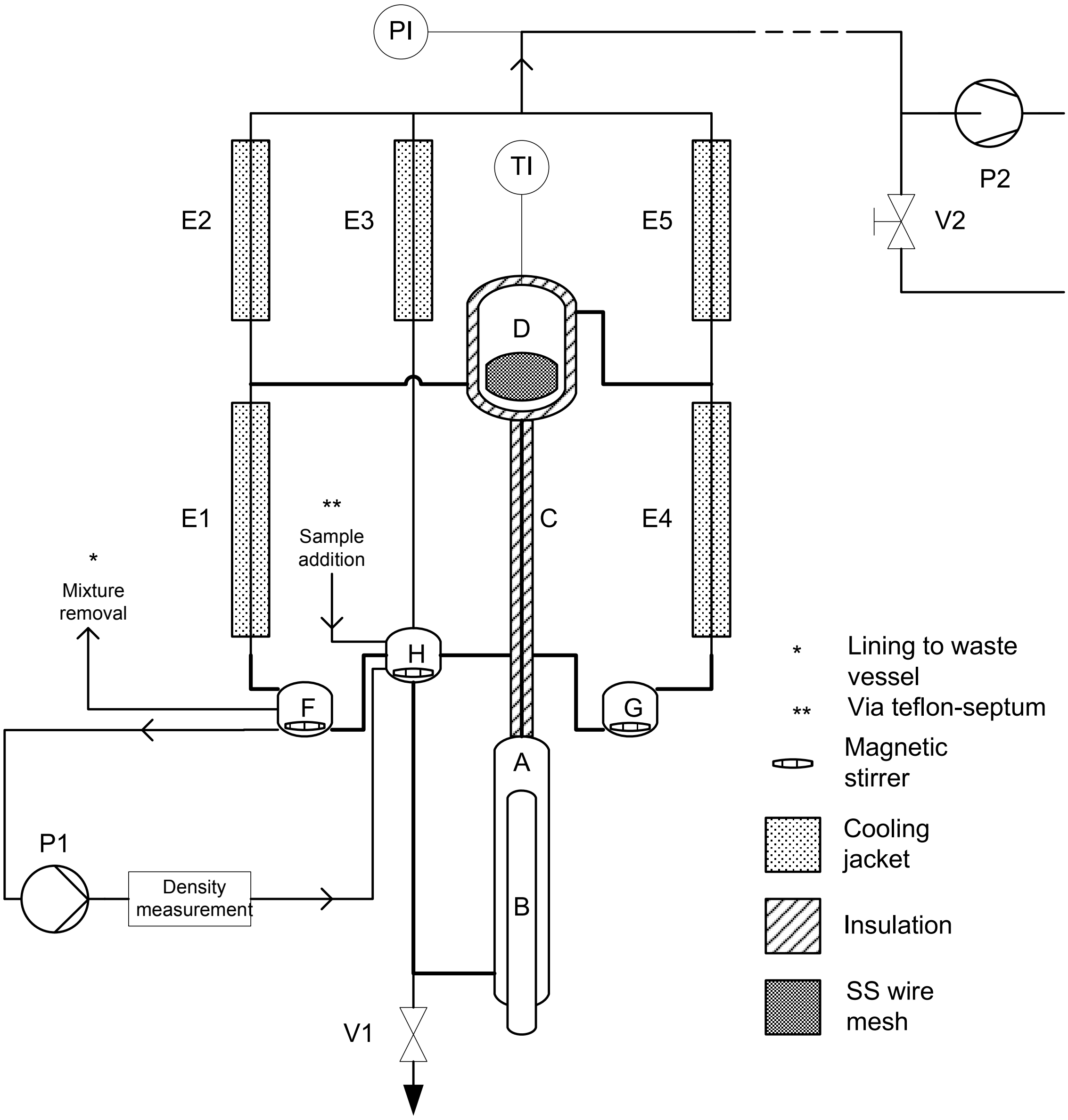

Figure 19 Modified Yerazunis *et al.* (1964) dynamic VLE still used in the measurements. A: reboiler, B: heating element, C: Cottrell tube, D: equilibrium chamber, E1-E5: water-cooled (10 °C) condensers, F: liquid-phase sample cell, G: vapour-phase sample cell, H: mixing chamber, P1: liquid sample circulation pump, P2: vacuum pump, V1: discharge valve (operated at shut-down), V2: pressure control valve. The temperature was measured with PT 100 temperature sensor and the pressure with a probe-type sensor. A liquid nitrogen trap was installed between the equipment and two 30 litre stabilizing tanks. The vacuum pump was attached to these tanks.

4.5.3 Measurements

The vapour phase composition was calculated based on the measured parameters (x, T, P). In accordance to the thermodynamic equilibrium of vapour and liquid phases ($y_iP = x_i\gamma_iP_i^0$), there are only two independent variables: activity coefficient and vapour phase composition. The parameter optimisation includes the Antoine correlation, which provides the information of pure component vapour pressure. The calculated pure component vapour pressure was compared against the measured pure component vapour pressures measured during start of the mixture experiments and vice versa.

The vapour phase composition was solved together with the optimisation of the activity coefficient parameters. The activity coefficients are dependent on both liquid mole fractions and temperature ($\gamma_i = f(x_i, x_j, T)$), and the actual activity coefficient model can be UNIQUAC, NRTL, Wilson etc. (any from Table VII). The Wilson activity coefficient model was used.

4.5.3.1 Calibration of the density measurement apparatus

The meter was first calibrated with pure deionised water and then with air. The system was flushed with toluene to remove all excess moisture and thereafter the readings of pure components and their gravimetric samples of a known composition (20, 60, 80 mol-%) were used for calibrating the density correlations. All measurements were performed in temperatures 15, 17, 20, 22 and 25 °C. The densities were compared with literature by Tret'yakova and Nisel'son (1967) for $TiCl_4$ and TRC Thermodynamic Tables for n-heptane and toluene.

4.5.3.2 Vapor pressure of titanium tetrachloride

The vapour pressure was measured with the described system. The measurement procedure was as follows:

1. Inertising the system via flushing the equipment and pressure stabilizing vessels with nitrogen.
2. Condenser water circulation on, T_{cw}=10 °C.
3. Feeding the system with pure compound, app. 80 ml.
4. Mixers on (liquid and vapour side collector cells and their mixing chamber), heater on, heat up to boiling at atmospheric pressure.
5. Let the system stabilize, *id est* reach steady state boiling conditions, takes ca. 15–20 min.
6. Measure temperature and pressure.
7. Lower the pressure and repeat steps 5-6 until 150 mbar, total 10 points.

Antoine equation coefficients were solved and compared against literature (NIST 2010).

4.5.3.3 Isobaric measurements at 1 atm

$Toluene+TiCl_4$ and $heptane+TiCl_4$ pairs were measured. The procedure was following:

1. Flushing the density meter, liquid sample circulation pump and connecting lines with toluene or heptane, depending on which pair was measured. By this way, free air and moisture was removed from this part of setup.
2. Inertising the system via flushing with nitrogen.
3. Condenser water circulation on, T_{cw}=10 °C.
4. Feeding the system with pure titanium tetrachloride, app. 80 ml (the first VLE pair, $toluene+TiCl_4$ was measured right after the vapour pressure measurements and therefore the system was not emptied in between).
5. Liquid sample circulation pump, mixers and heating on. Hydrocarbon holdup of circulation line, app. 5 ml of toluene, was thus fed to the system
6. Bring the solution up to boiling point at 1 atm (constant)
7. Let the mixture reach equilibrium at stabilized conditions at constant pressure, takes ca. 30 min. Sample circulation rate 2 drops/s.
8. Measure the boiling temperature, pressure and liquid-phase composition.
9. Remove mixture from the liquid collector cell via the waste line.
10. Add pure hydrocarbon to the system according to the target concentration.
11. Repeat steps 7–10 until $x_{Toluene}>0,8$, total 9 points for $toluene+TiCl_4$ pair and 10 for $heptane+TiCl_4$ pair

4.5.3.4 Isothermal measurements at 105 °C

Setup was similar to the equipment in isobaric measurements. The procedure of $toluene+TiCl_4$ isothermal measurements was as follows:

1. Flushing the density meter, liquid sample circulation pump and connecting lines with toluene. Connecting the lines to the VLE apparatus.
2. Inertising the system via flushing with nitrogen.
3. Condenser water circulation on, T_{cw}=10 °C.
4. Feeding the system with pure titanium tetrachloride, app. 80 ml
5. Liquid sample circulation pump, mixers and heating on. Hydrocarbon holdup of circulation line, app. 5 ml of HC, was thus fed to the system
6. Bring the solution up to boiling point at 1 atm (constant)
7. Pressure was gradually lowered to 450 mbar and then down to 414 mbar to have stable boiling conditions at 105 °C
8. Let the mixture reach equilibrium at stabilized conditions at constant temperature, takes ca. 30 min. Sample circulation rate 2 drops/s.
9. Measure the boiling temperature, pressure and liquid-phase composition.
10. Remove mixture from the liquid collector cell via the waste line.
11. Add pure hydrocarbon to the system according to the target concentration.
12. Adjust (increase) pressure to have steady state conditions at T=105 °C
13. Repeat steps 8–12 until $x_{Toluene}>0,8$, total 9 points

4.5.4 Results

4.5.4.1 $TiCl_4$ liquid vapour pressure

The measured vapour pressures were shown to be in good agreement with the literature. The Antoine equation (24) parameters for the given substances are presented in table XXXI. The vapour pressure was plotted with the Antoine parameters (Figure 20).

$$\ln P = A - \frac{B}{C+T} \tag{24}$$

, where A, B and C are Antoine equation parameters

Table XXXI Antoine parameters of titanium tetrachloride for temperature range 294,45–409,15 K. Temperature is given in K and pressure in MPa; * Values given for logarithm of base 10, temperature in K (249,93–409 K) and pressure in bar (NIST 2010)

	A	B	C
Experimental	8,79807	4534,5147	-
Literature *	4,84969	1990,235	2,0

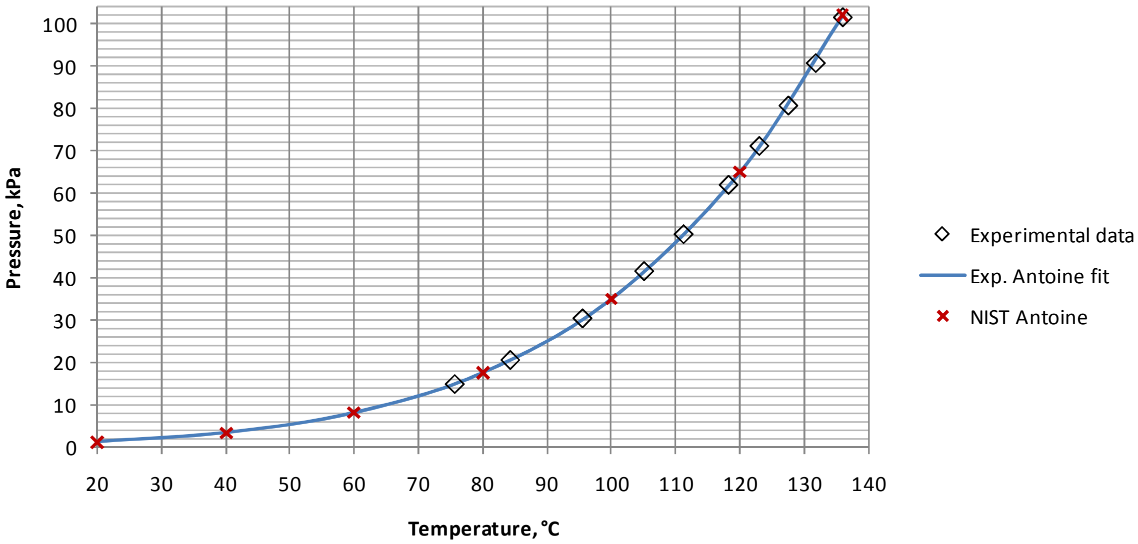

Figure 20 Vapour pressure experimental data and fitted Antoine equation curves of titanium tetrachloride (experimental and literature (NIST 2010))

4.5.4.2 Vapor-liquid equilibriums

The full data of measurements is given in the report by Räsänen and Lylykangas (internal Borealis report, confidential). The vapour-phase composition was calculated with ideal gas assumption. The toluene+$TiCl_4$ isobaric and isothermal VLEs were compared with Aspen ideally predicted VLEs. The VLEs did not deviate strongly.

4.5.4.3 Binary liquid-phase activity coefficients and Wilson parameters

The regressed parameters for Wilson/ideal gas property method are given in report by Räsänen and Lylykangas (internal Borealis report, confidential).

Table XXXII Regression results summary

Binary Pair	Toluene+$TiCl_4$	Heptane+$TiCl_4$
Objective function	Maximum-likelihood	Maximum-likelihood
Algorithm	New Britt-Luecke	New Britt-Luecke
Initialization method	Deming	Deming
Weighted sum of squares	412,095225	140,114273
Residual root mean square error	4,9235044	4,18500706

The binary mixture of toluene and $TiCl_4$, the molecule interaction does not consider H-bonds. Therefore, in accordance to literature (Seader and Henley, 2006), the deviation from Raoult's law is always positive if not ideal, and in our case positive. Because the slopes of activity coefficient increase towards smaller concentrations the mixture is non-ideal and deviates positively. The deviation is rather small (ideal activity coefficient equals one); however, the ideal-liquid solution assumption is invalid. The nonidealities can be corrected in Aspen by using Wilson property method and giving the binary mixture the regressed Wilson coefficients.

4.5.4.4 Evaluation of regression

All regression data was tested for consistency with the area test. Point test compares experimental vapour composition against calculated, and was not performed because the experimental vapour-phase composition was calculated based on the other measured variables (x, T, P). The toluene+$TiCl_4$ VLE was performed both at constant pressure and temperature in order to satisfy the requirement of high thermodynamic consistency (Raal and Ramjugernath 2005). The results of the area test are given in Table XXXIII.

Table XXXIII Results of the consistency test

Data set	Type	Test method	Tolerance	Value
Toluene+$TiCl_4$	IB+IT	Area	10 %	-11,23 %
n-heptane+$TiCl_4$	IB	Area	10 %	-12,95 %

Whereas the test methods for thermodynamic consistency are necessary for data evaluation, the results should still be reviewed with caution. Sometimes thermodynamically inconsistent data can pass the area test, and therefore it was appreciated that the regression was performed both with VLEfit and Aspen Plus. The regression results of VLEfit and Aspen were analogous and the VLE curves plotted with the regressed binary activity coefficients fitted well with the experimental values.

The toluene+$TiCl_4$ pair converged without errors, but failed to fit within the boundaries of area test (± 10 %): the value for area test was -11,23 %. Heptane+$TiCl_4$ VLE data regression converged without errors also outside the area test limits: the value for the area test was -12,95%. The data was not, however far from fitting within the test limits, and also from this point-of view it can also be considered more accurate than the standard state (ideal liquid and vapour phase) assumption.

4.6 Optimisation of the recovery section

In this chapter the methods of developing the recovery section to its optimal operation are discussed. The recovery section was optimised in respect to the experimental results acquired through this thesis. Variable cost was calculated for different optimised setups.

The recovery section was before the thesis modelled with NRTL property method, which did not include the binary liquid-phase activity coefficients for heptane+toluene binary pair. In result, the recovery was inaccurately modelled – especially the heptane column. Wilson property method, which includes these binary coefficients, was used in all simulations in combination with ideal gas EOS.

The experimental Antoine parameters (Table XXXI) for $TiCl_4$ vapour pressure were used. The binary liquid-phase nonidealities of toluene+$TiCl_4$ and heptane+$TiCl_4$ were corrected with the regressed Wilson coefficients.

4.6.1 Simulation in Aspen Plus 7.1

The design was to be optimised in respect to the material balances. In order to model the recovery section, the simulation had to incorporate also the washing stages. The washing stages are batch-wise (1 batch/x h) and separation processes continuous (units in kg/h); hence the material-flows on the batch side were multiplied to be x-times larger than on the continuous side. No thermal operations were on the batch-side, and thus the energy balance was not corrupted. The total amount of TWL was specified to be 1700 kg/100$kg_{catalyst}$. The TWL was divided into two washing stages 50:50 (weight). The amount of HWL was similarly 1700 kg/100$kg_{catalyst}$, divided into two washing stages 50:50. The other parameters defined in the simulation are given in Table XXXIV.

4.6.1.1 Importing updated physical property data

The experimental vapour pressure (Table XXXI) and binary Wilson were imported to the simulations. The pure vapour pressure (Antoine equation) was updated by giving new parameter values to function PLXANT (Data browser – Properties – Parameters – Pure component – PLXANT). The temperature and property units were changed to K and MPa. The Wilson parameters were given via Data browser – Properties – Parameters – Binary Interaction – WILSON.

Table XXXIV Unit ID's and parameters; *hours/batch

Block ID	Description	Parameters
a	ML syphonation	Siphonation efficiency 85 wt. %
b,c	Toluene wash stages	Siphonation efficiency 85 wt. %
d,e	Heptane wash stages	Siphonation efficiency 85 wt. %
f	Continuous evaporator	Pressure 300 mbar
g	Toluene column	Pressure 1 bar, 22 ideal stages
h	Heptane column	Pressure 1bar, 22 / 34 ideal stages
i / j	Stream multiplier / splitter	Multiply by x* / Divide by x*
C1-C7	Coolers, Toutlet=20 °C	Utility: water
CG, CH	Condensers	Total or partial (case C) water
H1, H2	Preheaters	Heat up to boiling point, steam
HG, HH	Reboilers	Utility: steam

4.6.1.2 Design variables and constraints

The common design specifications (Table XXXV) were based on the experimental results. The studied compositions of TWL and HWL had no significant effect on the catalyst polymerisation properties and thus were set as specifications. The effect of impurities in recovered $TiCl_4$ was not studied and therefore the specification for $TiCl_4$ purity (in toluene column bottom stream) was set to moderately high value, 99,5 wt-%.

Table XXXV Common design specifications; *for 34-stage column

Block	Parameter	Value	
TWL	Mass flow per washing stage	850	$kg/100kg_{catalyst}$
	Toluene	≥80	wt-%
	Heptane	≤15	wt-%
	$TiCl_4$	≤5	wt-%
HWL	Mass flow per washing stage	850	$kg/100kg_{catalyst}$
	Heptane	≥94	wt-%
	Toluene	≤6	wt-%
Evaporator	$TiCl_4$ recovery	≥90	wt-%
	Bottom Ti-alkoxide concentration	60	wt-%
Toluene column	Bottom $TiCl_4$ concentration	≥99,5	wt-%
	Feedstage = $(N_{stages}/2)-1$	10	
Heptane column	Feedstage = $(N_{stages}/2)-1$	10 and 16*	

4.6.1.3 Utilities

Steam was selected as the heating medium and conventional water as the coolant. Steam and cooling water properties used as utilities are given in Table XXXVI. The properties for steam were selected from the 8 bar steam and cooling water from 15 °C water. The temperature approach of cooling water was set to 5 K.

Table XXXVI Thermal properties and costs of utilities (Engineeringtoolbox 2010a and 2010b); * mainly power costs

	Temperature °C	Density kg/m3	Heat of evaporation kJ/kg	Specific Heat kJ/kgK	ΔT K	Price €/ton
Cooling water	15	999,2		4,186	5	0,0313*
8bar steam	170,4	4,16	2047			15

4.6.2 Evaporator design and results

The evaporation unit was modelled as a one-stage evaporator – a flash unit – and was specified to concentrate the Ti-haloalkoxides to 60 wt-% in the bottom stream (Table XXXV). $TiCl_4$ recovery was ~90 %. The operation pressure was set to 300 mbar and the temperature was in all study cases between 80 and 81 °C. The bottom flow was in all cases between 445–452 $kg/100kg_{catalyst}$. The corresponding residue per distillate ratio (R/D) was 0,19. The bottom flow, as well as the duty of the evaporator, was dependant on the studied toluene case. For toluene cases A, B, C and D the respective duties of the evaporator were: 24,6 kW, 24,2 kW, 24,4 kW and 24,4 kW.

4.6.3 Distillation design

Four case studies of different toluene column configurations and two different sized heptane columns were studied. Both of the columns were operated at 1 bar.

4.6.3.1 Toluene column

Via simulations, heptane was shown to accumulate in the TWL recycle loop. Heptane boils at lower temperatures than toluene and therefore is collected in the overhead of the evaporator and toluene column and is thereafter recycled back into process with TWL. The target was to meet the specified TWL composition without additional units. The possible configurations were limited to four alternatives (Figure 27):

A. Use column as it is: recycle overhead mixture until heptane content increses unacceptably high. After that the TWE is disposed and the next toluene wash is performed with pure toluene.
B. Bleedstream: toluene is recovered as a sidestream (stream 9c, Fig. 26) from the vapour phase. The overhead product (stream 8, Fig. 26), rich in heptane, is taken out of the process as a bleedstream to be collected as a second-grade burnable fuel.
C. Partial condenser: the overhead product is partially condensed. The condensed phase (stream 9a) is recovered toluene. The vapour phase (stream 8, Figure 26) is taken out and collected as a first-grade burnable fuel.
D. Partial recovery: a major part of the overhead is recycled (stream 9b, Fig. 26) and mixed with pure toluene to meet the required conditions (Table XXXV) for usage as TWL. The excess overhead product (stream 9d, Fig. 26) is taken out of the process to remove heptane from the recovery cycle as a burnable fuel.

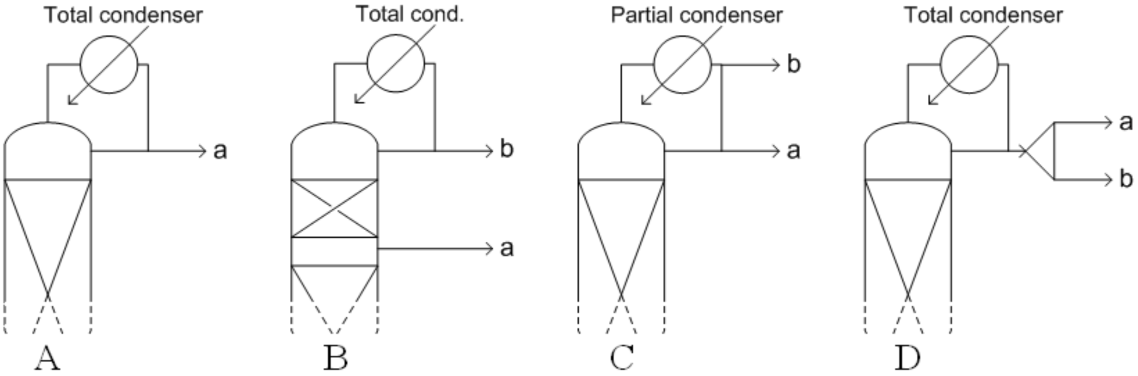

Figure 27 Alternative toluene column configurations (cases A-D) for recovering toluene for recycle (a) and heptane-rich overhead product as burnable fuel (b).

There were two types of burnable fuels generated: 1) those that could be directly fed to the burner as a first-grade fuel, and 2) those second-grade fuels that needed hydrolysis prior to be fed to the burner.

The recovered toluene is mixed with pure toluene to meet both the specified composition (<15 wt-% heptane, <5 wt-% $TiCl_4$) and mass flow (1700 kg/100$kg_{catalyst}$ in total, 850 kg/100$kg_{catalyst}$ per wash stage).

4.6.3.2 Heptane column

Mixtures of toluene and heptane are shown (Yerazunis *et al.* 1964) to be non-ideal most importantly in the region <20 mole-% toluene in heptane (liquid). Therefore, for practical reasons, some toluene has to be accepted in the recovered heptane. The recovered heptane is mixed with pure heptane before usage as HWL in order to achieve the design specifications (Table XXXV).

Two different cases of heptane column were studied: 22 stage and 34 stage columns. With 22 stages a larger bottoms rate is required to meet the specifications of HWL. The economic significance of increasing the recovery (and reducing the bottoms rate) by increased heptane column size was evaluated.

4.6.4 Results

4.6.4.1 Toluene column

The results of different simulated scenarios for toluene recovery are presented. The number of ideal stages (including the condenser and reboiler) was in all cases 22. The optimised operation parameters are given in Table XXXVII.

The case A (Figure O1) was shown to reach concentration of 16 wt-% of heptane in the recovered toluene (limit is ≤15 wt-%) after three recycles (Figure 28). TWL 1 was performed with pure toluene and the next three ones with the recovered toluene. Thus, if not mixed with pure toluene to decrease the amount of heptane, toluene can be recovered three times. Therefore, the TWL needs to be changed every fourth batch. The amount of recovered toluene was 1885 kg/100kg$_{catalyst}$, of which 185 kg/100kg$_{catalyst}$ was taken out as excess toluene (for fuel). The excess toluene was taken out to balance the washing amount to the specification, 1700 kg/100kg$_{catalyst}$. Every four batches the toluene is to be taken out of the process (first grade fuel) and replaced with pure toluene. $TiCl_4$ was recovered from the bottom of toluene column at 418 kg/100kg$_{catalyst}$.

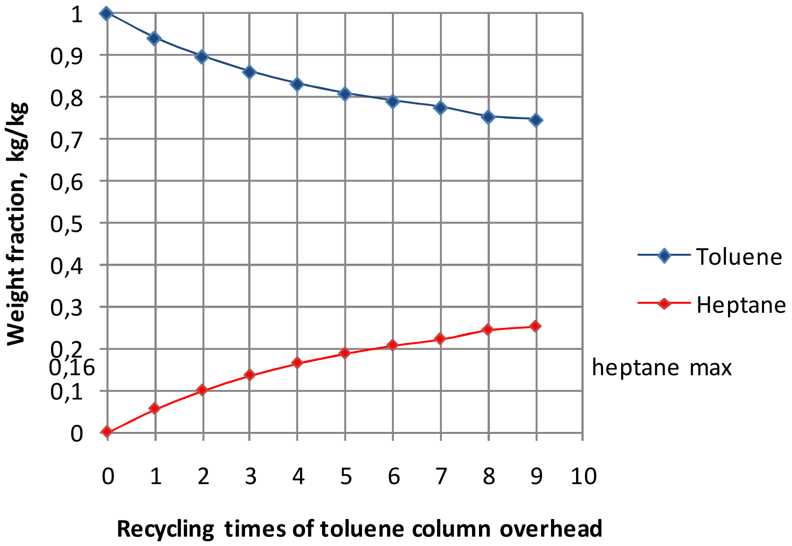

Figure 28 The composition of study case A TWL. The first wash was performed with pure toluene. The maximum allowable heptane content was 16 wt-%.

In case B the side takeout for toluene recovery was optimal at stage 3 vapour phase. Thus 1548 kg/100kg$_{catalyst}$ of toluene could be recovered for washing stages. The amount of pure toluene required for TWL was 152 kg/100kg$_{catalyst}$. The heptane-rich overhead product 360 kg/100kg$_{catalyst}$ was collected as a burnable fuel. However, the overhead product also had some $TiCl_4$ (2,7 wt-%), which needs to be neutralized prior to burning. The reflux ratio was rather high, 5, and in case of wanting to reduce the amount of high-boilers in the overhead stream would had been even higher. $TiCl_4$ was recovered from the bottom (99,5 wt-%) at 406 kg/100kg$_{catalyst}$. The composition of the heptane bleed in case B was: 22,3 % Heptane, 75 % Toluene and 2,7 % $TiCl_4$ (by weight).

In case C the required reflex was rather low, 2,5, even so resulting in a larger $TiCl_4$ recovery (421 kg/100kg$_{catalyst}$) compared to case B. The partial condenser vapour fraction was optimal at 0,17, thus resulting in heptane bleed of 324 kg/100kg$_{catalyst}$. Toluene was recovered at 1560 kg/100kg$_{catalyst}$. The composition of the heptane bleed was: 24,4 % Heptane, 75,3 % Toluene and 0,3 % $TiCl_4$ and the composition of the recovered toluene 15,2 % Heptane, 84,1 % Toluene and 0,7 % $TiCl_4$ (by weight).

Hence, the difference between vapour and liquid phase heptane concentration was 9,2 wt-%.

In case D the distillate was collected at 1881 kg/100kg$_{catalyst}$, of which 1450 kg/100kg$_{catalyst}$ was recycled for washing and 432 kg/100kg$_{catalyst}$ was taken out of the process as a burnable fuel. Pure toluene was to be added to the collected distillate to control the composition and adjust it to reach the design specifications. The amount of pure toluene required for TWL was 250 kg/100kg$_{catalyst}$. Titanium tetrachloride was concentrated in the bottom and collected at 424 kg/100kg$_{catalyst}$. The reflux was 3,5.

The optimised parameters for the distillation columns are given in Table XXXVII.

Table XXXVII Optimised operation parameters of the studied cases; *Toluene recovered from stage 3 vapour phase; **Partial condenser outlet vapour fraction 0,17 (heptane bleed); ***Values from the first run (pure toluene in TWL). The units were simulated as continuous unit operations, however the mass flows were fixed to per batch.

Unit		Case			
		A	B	C	D
Toluene column	*22 stages*				
Feed stage		10	10	10	10
Reflux ratio		3,5	5	2,5	3,5
Bottoms rate, kg/100kg$_{catalyst}$		418	406	421	424
Special specifications			*	**	
Heptane column	*22 stages*				
Feed stage		10	10	10	10
Reflux ratio		3,0	3,0	3,0	3,0
Bottoms rate, kg/100kg$_{catalyst}$		552***	432	456	456
Heptane column	*34 stages*				
Feed stage		16	16	16	16
Reflux ratio		4,0	4,0	4,0	4,0
Bottoms rate, kg/100kg$_{catalyst}$		186***	145	146	144

4.6.4.2 Heptane column

The heptane column was studied with 22 and 34 stages for all toluene study cases (A, B, C, D). The heptane recovery was maximized to meet the required HWL specifications (Table XXXV) after mixing with pure heptane. The optimised operation parameters are given in Table XXXVII. Increasing the column size from 22 to 34 ideal stages resulted, as expected, in a more efficient separation. The bottoms rate was reduced by 324 kg/100kg$_{catalyst}$ by average. However, the larger column increased the utility demand in average by over 56 %.

4.6.5 Variable operating cost

The cost of catalyst and motherliquor entering the recovery section was estimated as 100 €/$kg_{catalyst}$.

The residue of the evaporator was considered as a waste stream with a cost. The waste treatment of the residue was estimated 1,5 €/kg. The other “waste” streams, or bleed streams of the recovery section were the bleed from the toluene column and the bleed from the heptane column. These bleed streams were considered to be burnable, and thus would generate income. These burnable materials were classified into two grades:

- first-grade fuels (that could be fed directly to the burner) were given a value of 0,5 €/kg
- second-grade fuel (case B heptane bleed, needs hydrolysis prior to burning) was given a price of 95 % of the first-grade fuel

The recycled streams were considered also as an income. The incomes that the recovery generated were valued according to the pure component these streams replaced; as an example the recovered toluene stream (80 % toluene, max 15 % heptane, max 5 % $TiCl_4$) was valued according to the price of toluene (0,69 €/kg).

The costs of utilities, waste treatment and the prices of raw material burnable fuels are given in the following table (XXXVIII).

Table XXXVIII Estimated costs of utilities, raw materials, waste treatment and an estimated sale price for non-recycled toluene and heptane (sold as fuel)

Component	Price	
Cooling water	0,0313	€/1000 kg
Steam (8 bar)	15	€/1000 kg
Waste treatment	1,5	€/kg
$TiCl_4$	3,6	€/kg
Toluene	0,69	€/kg
n-Heptane	0,8	€/kg
Burnable fuels (no TiCl4)	0,5	€/kg
Burnable fuels (<3 % TiCl4)	0,475	€/kg

The results of the variable cost calculation for different cases are given in Table XXXIX. The achieved savings in the variable operating costs are summarized in Table XL. The cost of electricity or the fixed operating costs (labour, maintenance etc.) were not included in the variable cost calculations.

Table XXXIX Variable costs and intermediate costs and revenues for the studied cases (in €/kg$_{\text{catalyst}}$); T-Col 22: toluene column with 22 stages, H-Col22/H-Col 34: heptane column with 22 or 34 ideal stages; (values rounded)

	No	T-Col 22, H-Col 22				T-Col 22, H-Col 34			
	recovery	A	B	C	D	A	B	C	D
	€/kg	€/kg	€/kg	€/kg	€/kg	€/kg	€/kg	€/kg	€/kg
Material Costs									
Catalyst production and motherliquor	100	100	100	100	100	100	100	100	100
TWL, pure	11,7	2,9	1,1	1,0	1,7	2,9	1,1	1,0	1,7
HWL, pure	13,6	4,2	3,3	3,5	3,5	1,3	1,0	1,0	1,0
Waste treatment	41,3	6,8	6,7	6,8	6,8	6,8	6,7	6,8	6,7
Σ(costs)	166,7	114,0	111,0	111,2	112,0	111,0	108,7	108,7	109,4
Value of recovered components									
$TiCl_4$	0	15,1	14,6	15,2	15,3	15,0	14,6	15,2	15,3
Rec. TWL	0	8,8	10,7	10,8	10	8,8	10,7	10,8	10
Rec. HWL	0	9,4	10,3	10,2	10,2	12,3	12,6	12,6	12,6
Burnable fuels	8,6	5,8	3,9	3,9	4,4	4,0	2,4	2,3	2,9
Σ(revenues)	8,6	39,1	37,8	40,0	39,8	40,1	38,7	40,9	40,8
Direct Manufacturing Cost									
costs-revenues	158,0	74,8	73,2	71,2	72,1	70,9	70,1	67,8	68,6
Utility cost									
CW	0	0,08	0,05	0,07	0,08	0,1	0,07	0,08	0,1
Steam	0	0,48	0,37	0,43	0,48	0,55	0,42	0,50	0,55
Σ(utilities)	0	0,57	0,42	0,5	0,57	0,65	0,5	0,58	0,65
Variable cost	158	75,4	73,6	**71,7**	72,7	71,5	70,6	**68,4**	69,3

Table XL Savings achieved with the optimised recovery section; *compared to having no recovery; 'bolded'–case with lowest cost

		No	T-Col 22, H-Col 22				T-Col 22, H-Col 34			
		recovery	A	B	**C**	D	A	B	**C**	D
Variable cost	€/kg$_{\text{cat}}$	158,0	75,4	73,6	**71,7**	72,7	71,5	70,6	**68,4**	69,3
Saving *	€/kg$_{\text{cat}}$		82,6	84,4	**86,3**	85,4	86,5	87,5	**89,7**	88,8

The case C (partial condenser) was shown to have the lowest variable cost. The investment cost of different alternatives was not compared; however, the case C is simpler in construction than the second-best alternative, case B.

The variable cost of case C with 22-staged heptane column resulted in savings of 86,3 €/kg$_{\text{catalyst}}$ compared to having no recovery. The heptane column with 34 stages resulted in further 3,4 €/kg$_{\text{catalyst}}$ savings (case C toluene column). However, the design where both distillation columns had 22 ideal stages was proven adequate for the purposes.

5 Discussion

In this chapter the results will be briefly discussed in relationship to theory and methodology. The results are evaluated based on the introductory statement of purpose:

- Verify the suitability of the separation techniques
- Quantify the recoverable amounts of the key components
- Study the effect of impurities in washing liquids on the catalyst physical properties and on the catalyst polymerisation properties
- Deliver the vapour-liquid equilibriums of the key component mixtures and regress the binary activity coefficients for an appropriate property method
- Optimise the material balances of the recovery section

5.1 Suitability of the separation techniques and component recovery

Treatment of the combined motherliquor and toluene wash effluents was first tested with a laboratory-scale batch evaporator. Already the initial experiments revealed the weaknesses of such setup: the solidification reaction of titanium haloalkoxides was a very possible risk. Operation under vacuum, and correspondingly at lower temperature minimized the possibility; however the solidification reaction was also shown dependant on the residence time. The titanium haloalkoxides reacted to form a gel under storage even at room temperature (in dry, inert conditions).

The separation of valuable components from mixtures of motherliquor and toluene was shown to be most feasible with a continuous evaporator in vacuum conditions. The volatiles were successfully separated from the low-boilers without any significant entrainment. In addition, the highly concentrated residue was collected without clogging and was flowing in all of the trials. The continuous evaporator was thus proven feasible.

Despite the similar recovery rates as in batch evaporation, the continuous evaporator can be operated without the risk of the solidification reaction of titanium haloalkoxides. The continuous evaporator was operated at toluene boiling temperatures (below $TiCl_4$ boiling point) with successful recovery without any entrainment of DOP and very minor entrainment of haloalkoxides. With the evaporator toluene was recovered by over 93 % (weight, analysed) and $TiCl_4$ by over 91,5 % (molar).

The separation of toluene from solutions with titanium tetrachloride was studied in practice with a distillation setup. The efficiency of the lab-scale Vigreux-column was questionable, and distillation with a Raschig-ring packed-bed column was required. Nevertheless, the separation was performed successfully to recover $TiCl_4$ as the bottom product and toluene (together with heptane and small amount of $TiCl_4$) as distillate. According to the simulations the toluene column with 22 ideal stages is adequate.

The separation of heptane from toluene in very pure concentrations is expectedly difficult. As indicated by the “narrow” difference between the dew point and bubble point curves (VLE, Yerazunis *et al.* 1964), the separation of these components is nonideal. Via simulations it was verified that distillation column with 22 stages “limits” the rectification: there are simply too few steps for complete purification of heptane. In effect, a larger column, with (for example) 34 stages is preferred. However, the 22-staged column is also suitable, but requires a larger bottom mass flow.

5.2 Washing with recovered hydrocarbons

Washing the catalyst with recovered toluene was studied together with a synthetic sample of the following composition: 80 wt-% of toluene, 15 wt-% heptane and 5 wt-% $TiCl_4$. The studied conditions were shown to have diminutive, if any, effect on the catalyst morphology, composition or polymerisation properties. Therefore it is safe to conclude that the toluene can be recovered and reused in the washing stages at the studied conditions without apparent harmful side-effects.

Similarly, the extensive studies with toluene in the heptane wash liquid showed no indication that the studied conditions of HWL (6 wt-% of toluene in HWL) would harm the catalyst. In combination with the impurities also the effect of increased settling time was studied. Also the effect of the prolonged settling time was found trivial. Thus it can be concluded that also heptane can be recovered and reused in the washing stages at the studied conditions without clearly damaging the catalyst.

5.3 VLE and Wilson parameters

The vapour pressure of titanium tetrachloride was measured in addition to the vapour-liquid equilibriums of toluene+$TiCl_4$ and heptane+$TiCl_4$. Due to practical reasons, the vapour phase composition of the VLE measurements could not be measured. Hence,. The vapour-phase composition was calculated. The Antoine parameters – that were obtained from the $TiCl_4$ vapour pressure measurements – were used to correct the vapour-phase composition calculations.

Overall, the vapour-liquid equilibriums were measured with high-quality equipment and in co-operation with professionals. However, the regressed data (VLE) failed to pass the area test (Aspen Plus 7.1). The test methods are necessary for data evaluation, but must be reviewed with caution: sometimes even thermodynamically inconsistent data can pass the area test. Hence, the experimental VLEs was compared with the Wilson predicted VLEs. The predictions that were corrected with the regressed parameters were found to be in excellent agreement with the experimental results.

5.4 Optimised recovery section

The recovery section was updated with the regressed Wilson binary parameters. The Antoine equation was corrected with the experimentally acquired parameter values. Through the simulations the mass balances for different case studies were acquired, and for these different cases the variable costs were calculated.

The D/F ratio in the optimised evaporator was 83,6 %, R/D ratio was 19,6 % and $TiCl_4$ recovery 92,9 %. The vapour fraction of the distillate (heptane bleed fraction) in toluene column was 0,17 and the recovery of toluene 84,4 %. The recovery of heptane in heptane column was 78,8 %. The overall recovery of titanium tetrachloride was 90,4 %.

The setup with the lowest variable cost was case C (toluene column with a partial condenser). The heptane column with 34 ideal stages had a lower variable cost mainly due to the smaller bleed-stream compared to 22-staged heptane column. The addition of 12 stages to the original design (22 stages) results however in an increase of investment cost. The investment cost was to be kept unchanged, and thus the 22-staged heptane column was selected as the optimal case.

5.6 Deviating and unexpected results

The compositions were shown to be difficult to analyse with good consistency. The following sources of error were identified:

- Samples were analysed with three different methods: GC, LC and ICP → combining the results from the different methods does not add up to 100 %
- Samples were diluted prior to analysis in order to operate in the detection range
- Complexity of titanium haloalkoxide analysis: the sample needs to be first diluted, then hydrolyzed, analyzed with GC for 2-ethylhexanol and thereafter the content of Ti-haloalkoxide is back-calculated
- Lack of a secondary method for verifying the Ti-haloalkoxide quantity
- $TiCl_4$ analysis: the molar amount of titanium conserved by titanium haloalkoxide was subtracted from the total amount of titanium in solution to give the molar amount of titanium in titanium tetrachloride

Nevertheless, the methods are well established and the analyses were performed by a person skilled in the art.

Parts of the PPR polymerisation results deviated unexpectedly from the results acquired via batch polymerisations. The PPR polymerisations are performed in reactors with volume of 20 ml, of which 5 ml is active liquid volume. The maximum achievable yield is 500 mg_{PP} whilst a traditional yield is 100 mg_{PP}, depending on the purpose of polymerisations. In addition to the vast difference in yields between PPR and bench, the conditions are different: PPR polymerisations were performed in slurry, whereas bench polymerisations in bulk. Also, polymerisations in smaller scale (PPR) are more sensitive to catalyst poisoning. Nevertheless, polymerisation in PPR provided quick results and reliable indications of polymerisation activity. And via the PPR polymerisations a larger amount of data was acquired (compared to bench), as 48 polymerisations was performed simultaneously.

6 Conclusions

The purpose of this work was to optimise the recovery section of a polyolefin catalyst manufacturing plant. The initial design of the recovery section had been prepared according to assumptions of high uncertainty. Hence, in addition to studying the recovery and reuse of the components, the work included a secondary purpose of disproving common beliefs (such as the azeotropic mixture of toluene+$TiCl_4$ and deficient recovery of components from motherliquor).

It was shown that it is possible and economical to recover components from the motherliquor (if combined with toluene wash effluents). The recovery efficiency of a lab-scale batch evaporator was similar to a continuously operated bench-scale evaporator; however, the operability of the continuous evaporator was superior: the titanium haloalkoxides were successfully concentrated in the residue without harmful solidification reaction. In addition, the volatiles ($TiCl_4$, toluene, and heptane) were collected in the overhead with high recovery rates.

It has been shown via VLE measurements that none of the studied binary mixtures (toluene+$TiCl_4$, and n-heptane+$TiCl_4$) formed azeotropic systems. Hence, the studied components can be efficiently separated via conventional distillation. However, the studied binary systems were shown to deviate from ideal-liquid mixtures. Therefore the departures from ideal behaviour in liquid-phase were revised with liquid-phase activity coefficients. The Wilson binary interaction parameters were regressed from the VLE data in order to take the liquid-phase nonidealities into account in the simulations.

Impurities (heptane, $TiCl_4$) in toluene washing liquids were shown to have no effect on the catalyst composition, morphology or polymerisation properties. Neither was there any observed effect from possible products of thermal decomposition. Hence, toluene can be recovered and reused in the toluene washing stages at the studied conditions.

The studied amounts of toluene in heptane washing liquids had practically no effect on the catalyst composition, morphology or polymerisation properties. Therefore, heptane can also be recovered and reused in the heptane washing stages at the studied conditions without any harmful effect on the catalyst.

The concept used in the initial design of the recovery section is technically and economically feasible according to this study. However, prevention of heptane accumulation in toluene recovery cycle is proposed to be modified to study case C. In the study case C the toluene column has a partial condenser instead of a total condenser.

References

Akzo Nobel NV (2006) *Treatment of a titanium tetrachloride-containing waste stream.* US7045480 (B2).

Billet, R. (1992) Performance of Thin-film Distillation and its Application. *Sep. Technol.*, vol 2, October. Butterworth-Heinemann.

Billet, R. (2000) Evaporation. In *Ullmann's Encyclopedia of Industrial Chemistry*. 2010. John Wiley & Sons.

Business Wire. (2010) *Polypropylene (PP) 2010 World Market Outlook and Forecast Been Recently Added by MarketPublishers.com.* http://findarticles.com/p/articles/mi_m0EIN/is_20100310/ai_n52400321/ (2010-06-28)

Choi, W. and Lee, K. (1988) Purification of $TiCl_4$ by Adsorption Technique. *Bull. Korean Chem. Soc.*, Vol. 9, No. 1.

Dechema. (2010) *Detherm ...on the Web.* http://i-systems.dechema.de/detherm/mixture.php? (2010-06-28)

Engineeringtoolbox. (2010a) *Properties of Saturated Steam – SI Units.* http://www.engineeringtoolbox.com/saturated-steam-properties-d_101.html (2010-07-07)

Engineeringtoolbox. (2010b) *Water – Thermal Properties.* http://www.engineeringtoolbox.com/water-thermal-properties-d_162.html (2010-07-07)

Basell Poliolefine SRL (2010) *Method for recovering titanium tetrachloride from a waste liquid.* EP1834003 (B1).

Garoff, T., Leinonen, T, and Iiskola, E (1990) *Ziegler-Natta Catalysis in Polypropylene Polymerization*, 1990). Unpublished, confidential internal publication. Neste Chemicals, Porvoo Finland.

Glover, W. (2004) Scaleup of Agitated Thin-film Evaporators. *Eng. Practice. Chem. Eng.*, April.

Herington, E.F.G. (1947) A Thermodynamic Consistency Test for the Internal Consistency of Experimental Data of Volatility Ratios. *Nature*, 160, p. 610–611.

ICIS. (2010) *Polypropylene (PP) CAS No: 9003-07-0.* http://www.icis.com/v2/chemicals/9076428/polypropylene.html (2010-06-28)

Joseph, M.A., Ramjugernath, D., Raal, J.D. (2002) Computer-aided Measurement of Vapour-Liquid Equilibria in a Dynamic Still at Sub-Atmospheric Pressures. *Dev. Chem. Eng. Mineral Process*. 10(5/6), p. 615–637.

Lei, Z.; Chen, B. and Ding, Z. (2005) *Special Distillation Processes*. Elsevier. Netherlands.

Mitsui Chemicals Inc (2004) *Method for recovering titanium compound, process for preparing titanium halide, and process for preparing catalyst for polymer production*. US6790319 (B2).

Montgomery, D. (2009) *Design and Analysis of Experiments*. 7th Edition. John Wiley & Sons. Asia.

Moser, B. and Kistenmacher, H. (1987) An analysis of the industrial use of a phase equilibria prediction model based on thermodynamic perturbation theory. *Fluid Phase Equilib*. 34, p. 189–201.

Natta, G., Pino, P., Corradini, P., Danusso, F., Mantica, E., Mazzanti, G., and Moraglio, G. (1955) *J. Am. Chem. Soc.*, 77, 1708.

NIST. (2010) *Titanium tetrachloride. Phase change data.* http://webbook.nist.gov/cgi/cbook.cgi?Source=1966LUC593-598&Units=SI&Mask=4 (2010-09-20)

Ozzetti, R.; Filho, A.; Schuchardt, U. and Mandelli, D. (2002) Determination of tacticity in polypropylene by FTIR with multivariate calibration. *Journal of Applied Polymer Science*. Vol 85, Issue 4, p. 734–745.

Pillai, S.M.; Ravindranathan, M. and Sivram, M. (1986) Dimerization of ethylene and propylene catalyzed by transition-metal complexes. *Chem. Rev*., Vol 86, Issue 2.

Pradyot P. (2003) *Handbook of Inorganic Chemicals*. McGraw-Hill, p. 947–948.

Raal, J.D. and Mühlbauer, A.L. (1998) *Phase Equilibria: Measurement and Computation*. Taylor and Francis, Washington, DC.

Raal, J.D. and Ramjugernath, D., (2005) Vapor-Liquid Equilibrium at Low Pressure. In *Measurement of the Thermodynamic Properties of Multiple Phases*. International Union of Pure and Applied Chemistry.

Redlich, O.; Kister, A.T. (1948) Algebraic Representation of Thermodynamic Properties and the Classification of Solutions. *Industrial Engineering Chemistry*, 40, p. 345–348.

Roy, P.K.; Bhatt, A. and Rajagopal, C. (2003) Quantitative risk assessment for accidental release of titanium tetrachloride in a titanium sponge production plant, J. *Hazard. Mater*. A102, p. 167–186.

SciFinder. (2010) *Substance details*. https://scifinder.cas.org/scifinder/view/link_v1/substance.jsf?l=t7c60yhXV6tLsEBph1Nzgc0MeuOTFJexW24LeJxvgVWKSFRorN5U4Sbv5Th_otov (2010-07-27)

Seader, J. and Henley, E. (2006) *Separation Process Principles*. 2nd Edition. John Wiley & Sons, U.S.

Shell Int Research. (1990) *Process for removing contaminants from a liquid TiCl4 phase*. EP0202715 (B1).

Shell Oil CO. (1993) *Distillation separation process of titanium tetrachloride and halohydrocarbon.* US5242549 (A).

Sinnot, R. and Towler, G. (2009) Chemical Engineering Design. In *Coulson & Richardson's Chemical Engineering Series*. Fifth edition. Elsevier. UK.

Tret'yakova, K.V. Nisel'son, L.A. (1967) Orthobaric Density and Critical Parameters of $TiCl_4$ and $VOCl_3$ and Density of their Mixtures. *Russ. J. Inorg. Chem.* 12, 452

Tripathi, D. (2002) *Practical Guide to Polypropylene*. Rapra Technology Limited.

Union Carbide Chem Plastics. (2000) *Titanium separation process.* EP0837075 (B1)

Uusi-Kyyny, P. (2004) *Vapour-liquid equilibrium measurements for process design*. Espoo: Helsinki University of Technology. (Ph.D. thesis project, Department of Chemical Technology).

Van Ness, H.C.; Byter, S.M. and Gibbs R.E. (1973) Vapor-Liquid Equilibrium: Part I. An Appraisal of Data Reduction Methods. *AIChE Journal*, 19, p. 238–244.

Yerazunis, S.; Plowright, J. and Smola, F. (1964) Vapor-liquid Equilibrium Determination by a New Apparatus. *A.I.Ch.E. Journal*, Vol. 10, No. 5, September.

Ziegler, K., Breil, H., Holzkamp, E., and Martin, H. (1960) DE 973626, *Chem. Abstr.*, 54, 14794.

APPENDIX A SELECTION CRITERIA FOR VLE MODELS IN ASPEN

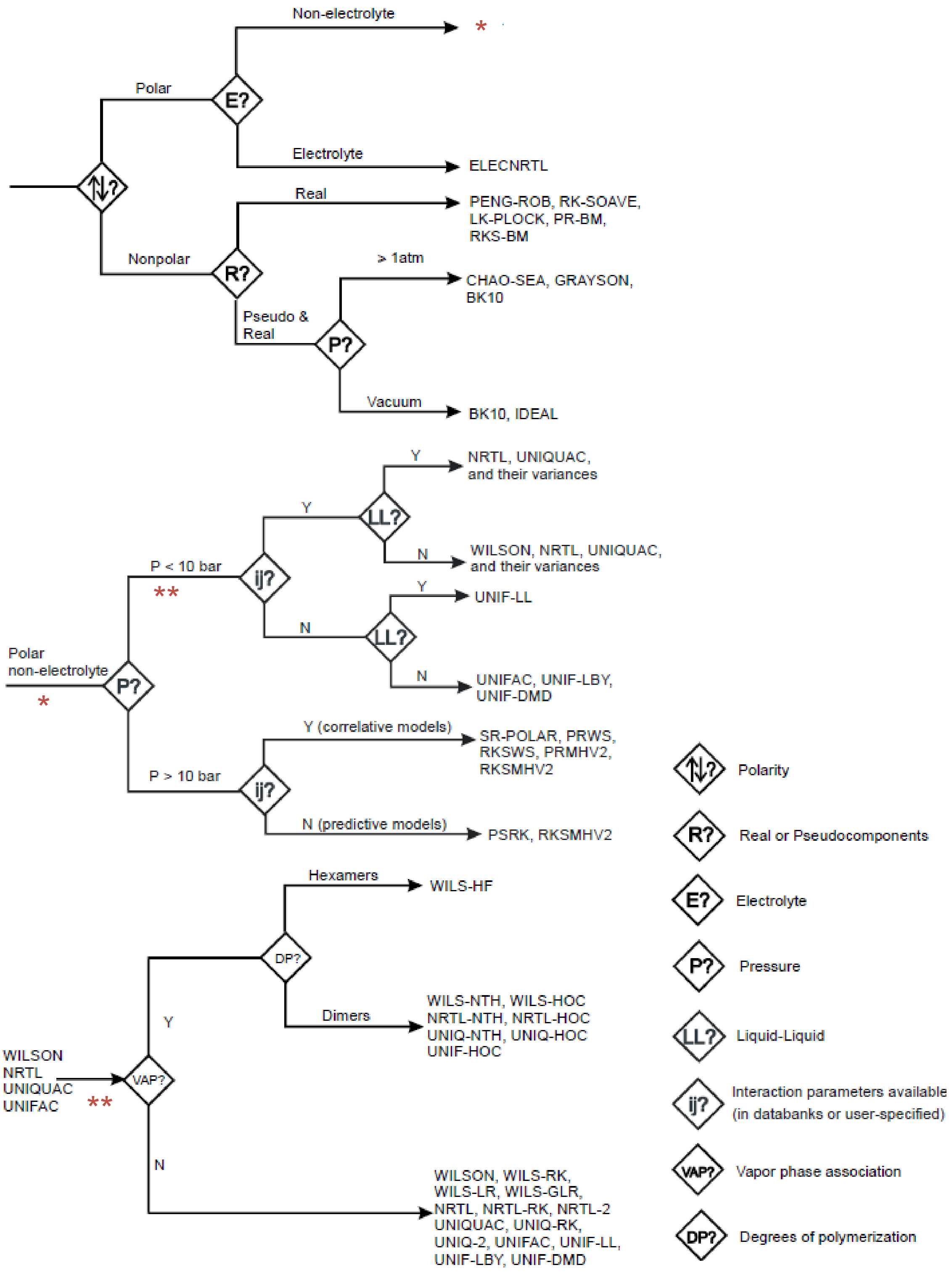

Figure A1 Property method selection map for Aspen Plus 7.1; * and ** are given to indicate the next stage on the selection path.

APPENDIX B SEM IMAGES OF THE CATALYSTS PREPARED FOR THE STUDY OF IMPURITIES IN TOLUENE WASHING LIQUIDS

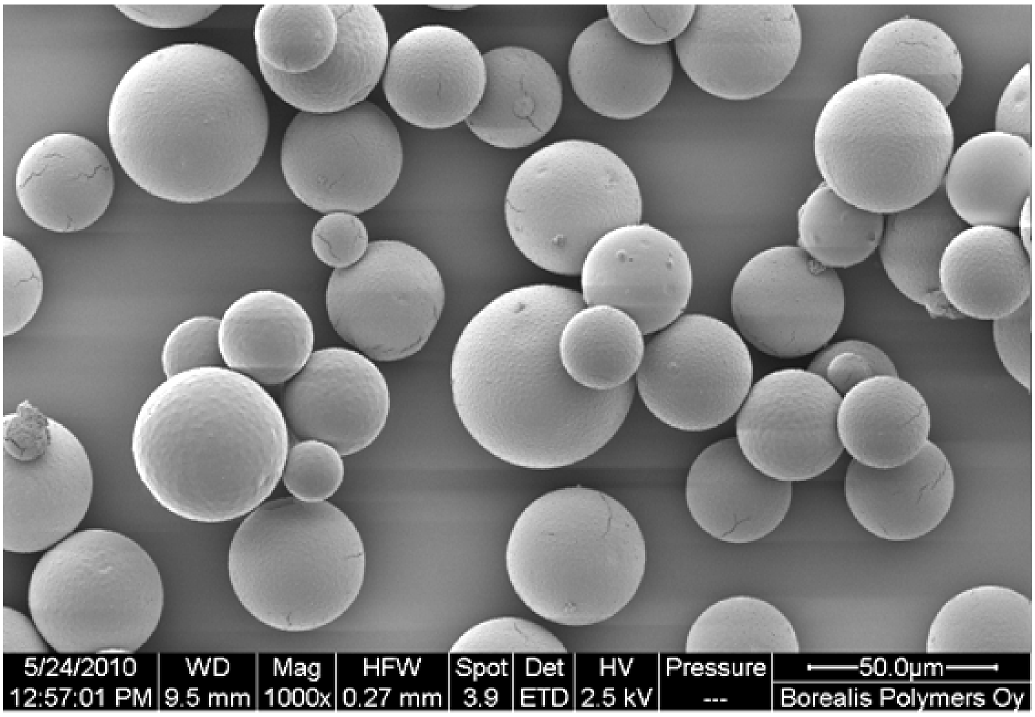

Figure B1 SEM image of the catalyst washed with the recovered toluene, RMAN077

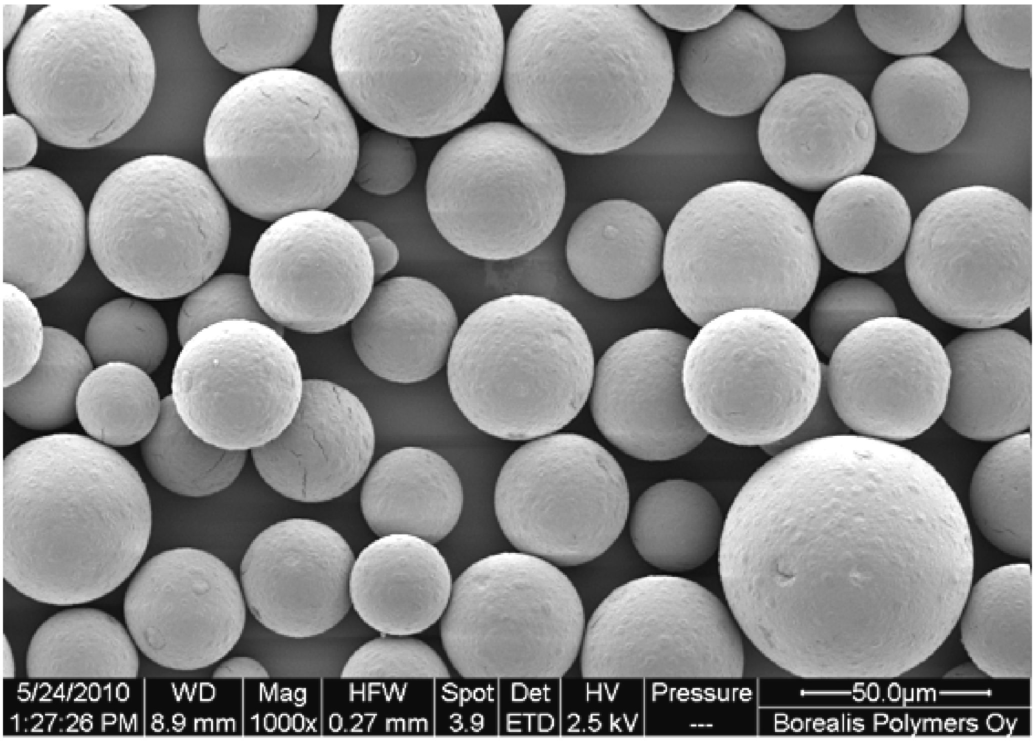

Figure B2 SEM image of the catalyst washed with the comparative mixture, RMAN078

APPENDIX C COULTERPARTICLE SIZE DISTRIBUTIONS OF CATALYSTS RMAN041-048

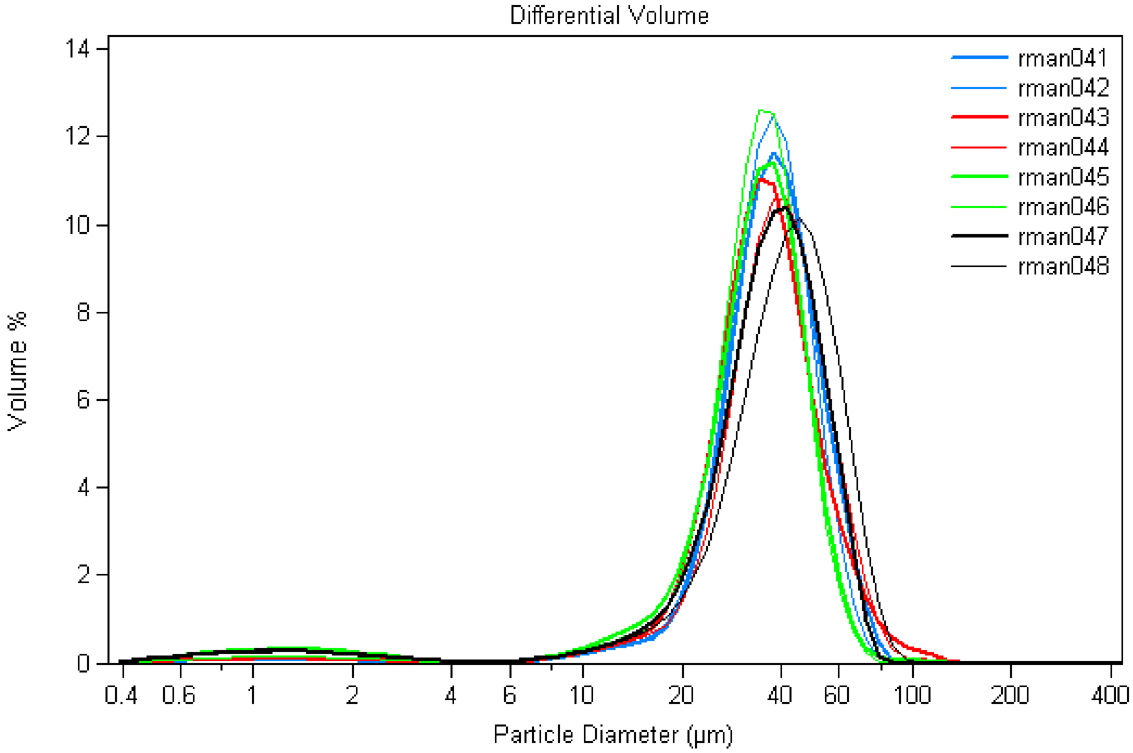

Figure C1 Coulter particle size distribution by differential volume of catalysts RMAN041-RMAN048.

The shapes of the size distributions are overlapping and regular: the peaks are smooth and do not have any “elbows”. No large diameter groups or peaks at >100 µm were identified. The three “lowest” peaks are RMAN044, 47 and 48, which are also broader at the top: the particle size distribution around the mode diameter is wider compared to others. Fine particles (<10 µm) are present only in very small amounts. If generalized, particle size distributions are “identical”.

APPENDIX D SEM IMAGES OF THE CATALYSTS PREPARED FOR THE STUDY OF IMPURITIES IN HEPTANE WASHING LIQUIDS

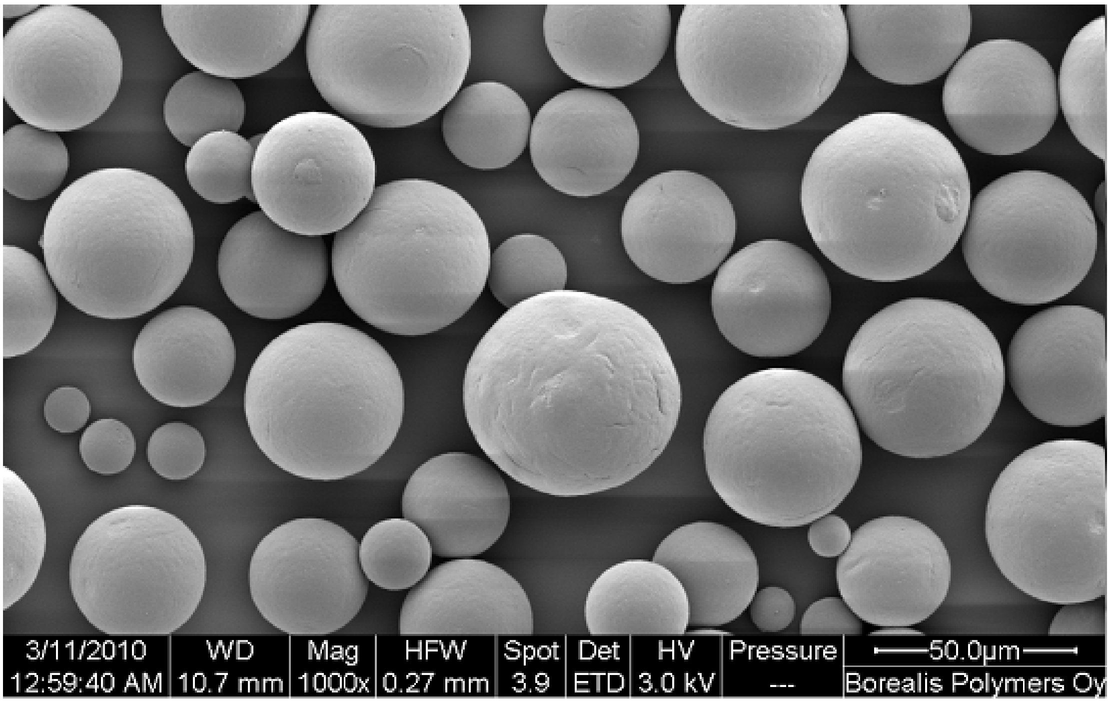

Figure D1 SEM image of the catalyst produced, batch code RMAN041 (reference catalyst)

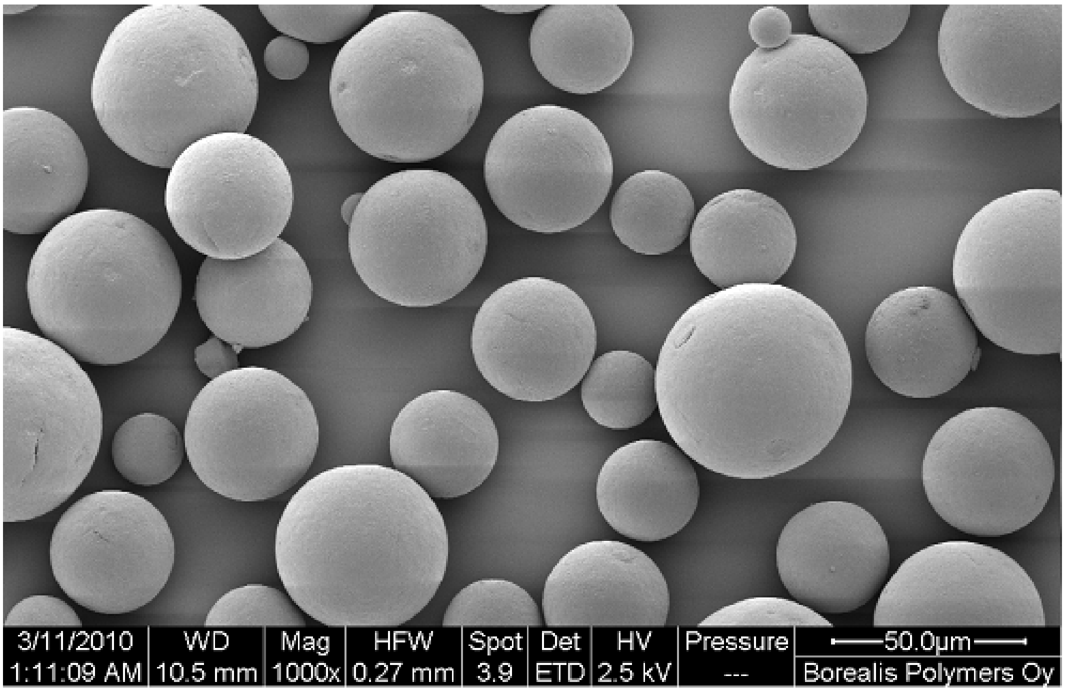

Figure D2 SEM image of the catalyst produced, batch code RMAN042 (reference catalyst)

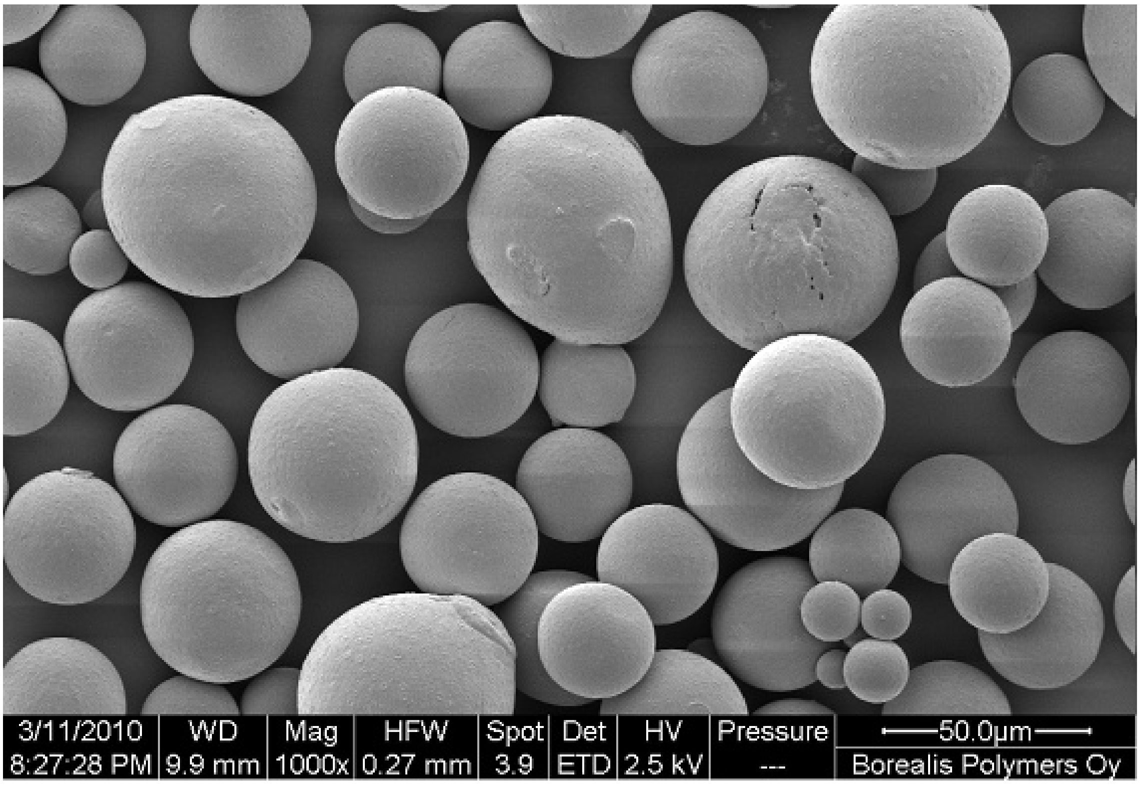

Figure D3 SEM image of the catalyst produced, batch code RMAN043

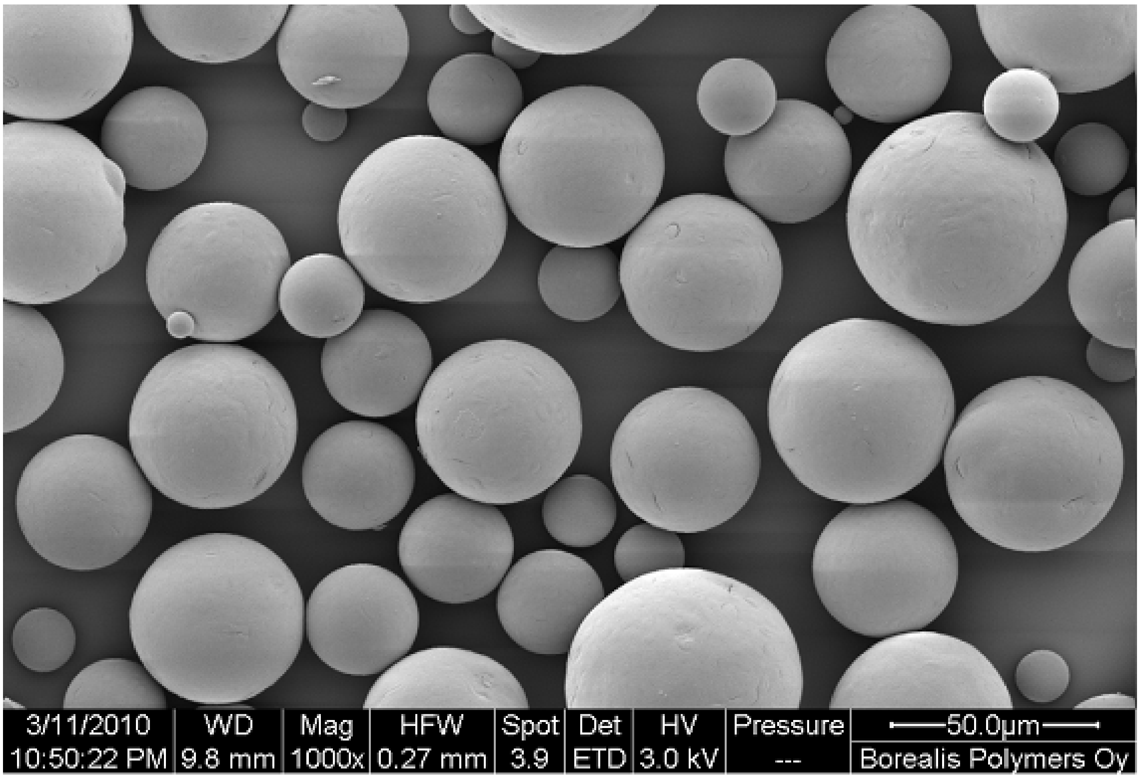

Figure D4 SEM image of the catalyst produced, batch code RMAN044

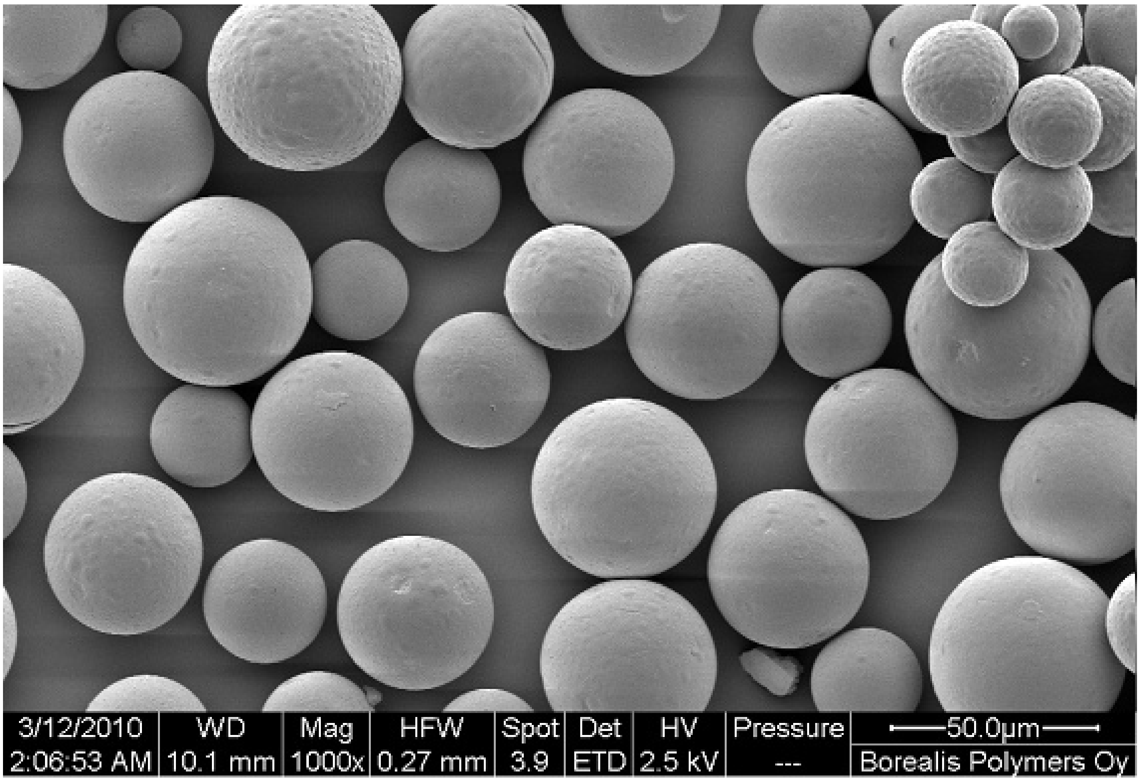

Figure D5 SEM image of the catalyst produced, batch code RMAN045

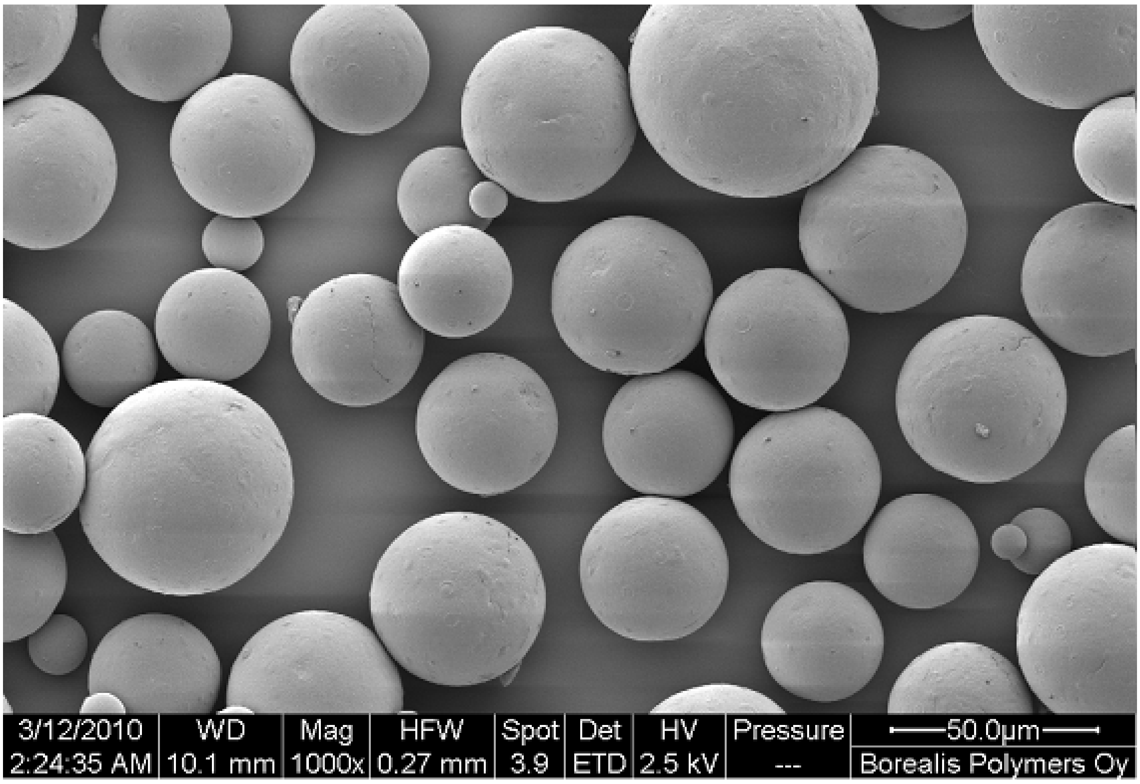

Figure D6 SEM image of the catalyst produced, batch code RMAN046

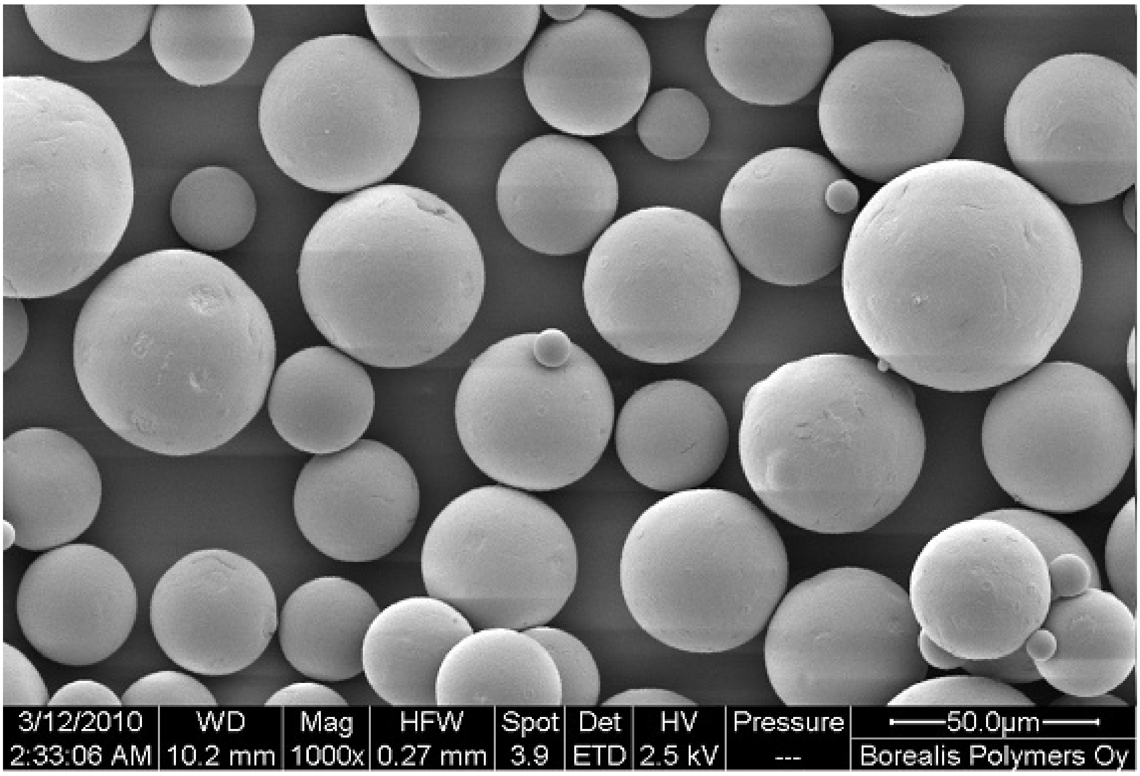

Figure D7 SEM image of the catalyst produced, batch code RMAN047

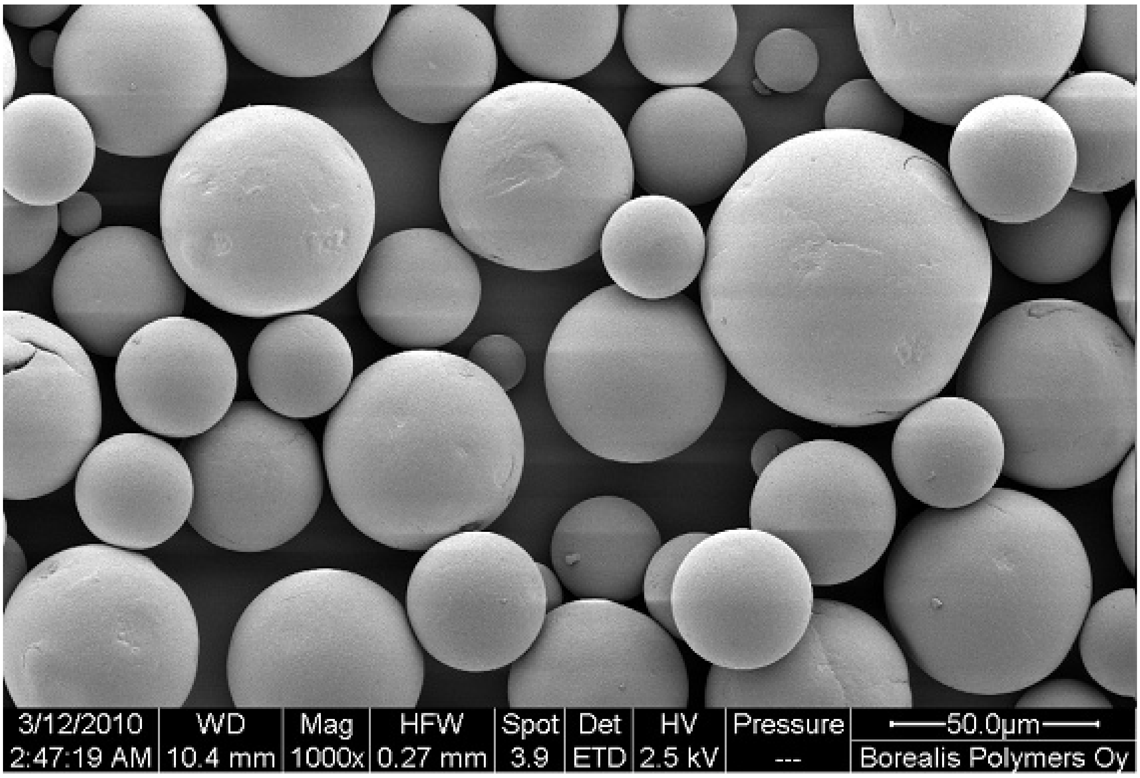

Figure D8 SEM image of the catalyst produced, batch code RMAN048

APPENDIX E NUMBER AVERAGE MOLECULAR WEIGHTS AND POLYDISPERSITY INDEXES OF PPR POLYMERISATIONS

Table E1 Number average molecular weights, Mn. Outliers (RMAN044 R_5 and RMAN045 R_3) were removed.

RMAN0--	R_1	R_2	R_3	R_4	R_5	R_6	Mean
41	94118	111204	109918	119626	105923	107161	107991,7
42	111225	95449	108376	119975	101830	106478	107222,2
43	99770	100395	118241	99759	92268	110252	103447,5
44	97909	90910	85428	110935	0	104063	97849
45	102500	111350	0	105469	104109	101259	104937,4
46	105358	97610	93662	97078	95473	101242	98403,83
47	87455	105641	102789	105149	88759	100719	98418,67
48	100211	102712	90653	105617	99218	86487	97483

Table E2 Polydispersity indexes, Mw/Mn. Outliers (RMAN044 R_5 and RMAN045 R_3) were removed.

RMAN0--	R1	R2	R3	R4	R5	R6	Mean
41	1,83	1,87	1,82	1,89	1,90	1,82	1,86
42	1,88	1,87	1,87	1,87	1,84	1,96	1,88
43	1,88	1,86	1,94	1,81	1,97	1,86	1,89
44	1,93	1,80	2,06	1,87		1,91	1,91
45	1,95	1,89		1,87	1,85	1,89	1,89
46	1,89	1,95	1,90	1,96	1,88	1,86	1,91
47	1,91	1,89	1,92	1,90	1,93	1,88	1,90
48	1,87	1,91	1,90	1,87	1,89	1,96	1,90

APPENDIX F NORMAL PROBABILITY PLOTS OF THE PPR POLYMERISATION RESULTS

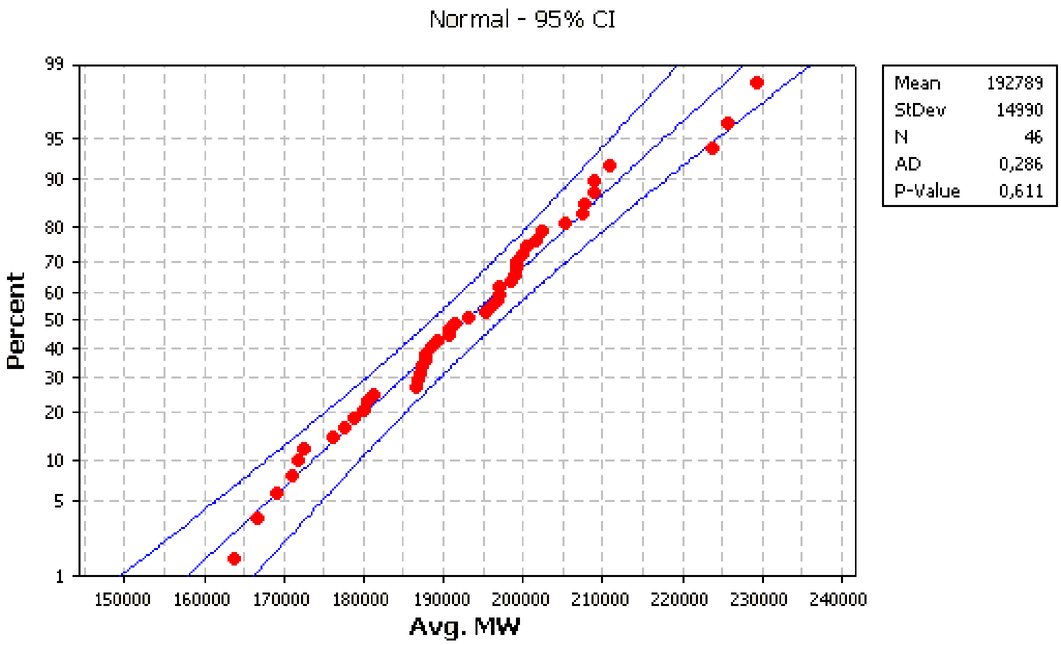

Figure F1 Normal probability plot of average Mw (Minitab 15.1.0.0). Outliers RMAN044 R_5 and 45 R_3 were removed prior to plotting. One possible outlier, RMAN042 R_4, identified, yet not removed at (223783;94,2).

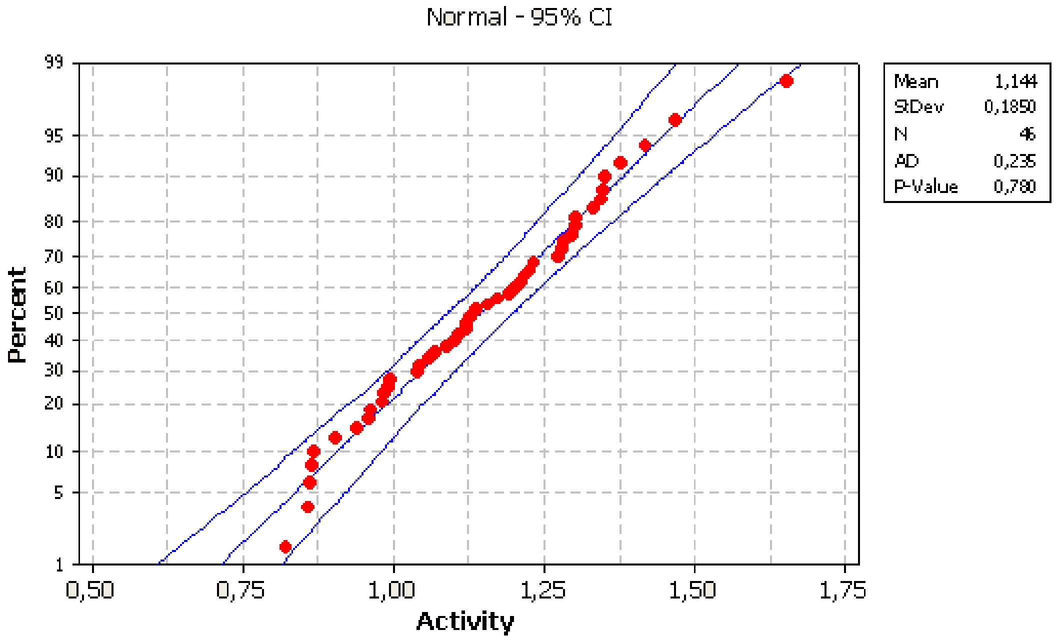

Figure F2 Normal probability plot of the calculated activities (Minitab 15.1.0.0), outliers RMAN044 R_5 and 45 R_3 were removed prior to plotting. One possible outlier, RMAN041 R_3, identified, yet not removed at (1,654;98,5).

APPENDIX G DSC RESULTS OF THE PPR POLYMERIZATIONS

Table G1 Results of differential scanning chromatography, DSC, of three selected polymerisations from each catalyst. T_m=melting temperature; T_c=crystallization temperature; Cr=percentage of crystalline material in sample.

Catalyst	Replica,	Avg. MW	T_m	T_c	Cr	Mean, T_m	Mean, T_c	Mean, Cr
RMAN0--	i=1...6	1000	°C	°C	%	°C	°C	%
41	R_1	173	160,8	114	45	161,8	113,4	45,0
41	R_3	200	161,9	113,3	45			
41	R_4	226	162,6	112,8	45			
42	R_2	179	161,7	112,1	45	161,1	112,7	43,3
42	R_3	202	160,4	112,5	40			
42	R_4	224	161,3	113,6	45			
43	R_1	187	160,3	113,1	46	160,8	113,5	45,0
43	R_3	229	160,7	115,2	44			
43	R_4	181	161,4	112,1	45			
44	R_1	189	160,2	114	46	161,2	114,5	45,0
44	R_2	164	160,8	114,2	43			
44	R_4	208	162,6	115,2	46			
45	R_2	211	162,3	112	45	161,1	112,5	45,0
45	R_4	197	160,4	112,4	45			
45	R_6	192	160,7	113,1	45			
46	R_1	199	161,1	114,7	44	161,1	114,9	43,3
46	R_3	178	161	115,1	44			
46	R_6	188	161,1	114,8	42			
47	R_1	167	162,9	113,6	44	160,6	112,5	43,7
47	R_4	199	158,4	112,4	42			
47	R_6	189	160,5	111,6	45			
48	R_4	197	160,7	114	45	161,0	113,9	44,0
48	R_5	187	161	114	44			
48	R_6	169	161,4	113,6	43			